Spring 1995

Component Mode Synthesis-Based Design Methodology for Structural Modification and Synthesis

Venkateshwarlu Maroju
Old Dominion University

COMPONENT MODE SYNTHESIS-BASED DESIGN METHODOLOGY FOR STRUCTURAL MODIFICATION AND SYNTHESIS

by

Venkateshwarlu Maroju

A Dissertation Submitted to the Faculty of
Old Dominion University in Partial Fulfillment of the
Requirements for the Degree of

DOCTOR OF PHILOSOPHY

in

MECHANICAL ENGINEERING

OLD DOMINION UNIVERSITY
May 1995

Approved by:

Gene J.-W. Hou, Director

Raymond G. Kvaternik

Samir R. Ibrahim

Jen K. Huang

ABSTRACT

COMPONENT MODE SYNTHESIS-BASED DESIGN METHODOLOGY FOR STRUCTURAL MODIFICATION AND SYNTHESIS

Venkateshwarlu Maroju
Old Dominion University, 1995
Director: Dr. Gene Hou

In this work, structural modification and synthesis techniques based on component mode synthesis are presented. The component mode synthesis method formulates the eigenvalue equation of an entire structure in terms of the vibration characteristics of individual components in the assembly. Through this functional relationship, the individual components are successfully treated as the design entities in the proposed methodology. Unlike conventional design modification techniques that can only treat the properties of the finite elements as the design variables, this technique uses the vibration and static responses of the individual components as the design entities. The sensitivity derivatives of the global responses with respect to the responses of the components are calculated to determine the contribution of each component to the vibration of the global structure.

The structural synthesis is formulated as an integer programming problem that treats the various choices of the components as the design variables; this problem is then solved with a genetic algorithm. After the required responses of the individual components have been obtained, the component mode synthesis method provides an efficient means of repetitively analyzing the global structure for the possible combinations of the assembled structure.

A structural modification technique called local vibration targeting is developed for the efficient modification of the structures. This method finds the most significant components in an assembly and determines the optimal values for their vibration and static responses to obtain the desired change in the performance of the global structure. These particular components are modified locally to achieve the target values. In this study, a linear programming technique is used to determine the target values for the individual components; gradient-based optimization techniques are used for the local design modification. Finally, a two-stage iterative design optimization scheme is developed to handle the local vibration targeting more rigorously. The developed methodologies are successfully demonstrated with two sample problems, and the numerical issues involved in the implementation are discussed.

ACKNOWLEDGMENT

To Dr. Gene Hou, my committee chairman, I would like to extend my deepest appreciation and gratitude for giving me the opportunity to work with him and for supporting me both academically and financially. I am thankful for the encouragement and motivation he has provided throughout my association with him.

I am grateful to Drs. Ibrahim, Kvaternik, and Huang for their valuable suggestions and support in serving on my dissertation committee. I am grateful to the National Science Foundation for their partial financial support of this work. I would like to thank Dr. R. J. Yang of the Ford Motor Company for many stimulating discussions that originated this work. Thanks are due to Ms. Diane Riddick of the Mechanical Engineering Department at ODU for her assistance in typing and to Ms. Jonay Campbell of NASA Langley Research Center for her assistance in proofreading this manuscript.

I thank my friend Vittal for his constant encouragement and help throughout my long association with him; without his understanding and patience, this work would not have been possible. In addition, I thank Satish for his timely help in completing this dissertation. Finally, I am deeply grateful to my parents and family, who have been a constant source of encouragement and inspiration in my studies.

TABLE OF CONTENTS

LIST OF FIGURES

LIST OF TABLES

LIST OF SYMBOLS

$\mathbf{K}$	Stiffness matrix of global structure
$\mathbf{M}$	Mass matrix of global structure
$\bar{\mathbf{K}}, \mathbf{K}^*$	Generalized stiffness matrices
$\bar{\mathbf{M}}, \mathbf{M}^*$	Generalized mass matrices
$\mathbf{K}^i$	Stiffness matrix of component i
$\mathbf{M}^i$	Mass matrix of component i
$\mathbf{G}$	Flexibility matrix
$\mathbf{A}$	Eigenvector expansion matrix
$\mathbf{B}$, $\mathbf{C}$	Compatibility matrices
λ^g	Eigenvalue of the global structure
$\mathbf{p}$	Reduced eigenvector of the global structure
$\mathbf{x}$	Eigenvector of the global structure
$\mathbf{a}$	Modal coefficients
$\mathbf{a_e}^i$	Modal coefficients that correspond to the eigenmodes of component i
$\mathbf{a_s}^i$	Modal coefficients that correspond to the static modes of component i
$\mathbf{f}^i$	Constraint forces along the interfaces of component i
u_g	Responses of global structure
u_i	Intermediate variables of components
$\mathbf{\Lambda}^i$	Diagonal matrix of eigenvalues of component i
λ^i	Eigenvalue of component i
ϕ^i	Eigenmode of component i

ψ^i	Static mode of component *i*
Φ^i	Eigenmode matrix of component *i*
Φ^i_k	Kept eigenmode of component *i*
Φ^i_r	Residual eigenmode of component *i*
Φ^i_o	Rigid-body modes of component *i*
Ψ^i_a	Attachment modes of component *i*
Ψ^i_c	Constraint modes of component *i*
Ψ^i_{ra}	Residual attachment modes of component *i*
Φ^i_s	Boundary degrees of freedom of eigenmodes of component *i*
Ψ^i_s	Boundary degrees of freedom of attachment modes of component *i*
$\Psi^i_{s_{ra}}, K^i_s$	Boundary degrees of freedom of residual attachment modes of component *i*
R_r	Reaction forces at the rigid-body degrees of freedom
n_s	Number of interface degrees of freedom
n_r	Number of rigid-body degrees of freedom
n_s	(n_s - n_r) number of interface degrees of freedom
Ψ_I	Static displacement obtained by applying unit forces
Ψ_{Is}	Interface degrees of freedom of Ψ_I

Chapter 1

INTRODUCTION

1.1 Motivation

Most complex structures are usually manufactured as assemblies of components which in turn are made up of smaller components. In practice, each component in the global structure may be designed, analyzed, and fabricated separately from other components. Obviously, the performance of the global structure is closely related to the characteristics of each individual component. Therefore, to accurately analyze the performance of the global structure requires detailed information about each individual component, which may not be available at earlier design stages. This lack of information early in the process creates a dilemma for design engineers who must know the design criteria of the component so that the specific component can be designed separately from the rest of the structure; however, the design criteria of the component cannot be specified quantitatively unless the performance of the assembled structure can be analyzed accurately. Furthermore, such an analysis cannot be done without detailed information on the components. Usually, design criteria are obtained based on similar design experience and are modified continuously on a trial-and-error procedure until the performance required of the global structure is met.

Recently, many computer-aided design (CAD) and analysis tools have been developed to alleviate problems in structural design. However, none of the tools currently available address the above dilemma. Existing tools directly relate the design of the global structure to the very detailed design variables of the components, such as the thickness of individual elements or groups of elements. In general, a realistic structure is discretized into a large

number of finite elements; hence, it becomes highly detailed. This detail may be necessary from an analysis point of view for obtaining accurate responses, but not from a design point of view. On the other hand, a large number of design variables will result from a large number of finite elements, which makes the design modification procedure not only cumbersome but also computationally expensive. Furthermore, each of the components may be fabricated by a different manufacturing process. Hence, any design modification considered should be confined to only selected components, so that a minimal change occurs in the existing manufacturing process. However, available CAD and analysis tools cannot easily accommodate the design and manufacturing considerations mentioned above because these techniques can only treat the properties of finite elements as design variables and are unable to consider a single component as a design entity.

In conclusion, although the existing CAD tools can be effectively used for the detailed design of the structures on the component level, these tools fail to address the following questions in regard to the design modification of large structures:

1. Which component must be modified in order to achieve the required global performance?
2. How can the design criteria be determined for local component design?
3. How can a new structure be synthesized from a group of given components?

To answer the above questions, the contribution of the individual components to the global performance of the structure must be known. To this end, the component mode synthesis technique based on the residual-attachment-mode set can be used for vibration analysis of the global structure, in which the eigenvalues and components of the eigenvectors and static deflection can be used to characterize the dynamic behavior of the components. This process produces a reduced-order eigenvalue equation that directly relates the global structural responses to the component responses in mathematical terms. In other words, the component mode synthesis method provides a rigorous mathematical formulation that includes independent variables that represent the structural components. With the help of the component mode synthesis, the effects on the performance of

the assembled structure can be studied by modifying and even replacing its structural components. Based on this mathematical foundation, computational methodologies can be developed for vibration modification and structural synthesis in which the structural components, rather than the detailed design variables, can be treated as design entities.

Component mode synthesis can be viewed as a two-stage analysis method. In the first stage, each component is analyzed independently to obtain the required component responses; in the second stage, these responses are assembled into a reduced eigenproblem that is solved to obtain the eigenvalues and eigenvectors of the complete structure. The conventional design modification problem can be reformulated to take advantage of the analysis procedure of the component mode synthesis in such a way that it allows the individual components to be treated as the design entities. This reformulation can be primarily done by dividing the problem into two independent design optimization problems. The first problem, called "upper-level design optimization," can be formulated by treating the individual component responses as the design variables and by treating the reduced-eigenvalue problem (that relates the component responses to the global responses) as the state equation. The optimal solution of this problem yields the required responses that must be exhibited by the individual components so that the desired criteria for the global structure will be met. These optimal values are simply the required design criteria for the individual components. Then, the individual components can be designed and manufactured independently to meet the specified design criteria. The second problem involves the solution of a conventional design modification problem for each component of concern, in which the sizing variables of the finite elements, such as thickness and cross-sectional areas, can be treated as design variables; this procedure is called a "lower-level design optimization." To solve these optimization problems, linear programming algorithms can be used at the upper-level to determine the required perturbations in the component responses; at the lower-level, gradient-based algorithms can be used.

From the optimization point of view, the above procedure is simply a multilevel decomposition of the optimization problem into smaller and more tractable subproblems. However, the success of the above procedure lies in the efficiency of the lower-level optimization in achieving the target values for the component responses. To this end, a more rigorous iterative multilevel optimization scheme has been developed. In this scheme, the upper-level design optimization problem is also solved with a gradient-based algorithm, and the above-described process will be iterated between the upper- and lower-levels until convergence is reached between the target values and the actual component responses.

In many engineering applications, the proper selection of the components needed to assemble a useful structure is more important than modifying the detailed dimensions of the members in the components. To address such cases, a structural synthesis tool has been developed in conjunction with the genetic algorithm for selecting the optimal set of cross members and their locations from a group of available stiffeners. This tool uses component mode synthesis as a reanalysis technique for the efficient evaluation of the global structural performance after the individual components have been analyzed; then, only a small reduced-eigenvalue problem must be solved repeatedly to obtain the eigenvalues and eigenvectors of the assembled structure for each new design.

1.2 Objective and Scope of the Study

The primary focus of this study is to develop a preliminary design tool that provides an efficient method for defining "consistent" design criteria for designing or modifying the individual components of a structure. Specifically, this design tool can assist engineers in performing

1) Structural modifications to the global structure (i.e., local vibration targeting). In this case, an improvement in the performance of an existing structure is sought by modifying a few significant components in the structure.

2) Structural synthesis to create a global structure by assembling a set of given components. In this case, no structure exists yet.

The above tasks were accomplished with component mode synthesis, which essentially enables the individual component to be treated as a design entity and uses the structural responses of the individual component as the representative variables. This concept enables performance of the sensitivity analysis of the global responses with respect to the responses of the individual components, which in turn enables an understanding of the contribution of the individual components to the global structural responses. Along the lines of the component mode synthesis procedure, a multilevel optimization scheme has been developed for local structural modification. Finally, by combining this analysis procedure with a genetic algorithm, a practical structural synthesis tool has been developed.

The literature related to this study is reviewed in the next section. Chapter 2 describes the formulation of component mode synthesis based on the residual-attachment-mode set and the reduced-eigenvalue problem that results. This chapter also explains how this method can be generalized for rigid bodies, as well as for multilevel analysis. Chapter 3 shows how an individual component can be characterized as a design entity using its component responses. Various sensitivity derivatives of the global eigenvalues and eigenvectors with respect to the individual component responses are calculated. Chapter 4 describes the general methodology for structural synthesis with a genetic algorithm. The genetic representation and the computational procedure are explained in detail with a sample problem. In chapter 5, the method of local vibration targeting for structural modification is discussed. This chapter, explains how the conventional structural modification problem has been reformulated so that an individual component can be treated as a design entity. Chapter 6 discusses a multilevel design optimization scheme that deals more rigorously with the problem of local vibration targeting. Concluding remarks and recommendations for future work are presented in Chapter 7.

1.3 Literature Review

Hurty [1]* presented the first paper on component mode synthesis. Since then, many researchers have developed numerous methods for vibration analysis of large structures by using various eigenmodes and static modes of the individual components. These methods differ from one another, depending on the type of component modes used in the eigenvector approximation and the type of coupling used to combine the components. Through the years, the component mode synthesis technique has become very well established. Several review papers are available in the literature [2–7]. The next chapter discusses the formulation of component mode synthesis in detail; the literature related to structural modification methods that incorporate substructuring techniques, which is of specific interest to the current research, is reviewed here.

Kirsch et al. [8–9] were the first researchers to perform an optimization of a structure by partitioning it into a number of substructures. They performed successive optimizations on substructures by considering only some of the design variables and the constraints that pertain to a particular substructure. They repeated this procedure iteratively until no additional improvement was noted in the objective function. In the optimization of each substructure, they used the approximate reanalysis of a reduced structure. The basis for such an approximate analysis and the reduction of the constraints in the optimization of the substructure was the assumption that the behavior of the structure was not sensitive to the distribution of the stiffness.

Arora and Govil [10] developed an algorithm for calculating the static-displacement sensitivity derivatives and incorporated the substructuring technique into their formulation. The sensitivity calculations were performed with the same concept of static condensation employed in the substructure analysis technique. With these sensitivity derivatives, they developed an integrated design optimization methodology based on the Kuhn-Tucker necessary conditions for the nonlinear programming problem.

*The numbers in brackets indicate references.

Okuma et al. [11] used the component mode synthesis method in conjunction with the mathematical pseudo-inverse method for structural dynamic modification. They used only component mode synthesis to obtain the eigenvalues and eigenvectors so that the reanalysis of the structural responses during the iterative design procedure did not require the analysis of the unmodified components in the structure. However, the sensitivity derivatives were calculated with the full system of matrices of the assembled structure, and the required changes in the design variables were obtained, based upon the first-order Taylor-series approximation of the natural frequency at the current design.

Heo and Ehmann [12] incorporated the component mode synthesis technique for calculating the sensitivity derivatives of the eigensolutions of the assembled structure. They established the sensitivity equations with respect to design variables that pertained to a particular modifiable substructure; this was accomplished as a chain rule of differentiation with the derivatives of the component modes of the modifiable substructure and the component mode synthesis procedure. Fixed-interface eigenmodes and the constraint modes of the substructures were used to obtain the reduced-eigenvalue problem.

In an effort to make the optimum design of large and complex structures feasible and tractable, many researchers have explored and successfully applied multilevel design optimization schemes [9, 13–22]. Although these methods have been applied to structural problems for the past 20 years, research continues in this area; a large number of papers have been published in the past couple of years. A brief review of some of this research is given in the following.

Kirsch [9] decomposed the optimization problem into a number of smaller problems. These smaller optimization problems were solved independently with their own objective functions and constraints at one level; on the other level, the independent subproblems were coordinated to converge to a single solution. The optimum solutions of the subproblems together produced an optimum overall system. For both levels, mathematical programming techniques were employed to solve the optimization problems.

Schmit and Ramanathan [13] applied the multilevel optimization approach to the optimum design of truss and wing structures. The overall structural optimization was performed for strength, displacement, and global buckling constraints. Then at the component level, the detailed design was carried out for the local buckling constraints. The system-level objective function was the total weight of the structure; the change in the stiffness was the objective function at the component level.

Sobieski et al. [14] presented a multilevel optimization procedure in which the optimization problem was decomposed into a number of subproblems; the coupling between these subproblems was coordinated by another optimization problem at the system level. The subproblems were simply optimizations of the individual components in a structure. At the component level the element cross-sectional areas and at the system level the quantities that affect the mass and stiffness distribution were considered as design variables. Because this entire process is iterative between the subproblems and the system-level optimization, the component optimum solutions were extrapolated linearly by using the optimum sensitivity derivatives with respect to the system-level design variables.

Haftka [15] dealt with discontinuous derivatives of the lower-level optimum in a multilevel optimization problem. He developed an algorithm that employs the penalty function method in conjunction with Newton's method and uses the approximate second derivatives to avoid the problem of nondifferentiability of the lower-level optimum. This algorithm was computationally more efficient in comparison with the conventional single-level optimization. Barthelemy [16] explored methods for improving the computational efficiency of the multilevel optimization. He successfully reduced the cost of optimization by employing a sequence of convex approximations in place of the initial design problem and performing the reoptimization of only those subproblems that violated the constraints. However, these savings in the computational cost were limited to problems that involved only a small number of design variables.

The above multilevel optimization schemes have been developed primarily to address the problem of structural design for static responses. Thus far, no multilevel optimization schemes have been applied to the dynamic modification of structures, although implementation of one of these schemes into a component mode synthesis procedure is certainly feasible. On the other hand, in regard to the use of substructuring the above studies simply apply substructuring as an efficient analysis tool to support the design optimization process. Hence, the motivation in the above studies for applying substructuring techniques and multilevel optimization schemes to structural optimization problems was to improve the tractability and computational efficiency of the conventional design optimization problem. Nevertheless, the determination and examination of individual-component contributions to the global responses are not addressed in the literature, although this concept has great potential in making the component design more independent and efficient in an industrial design environment. To this end, in the proposed approach the design modification formulation has been modified to accommodate the solution procedure of component mode synthesis. This arrangement not only allows a complex problem to be divided into several smaller and more tractable subproblems for design and analysis but enables the individual components to be treated as design entities.

Chapter 2

COMPONENT MODE SYNTHESIS

2.1 Introduction

The method of component mode synthesis plays a crucial role in the proposed study. It is primarily employed to describe the contribution of the vibration characteristics of local structural components to that of the global structure. Component mode synthesis is a substructuring technique commonly used for the dynamic analysis of large structures [1–7, 23–28]. In this method, the vibration characteristics of each component are represented as a summation of its modal contributions. By enforcing the compatibility conditions along the interfaces between structural components, a reduced-order eigenvalue equation is obtained that can be solved efficiently for the first few eigenmodes of the assembled structure. To provide a foundation for the work in the following chapters, this chapter outlines the basic procedure for component mode synthesis.

To facilitate the discussion, consider a structure divided into two components α and β at a common interface S, as shown in Fig. 2.1. For simplicity, none of the components is assumed to have any rigid-body motion.

The eigenvalue equation of the complete structure, shown in Fig. 2.1(a), is given as

$$\mathbf{K}\mathbf{x} = \lambda^g \mathbf{M}\mathbf{x} \tag{2.1}$$

where $\mathbf{K}$ and $\mathbf{M}$ are the stiffness and mass matrices of the global structure. The preceding equation can be rewritten to account for the contribution of each component to the global structure as

$$\begin{bmatrix} \mathbf{K}^\alpha & 0 \\ 0 & \mathbf{K}^\beta \end{bmatrix} \begin{Bmatrix} \mathbf{x}^\alpha \\ \mathbf{x}^\beta \end{Bmatrix} = \lambda \begin{bmatrix} \mathbf{M}^\alpha & 0 \\ 0 & \mathbf{M}^\beta \end{bmatrix} \begin{Bmatrix} \mathbf{x}^\alpha \\ \mathbf{x}^\beta \end{Bmatrix} + \begin{Bmatrix} \mathbf{f}^\alpha \\ \mathbf{f}^\beta \end{Bmatrix} \tag{2.2}$$

where $\mathbf{K}^{\alpha}$ and $\mathbf{M}^{\alpha}$ are the stiffness and mass matrices and $\mathbf{x}^{\alpha}$ is the displacement vector of component α with dimensions $n^{\alpha}xn^{\alpha}$, $n^{\alpha}xn^{\alpha}$, and $n^{\alpha}x1$, respectively. Similarly, $\mathbf{K}^{\beta}$, $\mathbf{M}^{\beta}$, and $\mathbf{x}^{\beta}$ can be defined accordingly. The vectors $\mathbf{f}^{\alpha}$ and $\mathbf{f}^{\beta}$ represent the constraint forces to preserve the compatibility conditions between the components; that is

$$\mathbf{x}_s^{\alpha} = \mathbf{x}_s^{\beta} \tag{2.3}$$

where the subscript s indicates the degrees of freedom along the interface boundary. As a result, the solution of Eq. (2.2) will be the same as that of Eq. (2.1); that is, $\lambda^g = \lambda$ and $\mathbf{X} = \mathbf{X}^{\alpha} \cup \mathbf{X}^{\beta}$. To solve Eqs. (2.2) and (2.3) simultaneously, the solution vectors $\mathbf{x}^{\alpha}$ and $\mathbf{x}^{\beta}$ are expanded with the basis vectors associated with the corresponding components and an alternate reduced eigenvalue equation (instead of Eqs. (2.2) and (2.3)) is solved in terms of the modal coefficients that pertain to the basis vectors. The basis vectors can be a combination of several types of eigenmodes of free vibration $\mathbf{\Phi}$ and static modes $\mathbf{\Psi}$ of the undamped components.

2.2 Component Modes

The vector $\mathbf{x}$ can be written as a linear combination of component modes as

$$\mathbf{x} = \mathbf{A}\,\mathbf{a} \tag{2.4}$$

where the eigenvector expansion matrix $\mathbf{A}$ contains the preselected component modes and the vector $\mathbf{a}$ is simply the modal coefficient of the components [1, 2]. Although several types of component modes can be used for the modal expansion in Eq. (2.4), they can be primarily classified into two types: the eigenmodes of free vibration and the static modes.

2.2.1 Eigenmodes

Eigenmodes of free vibration can be of two types, depending on whether the interface degrees of freedom are kept fixed or free (i.e., fixed-interface modes and free-interface modes). Eigenmodes of a component are obtained by solving the following eigenvalue problem:

$$\mathbf{K}^i\mathbf{\Phi}^i = \lambda^i\mathbf{M}^i\mathbf{\Phi}^i \tag{2.5}$$

where the superscript i indicates that the quantity is associated with component i. For notational convenience, the superscript i is dropped from the equation. By partitioning the above equation into interior and boundary degrees of freedom, it can be rewritten as

$$\begin{bmatrix} \mathbf{K}_{ii} & \mathbf{K}_{is} \\ \mathbf{K}_{si} & \mathbf{K}_{ss} \end{bmatrix} \begin{Bmatrix} \mathbf{\Phi}_i \\ \mathbf{\Phi}_s \end{Bmatrix} = \lambda \begin{bmatrix} \mathbf{M}_{ii} & \mathbf{M}_{is} \\ \mathbf{M}_{si} & \mathbf{M}_{ss} \end{bmatrix} \begin{Bmatrix} \mathbf{\Phi}_i \\ \mathbf{\Phi}_s \end{Bmatrix} \tag{2.6}$$

where the subscript i represents the interior degrees of freedom and the subscript s represents the degrees of freedom at the boundary. For free-interface modes, Eq. (2.6) is solved and the mode $\mathbf{\Phi}$ has the following form:

$$\mathbf{\Phi} = \begin{Bmatrix} \mathbf{\Phi}_i \\ \mathbf{\Phi}_s \end{Bmatrix} \tag{2.7}$$

Fixed-interface modes are obtained by solving Eq. (2.6) after setting the displacements at the interface degrees of freedom (i.e., $\mathbf{\Phi}_s$ terms) to zero. This step leads to the eigenvalue problem

$$\mathbf{K}_{ii}\mathbf{\Phi}_i = \lambda\mathbf{M}_{ii}\mathbf{\Phi}_i \tag{2.8}$$

which is solved for λ and $\mathbf{\Phi}_i$. Then, the complete mode has the form

$$\mathbf{\Phi} = \begin{Bmatrix} \mathbf{\Phi}_i \\ 0 \end{Bmatrix} \tag{2.9}$$

2.2.2 Static Modes

Static modes can be of two types: constraint modes and attachment modes. A constraint mode is defined as the static displacement obtained from an imposed unit displacement on one of the boundary degrees of the freedom and zero displacement on the rest of the degrees of freedom at the boundary. Several authors in the past have employed the constraint modes to supplement the eigenmodes [4, 5, 25]. For a typical structure, the stiffness matrix can be partitioned according to the interior and boundary degrees of freedom. By imposing the unit displacement once at each degree of freedom at the boundary, the equation for static displacement can be written as

$$\begin{bmatrix} \mathbf{K}_{ii} & \mathbf{K}_{is} \\ \mathbf{K}_{si} & \mathbf{K}_{ss} \end{bmatrix} \begin{bmatrix} \mathbf{u}_{is} \\ \mathbf{I}_{ss} \end{bmatrix} = \begin{bmatrix} 0 \\ \mathbf{R}_{ss} \end{bmatrix} \tag{2.10}$$

where $\mathbf{I}_{ss}$ and $\mathbf{R}_{ss}$ are the identity and reaction-force matrices, respectively, with dimensions $n_s \times n_s$. By solving the above equations, one can obtain n_s constraint modes Ψ_c as follows:

$$\Psi_c = \begin{bmatrix} \mathbf{u}_{is} \\ \mathbf{I}_{ss} \end{bmatrix} = \begin{bmatrix} -\mathbf{K}_{ii}^{-1}\mathbf{K}_{ss} \\ \mathbf{I}_{ss} \end{bmatrix} \tag{2.11}$$

An attachment mode is defined as the static displacement obtained by applying a unit force at a boundary degree of freedom. Thus, one can obtain n_s attachment modes Ψ_a by solving the following static equation:

$$[\mathbf{K}][\Psi_a] = \begin{bmatrix} 0 \\ \mathbf{I}_s \end{bmatrix} \tag{2.12}$$

or

$$[\Psi_a] = [\mathbf{G}] \begin{bmatrix} 0 \\ \mathbf{I}_s \end{bmatrix} \tag{2.13}$$

where **G** is the elastic flexibility matrix, which is simply the inverse of the stiffness matrix **K**. Attachment modes were used to supplement the eigenmodes by several researchers in the literature [4, 6–7, 23–25].

To obtain the attachment modes, the stiffness matrix **K** must be nonsingular. However, for an unconstrained component, the stiffness matrix is singular. To accommodate this situation, a procedure has been developed to deal with unconstrained components with rigid-body motion. This procedure is explained in detail in section 2.6; until then our discussion will assume that none of the components has rigid-body motion.

2.3 Eigenvector Approximation

This section outlines the procedure for eigenvector approximation with the component modes and shows how it will reduce the system model to a simpler and smaller eigenvalue problem. To facilitate the discussion, we use the example given in Fig. 2.1. For simplicity, let the component modes selected for the approximation include only a subset of the free-interface eigenmodes of free vibration Φ and the attachment modes Ψ of the undamped components.

The eigenvector of the α component $\mathbf{x}^\alpha$ can then be written as a linear combination of Φ^α and Ψ^α as

$$\begin{aligned}\mathbf{x}^\alpha &= \sum_{i=1}^{m^\alpha} \mathbf{a}_i^\alpha \Phi_i^\alpha + \sum_{i=m^\alpha+1}^{m^\alpha+n_s^\alpha} \mathbf{a}_i^\alpha \Psi_{i-m^\alpha}^\alpha \\ &= [\,\Phi^\alpha \quad \Psi^\alpha\,] \begin{Bmatrix} \mathbf{a}_e^\alpha \\ \mathbf{a}_s^\alpha \end{Bmatrix}\end{aligned} \tag{2.14}$$

where the modal coefficients $\mathbf{a}_e^\alpha$ and $\mathbf{a}_s^\alpha$ are m^αx1 and $n^\alpha{}_s$x1 vectors that correspond to the eigenmodes and static modes, respectively; m^α is the number of eigenmodes, and n_s^α is the number of static modes, which is generally equal to the number of interface degrees of freedom (although this is not a necessity). Similarly, the eigenvector approximation for the component β can be written as

$$\mathbf{x}^\beta = [\,\Phi^\beta \quad \Psi^\beta\,] \begin{Bmatrix} \mathbf{a}_e^\beta \\ \mathbf{a}_s^\beta \end{Bmatrix} \tag{2.15}$$

With the aid of Eqs. (2.14) and (2.15), the eigenvalue equation (2.2) can be reformulated in terms of modal coefficients as

$$\bar{\mathbf{K}}\mathbf{a} = \lambda \bar{\mathbf{M}}\mathbf{a} + \mathbf{f} \tag{2.16}$$

where

$$\bar{\mathbf{K}} = \begin{bmatrix} \boldsymbol{\Phi}^{\alpha^T} & 0 \\ \boldsymbol{\Psi}^{\alpha^T} & 0 \\ 0 & \boldsymbol{\Phi}^{\beta^T} \\ 0 & \boldsymbol{\Psi}^{\beta^T} \end{bmatrix} \begin{bmatrix} \mathbf{K}^{\alpha} & 0 \\ 0 & \mathbf{K}^{\beta} \end{bmatrix} \begin{bmatrix} \boldsymbol{\Phi}^{\alpha} & \boldsymbol{\Psi}^{\alpha} & 0 & 0 \\ 0 & 0 & \boldsymbol{\Phi}^{\beta} & \boldsymbol{\Psi}^{\beta} \end{bmatrix}$$
$$= \begin{bmatrix} \boldsymbol{\Lambda}^{\alpha} & \boldsymbol{\Phi}_s^{\alpha^T} & 0 & 0 \\ \boldsymbol{\Phi}_s^{\alpha} & \mathrm{K}_s^{\alpha} & 0 & 0 \\ 0 & 0 & \boldsymbol{\Lambda}^{\beta} & \boldsymbol{\Phi}_s^{\beta^T} \\ 0 & 0 & \boldsymbol{\Phi}_s^{\beta} & \mathrm{K}_s^{\beta} \end{bmatrix} \tag{2.17}$$

The matrix $\bar{\mathbf{K}}$ is symmetric; $\boldsymbol{\Phi}_s^{\alpha}$ and K_s^{α}, with the respective dimensions of $m^{\alpha} \times n_s^{\alpha}$ and $n_s^{\alpha} \times n_s^{\alpha}$, are obtained as follows with the definition of the attachment modes from Eq. (2.12):

$$\boldsymbol{\Phi}^{\alpha^T} \mathbf{K}^{\alpha} \boldsymbol{\Psi}^{\alpha} = \begin{bmatrix} \boldsymbol{\Phi}_i^{\alpha} \\ \boldsymbol{\Phi}_s^{\alpha} \end{bmatrix}^T \begin{bmatrix} 0 \\ \mathbf{I}_{ss} \end{bmatrix} = \boldsymbol{\Phi}_s^{\alpha^T} \tag{2.18}$$

and

$$\boldsymbol{\Psi}^{\alpha^T} \mathbf{K}^{\alpha} \boldsymbol{\Psi}^{\alpha} = \begin{bmatrix} \boldsymbol{\Psi}_i^{\alpha} \\ \boldsymbol{\Psi}_s^{\alpha} \end{bmatrix}^T \begin{bmatrix} 0 \\ \mathrm{I}_{ss} \end{bmatrix} = \boldsymbol{\Psi}_s^{\alpha^T} \tag{2.19}$$

where $\boldsymbol{\Psi}_s^{\alpha^T}$ (defined as K_s^{α} in Eq. (2.17)) is the boundary partition of the attachment modes; that is, $\boldsymbol{\Psi}_s^{\alpha^T}$ is the same as the boundary partition of the flexibility matrix **G**, and $\boldsymbol{\Phi}_s^{\alpha}$ is the boundary partition of the eigenmodes.

The matrix $\bar{\mathbf{M}}$ in Eq. (2.16) is given as

$$\bar{\mathbf{M}} = \begin{bmatrix} \boldsymbol{\Phi}^{\alpha^T} & 0 \\ \boldsymbol{\Psi}^{\alpha^T} & 0 \\ 0 & \boldsymbol{\Phi}^{\beta^T} \\ 0 & \boldsymbol{\Psi}^{\beta^T} \end{bmatrix} \begin{bmatrix} \mathbf{M}^{\alpha} & 0 \\ 0 & \mathbf{M}^{\beta} \end{bmatrix} \begin{bmatrix} \boldsymbol{\Phi}^{\alpha} & \boldsymbol{\Psi}^{\alpha} & 0 & 0 \\ 0 & 0 & \boldsymbol{\Phi}^{\beta} & \boldsymbol{\Psi}^{\beta} \end{bmatrix}$$
$$= \begin{bmatrix} \mathbf{I}^{\alpha} & \boldsymbol{\Lambda}^{\alpha^{-1}} \boldsymbol{\Phi}_s^{\alpha} & 0 & 0 \\ \boldsymbol{\Phi}_s^{\alpha^T} \boldsymbol{\Lambda}^{\alpha^{-1}} & \mathbf{M}_s^{\alpha} & 0 & 0 \\ 0 & 0 & \mathbf{I}^{\beta} & \boldsymbol{\Lambda}^{\beta^{-1}} \boldsymbol{\Phi}_s^{\beta} \\ 0 & 0 & \boldsymbol{\Phi}_s^{\beta^T} \boldsymbol{\Lambda}^{\beta^{-1}} & \mathbf{M}_s^{\beta} \end{bmatrix} \tag{2.20}$$

where $\mathbf{I}^{\alpha}$ and $\mathbf{I}^{\beta}$ are the identity matrices with the dimensions $m^{\alpha} \times m^{\alpha}$ and $m^{\beta} \times m^{\beta}$. In regard to the other terms in $\bar{\mathbf{M}}$, note the following:

$$\boldsymbol{\Phi}^{\alpha^T} \mathbf{M}^{\alpha} \boldsymbol{\Psi}^{\alpha} = \boldsymbol{\Lambda}^{\alpha^{-1}} \boldsymbol{\Phi}^{\alpha^T} \mathbf{K}^{\alpha} \boldsymbol{\Psi}^{\alpha} = \boldsymbol{\Lambda}^{\alpha^{-1}} \boldsymbol{\Phi}_s^{\alpha^T} \tag{2.21}$$

and

$$\mathbf{M}_s^{\alpha} = \boldsymbol{\Psi}^{\alpha^T} \mathbf{M}^{\alpha} \boldsymbol{\Psi}^{\alpha} \tag{2.22}$$

The rest of the terms in $\bar{\mathbf{K}}$ and $\bar{\mathbf{M}}$ have similar definitions for the β structure. Note that the constituent terms of the generalized stiffness matrix $\bar{\mathbf{K}}$ and the mass matrix $\bar{\mathbf{M}}$ of the reduced-order eigenvalue problem in Eq. (2.16) depend on the type of the basis vectors selected for the eigenvector approximation [2].

2.4 Residual-Attachment-Mode Set

The attachment modes Ψ_a may be linearly dependent on the free-interface eigenmodes if Φ includes either all or a large fraction of the component eigenmodes. In this case, the contribution of the eigenmodes must be removed from the attachment modes in order to ensure a set of linearly independent basis vectors [2, 7]. The modified attachment modes obtained by this process are called residual attachment modes. This step is accomplished by defining the residual flexibility matrix $\mathbf{G}_r$. The elastic flexibility matrix, $\mathbf{G}$, which is the pseudo inverse of the stiffness matrix $\mathbf{K}$, can be written as a combination of the contribution from all elastic modes Φ as follows:

$$\mathbf{G} = \Phi \Lambda^{-1} \Phi^T \tag{2.23}$$

If a truncated set of eigenmodes is used to represent the component, then the elastic flexibility matrix be written as the sum of the contribution from the kept modes and the mode residual modes as flexit

$$\begin{aligned} \mathbf{G} &= \mathbf{G}_k + \mathbf{G}_r \\ &= \Phi_k \Lambda_k^{-1} \Phi_k^T + \Phi_r \Lambda_r^{-1} \Phi_r^T \end{aligned} \tag{2.24}$$

residu

where $\mathbf{G}_r = \Phi_r \Lambda_r^{-1} \Phi_r^T$ is called the residual flexibility matrix and represents the flexi-

$= \Psi_k \Lambda_k^{-1} \Psi_k + \Psi_r \Lambda_r^{-1} \Psi_r^T$

where $\mathbf{G}_r = \Phi_r \Lambda_r^{-1} \Phi_r^T$ is called the residual flexibility matrix and represents the flexibility of the structure that is not reflected in the kept modes. Now, one can define the contribution of the kept eigenmodes to the attachment modes as

$$\Psi_{ka} = [\mathbf{G}_k] \begin{bmatrix} 0 \\ \mathbf{I}_{ss} \end{bmatrix} \tag{2.25}$$

With the definition of $\mathbf{G}_k$, the above expression can be simplified as:

$$\begin{aligned}\boldsymbol{\Psi}_{ka} &= \boldsymbol{\Phi}_k \boldsymbol{\Lambda}_k^{-1} \boldsymbol{\Phi}_k^T \begin{bmatrix} 0 \\ \mathbf{I}_{ss} \end{bmatrix} \\ &= \boldsymbol{\Phi}_k \boldsymbol{\Lambda}_k^{-1} \boldsymbol{\Phi}_{sk}^T\end{aligned} \tag{2.26}$$

where $\boldsymbol{\Phi}_{sk}$ represents the boundary partition of the eigenmodes. Then, the residual attachment mode $\boldsymbol{\Psi}_{ra}$ can be obtained by simply subtracting the contribution of the kept eigenmodes from the attachment modes as

$$\boldsymbol{\Psi}_{ra} = \boldsymbol{\Psi}_a - \boldsymbol{\Phi}_k \boldsymbol{\Lambda}_k^{-1} \boldsymbol{\Phi}_{sk}^T \tag{2.27}$$

Alternatively, the residual attachment mode $\boldsymbol{\Psi}_{ra}$ can also be written as a summation of the contributions from the residual modes $\boldsymbol{\Phi}_r$ as

$$\boldsymbol{\Psi}_{ra} = \boldsymbol{\Phi}_r \boldsymbol{\Lambda}_r^{-1} \boldsymbol{\Phi}_{sr}^T \tag{2.28}$$

However, the definition for $\boldsymbol{\Psi}_{ra}$ given in Eq. (2.27) is more appropriate because it expresses the residual attachment modes in terms of the kept eigenmodes and the attachment modes of the component. In Eq. (2.28), it is expressed in terms of the residual modes; hence, all higher frequency modes of the component must be known.

In this study, these residual attachment modes will be employed to supplement the free-interface modes of the components for the eigenvector expansion because this particular combination of component modes, in addition to ensuring a linearly independent set of basis vectors, reduces the constituent terms of $\bar{\mathbf{K}}$ and $\bar{\mathbf{M}}$ in Eq. (2.17) and Eq. (2.20) to a considerably simpler form such that they can be easily obtained by component testing [23–24, 27]. This particular combination of component modes is called the dynamic residual attachment-mode set [2, 3]. Because the residual-attachment modes $\boldsymbol{\Psi}_{ra}^{\alpha}$ and $\boldsymbol{\Psi}_{ra}^{\beta}$ are orthogonal to the kept eigenmodes $\boldsymbol{\Phi}_k^{\alpha}$ and $\boldsymbol{\Phi}_k^{\beta}$, respectively, the cross-diagonal terms in the submatrices that correspond to the α and β components become zero. Hence, Eqs. (2.17) and (2.20) simplify to

$$\bar{\mathbf{K}} = \begin{bmatrix} \boldsymbol{\Lambda}^{\alpha} & 0 & 0 & 0 \\ 0 & \mathbf{K}_s^{\alpha} & 0 & 0 \\ 0 & 0 & \boldsymbol{\Lambda}^{\beta} & 0 \\ 0 & 0 & 0 & \mathbf{K}_s^{\beta} \end{bmatrix} \tag{2.29}$$

and

$$\bar{\mathbf{M}} = \begin{bmatrix} \mathbf{I}^{\alpha} & 0 & 0 & 0 \\ 0 & \mathbf{M}_s^{\alpha} & 0 & 0 \\ 0 & 0 & \mathbf{I}^{\beta} & 0 \\ 0 & 0 & 0 & \mathbf{M}_s^{\beta} \end{bmatrix} \tag{2.30}$$

In the above matrices, only $\mathbf{K}_s^{\alpha}$, $\mathbf{M}_s^{\alpha}$ and $\mathbf{K}_s^{\beta}$, $\mathbf{M}_s^{\beta}$ must be defined. For convenience, the superscripts α and β are discarded. Then from Eq. (2.19),

$$\mathbf{K}_s = \boldsymbol{\Psi}_{ra}^T \mathbf{K} \boldsymbol{\Psi}_{ra}$$

If $\boldsymbol{\Psi}_{ra}$ is substituted from Eq. (2.27) into Eqs. (2.18) and (2.19), then

$$\begin{aligned} \mathbf{K}_s &= \left(\boldsymbol{\Psi}_a - \boldsymbol{\Phi}_k \boldsymbol{\Lambda}_k^{-1} \boldsymbol{\Phi}_{sk}^T\right)^T \mathbf{K} \left(\boldsymbol{\Psi}_a - \boldsymbol{\Phi}_k \boldsymbol{\Lambda}_k^{-1} \boldsymbol{\Phi}_{sk}^T\right) \\ &= \boldsymbol{\Psi}_{ss} - \boldsymbol{\Phi}_{sk} \boldsymbol{\Lambda}_k^{-1} \boldsymbol{\Phi}_{sk}^T \end{aligned} \tag{2.32}$$

where $\boldsymbol{\Psi}_{ss}$ is the boundary partition of the attachment modes (which is simply the partition of the flexibility matrix that corresponds to the boundary degrees of freedom). Similarly, we can simplify $\mathbf{M}_s$ with the definition of $\boldsymbol{\Psi}_{ra}$ given in Eq. (2.28) (instead of Eq. (2.27)) as follows:

$$\begin{aligned} \mathbf{M}_s &= \boldsymbol{\Psi}_{ra}^T \mathbf{M} \boldsymbol{\Psi}_{ra} \\ &= \boldsymbol{\Phi}_{sr} \boldsymbol{\Lambda}_r^{-1} \boldsymbol{\Phi}_r^T \mathbf{M} \boldsymbol{\Phi}_r \boldsymbol{\Lambda}_r^{-1} \boldsymbol{\Phi}_{sr}^T \\ &= \boldsymbol{\Phi}_{sr} \boldsymbol{\Lambda}_r^{-2} \boldsymbol{\Phi}_{sr}^T \end{aligned} \tag{2.33}$$

Obviously (from the above expression), these values are small in comparison with unity because $\boldsymbol{\Lambda}_r$ contains all higher frequency modes that are not used in the synthesis. Hence, $\mathbf{M}_s$ terms can be neglected without incurring a large error in the computation of the eigenvalues and eigenvectors of the global structure [23–26].

2.5 Compatibility Conditions

To assemble the structure, the compatibility conditions between components must be enforced. This is achieved by requiring that the displacements at each degree of freedom along the interface boundaries be continuous [2, 3]. In other words,

$$x_s^{\alpha} = x_s^{\beta} \tag{2.34}$$

which implies a set of n_s equations

$$\Phi_s^{\alpha} a_e^{\alpha} + \Psi_s^{\alpha} a_s^{\alpha} = \Phi_s^{\beta} a_e^{\beta} + \Psi_s^{\beta} a_s^{\beta} \tag{2.35}$$

The above equation can be rewritten in matrix form as

$$\mathbf{C}\,\mathbf{a} = 0 \tag{2.36}$$

where $\mathbf{C}$ is a $n_s \times n$ matrix, in which n is the total number of modes of all components used in the eigenvector expansion.

The preceding equation can help to represent the n_s number of the modal coefficients in terms of the rest of the independent coefficients. This step can be accomplished by partitioning the vector $\mathbf{a}$ into the dependent and independent coefficients $\mathbf{a}_1$ and $\mathbf{a}_2$, respectively. Then, Eq. (2.36) can be rewritten as

$$[\mathbf{C}_1 \quad \mathbf{C}_2]\begin{Bmatrix} \mathbf{a}_1 \\ \mathbf{a}_2 \end{Bmatrix} = 0 \tag{2.37}$$

where $\mathbf{C}_1$ and $\mathbf{C}_2$ are of the dimensions $n_s \times n_s$ and $n_s \times (n - n_s)$, respectively. With the above equation, the dependent coefficients $\mathbf{a}_1$ can be written in terms of the independent coefficients $\mathbf{a}_2$ as

$$\{\mathbf{a}_1\} = -[\mathbf{C}_1^{-1}\mathbf{C}_2]\ \{\mathbf{a}_2\} \tag{2.38}$$

With the above relationship, the vector $\mathbf{a}$ can be written in terms of $\mathbf{a}_2$ alone as

$$\{\mathbf{a}\} = \begin{Bmatrix} \mathbf{a}_1 \\ \mathbf{a}_2 \end{Bmatrix} = \begin{bmatrix} -\mathbf{C}_1^{-1}\mathbf{C}_2 \\ \mathbf{I} \end{bmatrix}\{\mathbf{a}_2\} \tag{2.39}$$

where **I** is the identity matrix with a dimension of $(n - n_s) \times (n - n_s)$. Throughout the remainder of this work, the independent coefficients $\mathbf{a}_2$ are referred to as the vector **p** with a dimension of $(n - n_s) \times 1$. Then, the above equation can be simply written as

$$\mathbf{a} = \mathbf{B}\mathbf{p} \tag{2.40}$$

where **B** is simply the transformation matrix $\begin{bmatrix} -\mathbf{C}_1^{-1}\mathbf{C}_2 \\ \mathbf{I} \end{bmatrix}$ with a dimension of $n \times (n - n_s)$. The compatibility condition in Eq. (2.3) or (2.34) can then be imposed on Eq. (2.16) with the help of Eq. (2.40), which results in the further reduced eigenvalue problem

$$\mathbf{K}^*\mathbf{p} = \lambda\mathbf{M}^*\mathbf{p} \tag{2.41}$$

where $\mathbf{K}^* = \mathbf{B}^T\bar{\mathbf{K}}\mathbf{B}$ and $\mathbf{M}^* = \mathbf{B}^T\bar{\mathbf{M}}\mathbf{B}$. The internal forces **f** in Eq. (2.16) cancel each other out because they must satisfy the force-equilibrium equation $\mathbf{B}^T\mathbf{f} = 0$.

After the eigensolution (λ and **p** in Eq. (2.41)) is found, Eq. (2.40) and Eqs. (2.14) and (2.15) can be used to compute the eigenvectors in discrete coordinates.

2.6 Components with Rigid-Body Motion

The component mode synthesis method proposed in this chapter is based on the residual-attachment-mode set, which requires the free-interface eigenmodes and the residual attachment modes of all components in the assembly. However, all previous derivations were done under the assumption that none of the components in the assembly are subject to rigid-body motion. In practice, however, some components will have rigid-body motion. Hence, the proposed component mode synthesis method must be generalized to handle unconstrained components. The only difficulty in employing the above method for unconstrained components is in finding the static attachment modes because the stiffness matrix of the unconstrained component is singular. Therefore, as long as the residual attachment modes of any component can be found, then this method can be applied to that component.

If the eigenmodes of the component are known, then (as shown in Eq. (2.28)), the residual flexibility matrix of the component can easily be built as a summation of the contribution of all residual modes, which then can be directly used to find the required residual attachment modes. However, generally the calculation of all eigenmodes for a structure is not possible because of the computational cost involved. However, for the constrained component the residual attachment modes can be obtained by subtracting the contribution of the kept eigenmodes from that of the attachment modes. The attachment modes for a constrained structure can be obtained easily by applying unit forces at the interface degrees of freedom. The attachment modes for an unconstrained component, on the other hand, are difficult to determine because the stiffness matrix of the unconstrained structure is singular.

To overcome this difficulty, one can constrain the rigid-body degrees of freedom at an arbitrary nodal point. By applying unit forces at the interface degrees of freedom, the attachment modes for the constrained component can be found as follows:

$$\begin{bmatrix} \mathbf{K}_{uu} & \mathbf{K}_{ui} & \mathbf{K}_{ur} \\ \mathbf{K}_{iu} & \mathbf{K}_{ii} & \mathbf{K}_{ir} \\ \mathbf{K}_{ru} & \mathbf{K}_{ri} & \mathbf{K}_{rr} \end{bmatrix} \begin{bmatrix} \boldsymbol{\Psi}'_u \\ \boldsymbol{\Psi}'_i \\ 0 \end{bmatrix} = \begin{bmatrix} \mathbf{I} \\ 0 \\ \mathbf{R}_r \end{bmatrix} \tag{2.42}$$

In the above equation, the subscript u represents the degrees of freedom at which the unit forces are applied, and the subscripts i and r represent the interior and rigid-body degrees of freedom, respectively. In the force matrix, $\mathbf{I}$ is an identity matrix of dimension $n_u \times n_u$, where n_u is the number of degrees of freedom at which the unit forces are applied, which is also equal to the number of attachment modes. The matrix $\mathbf{R}_r$ represents the reaction forces at the constrained degrees of freedom r with dimension $n_r \times n_u$, where n_r is the number of rigid-body degrees of freedom.

The attachment modes $\boldsymbol{\Psi}_a$ obtained for an unconstrained component as a result of Eq. (2.42) are not orthogonal to the rigid-body modes $\boldsymbol{\Phi}_0$ with respect to the mass matrix, although they are orthogonal to each other with respect to the stiffness matrix. Hence, the off-diagonal terms in the corresponding submatrices of the generalized mass matrix

$\bar{\mathbf{M}}$ in Eq. (2.20) will not become zero. Therefore, forcing the attachment modes Ψ_a to be orthogonal to the rigid-body modes is beneficial. After the orthogonality is forced, the new attachment modes Ψ_{na} are obtained as

$$\Psi_{na} = \Psi_a - \Phi_0 \Gamma \tag{2.43}$$

where the matrix Γ, with the dimension $n_r \times n_a$ (n_r is the number of rigid-body modes and n_a is the number of attachment modes), is defined as

$$\Gamma = \Phi_0^T \mathbf{M} \Psi_a \tag{2.44}$$

where $\mathbf{M}$ is the mass matrix of the component.

Thus, the attachment modes can be directly used in the eigenvector expansion after the contribution is subtracted from the kept elastic modes. This process of eliminating the rigid-body degrees of freedom to find the attachment modes of the unconstrained component will not incur any error in computing the global responses of the assembled structure because the rigid-body motion of the component is already represented by its first few eigenmodes. If the number of eigenmodes used in the expansion is greater than the number of rigid-body modes of that component, then the contribution of the kept elastic modes must be eliminated from the set of attachment modes to obtain the residual attachment modes:

$$\Psi_{ra} = \Psi_{na} - \Phi_k \Lambda_k^{-1} \Phi_k^T \begin{bmatrix} \mathbf{I} \\ 0 \\ \mathbf{R}_r \end{bmatrix} \tag{2.45}$$

In the above equation, the summation $\Phi_k \Lambda_k^{-1} \Phi_k^T$ is the flexibility matrix of the kept elastic modes G_k, as defined in Eq. (2.24). Note that the force matrix in Eq. (2.45) is expanded to the full size of the component degrees of freedom by inserting the reaction forces at the constrained degrees of freedom. This step forces the attachment modes to be consistent in size with the eigenmodes of the component, which are spanned to the full size of the component degrees of freedom, including the rigid-body degrees of freedom. Hence, the reaction forces at the constrained degrees of freedom are also necessary in calculating the residual attachment modes of the unconstrained component.

2.7 Multilevel Component Mode Synthesis

Normally, the components in an assembly are formed by assembling the various subcomponents. In such a situation, application of component mode synthesis in a multilevel manner is necessary to find the eigenvalues and eigenvectors of the global structure. As mentioned earlier, the component mode synthesis employed here requires knowledge of the free-interface eigenmodes and the residual attachment modes for the eigenvector expansion. Hence, in order to apply this method in a multilevel process, the eigenmodes as well as the attachment modes of the subassemblies at each level must be known. The component mode synthesis method provides the first few eigenmodes of the subassemblies very accurately; however, the difficulty lies in finding the attachment modes of the subassemblies because the stiffness matrices of the subassemblies at each level are not known.

Our first attempt was to use the generalized stiffness matrix $\bar{\mathbf{K}}$ in Eq. (2.16) to find an approximate attachment mode of the subassembly for subsequent use in the analysis for the next level. However, the results obtained were inaccurate because of the use of an approximate attachment mode. The reason for the inaccurate results can be attributed to the fact that, although the low-frequency eigenmodes are supplemented with static modes, the generalized stiffness matrix can only represent the partial contribution of high-frequency component modes to find the attachment modes. Therefore, use of the generalized stiffness matrix, which is primarily made up of a small portion of the eigenmodes, will not yield an attachment mode that is representative of the high-frequency modes of the assembly. Numerical experience has shown that component mode synthesis does not perform satisfactorily without accurate attachment modes. This experience leads to our second attempt to find the exact attachment modes of the subassembly by using the substructuring technique.

In this study, a static substructuring technique was developed to find the attachment modes of the subassembly with only certain selected static modes of the components

and without exact assembly of the subassembly stiffness matrix. This procedure was accomplished by writing the displacement of the components as a summation of the displacement vectors due to the unit forces, at the interface degrees of freedom, due to the external forces and the rigid-body displacement, if any. The resulting displacement vector is subjected to the compatibility and force equilibrium conditions at the interfaces of the components to obtain the static modes of the subassembly due to the respective external forces.

Detailed procedures for the substructuring technique are outlined in the next section with a sample problem. For generality, one of the components is assumed to have rigid-body motion.

2.8 Static Substructuring Technique

Let components α and β form the subassembly; component α is constrained and component β is unconstrained. The components α and β are subjected to external forces F^{α} and F^{β}, respectively. For generality, let the number of interface degrees of freedom n_s be greater than the rigid-body degrees of freedom n_r of the β component. The procedure for finding the static modes of the subassembly is outlined below (see Fig. 2.2).

1. Find the displacement Ψ_I^{α} of the component α by applying the unit forces at each successive interface degree of freedom. Collect the resulting displacements at the interface degrees of freedom as Ψ_{Is}^{α}.

2. Apply the external force F^{α} to the α component and obtain the corresponding displacement vector ψ_f^{α}.

3. Find the rigid-body displacement of component β, Ψ_r^{β}, due to the prescribed displacement of component α, Ψ_{Ir}^{α}, at the constrained rigid-body degrees of freedom $n_r{}^{\beta}$ of the β component. Note that Ψ_{Ir}^{α} is part of the Ψ_{Is}^{α} that corresponds to the constrained rigid-body degrees of freedom at the interface between components α and β.

4. Similarly, find the rigid-body displacement of component β, ψ_r^β, due to the prescribed displacement of component α, ψ_{fr}^α, at the constrained rigid-body degrees of freedom η_r^β of the β component. The displacement ψ_{fr}^α is part of ψ_f^α.

5. For component β, fix the rigid-body degrees of freedom $n_r{}^\beta$ at the interface. Apply a unit force at each of the remaining interface degrees of freedom ($n_s' = n_s - n_r{}^\beta$) to obtain the displacement vectors Ψ_I^β and the corresponding reaction forces $\mathbf{R}_{Ir}^\beta$ at $n_r{}^\beta$.

6. Apply the external force F^β to the β component constrained at $n_r{}^\beta$ to find the corresponding displacement vector ψ_f^β and the reaction forces $\mathbf{r}_f^\beta$ at $n_r{}^\beta$.

7. If (a) the reaction forces at the interface degrees of freedom are $[\lambda_r^\alpha \quad \lambda_{s'}^\alpha]^T$ and $[\lambda_r^\beta \quad \lambda_{s'}^\beta]^T$ for components α and β, respectively; (b) the reaction forces λ_r^α and λ_r^β correspond to the constrained rigid-body degrees of freedom n_r; and (c) $\lambda_{s'}^\alpha$ and $\lambda_{s'}^\beta$ are the reaction forces that correspond to the rest of the interface degrees of freedom n_s' of components α and β, respectively; then the total displacement of the α component is obtained as follows:

$$X^\alpha = \Psi_I^\alpha \cdot \begin{Bmatrix} \lambda_r^\alpha \\ \lambda_{s'}^\alpha \end{Bmatrix} + \psi_f^\alpha \tag{2.46}$$

For component β, the total displacement is written as the summation of the displacements due to the external force, the rigid-body motion, and the reaction forces at the constrained degrees of freedom, as shown:

$$X^\beta = \Psi_I^\beta \cdot \begin{Bmatrix} \lambda_r^\beta \\ \lambda_{s'}^\beta \end{Bmatrix} + \psi_f^\beta + \Psi_r^\beta \cdot \begin{Bmatrix} \lambda_r^\alpha \\ \lambda_{s'}^\alpha \end{Bmatrix} + \psi_r^\beta \tag{2.47}$$

In the above equations, the unknowns are the reaction forces $[\lambda_r^\alpha \quad \lambda_{s'}^\alpha]^T$ and $[\lambda_r^\beta \quad \lambda_{s'}^\beta]^T$.

8. If the compatibility conditions for displacements at the interface degrees of freedom n_s' are imposed, then n_s' equations are obtained as shown:

$$\Psi_{Is'}^\alpha \cdot \begin{Bmatrix} \lambda_r^\alpha \\ \lambda_{s'}^\alpha \end{Bmatrix} + \psi_{fs'}^\alpha = \Psi_{Is'}^\beta \cdot \begin{Bmatrix} \lambda_r^\beta \\ \lambda_{s'}^\beta \end{Bmatrix} + \psi_{fs'}^\beta + \Psi_{rs'}^\beta \cdot \begin{Bmatrix} \lambda_r^\alpha \\ \lambda_{s'}^\alpha \end{Bmatrix} + \psi_{rs'}^\beta \tag{2.48}$$

where $\Psi_{Is'}^\alpha$, Ψ_{Is}^β, and $\Psi_{rs'}^\beta$ have the dimension $n_{s'}\mathrm{x}n_s$ and the vectors $\psi_{fs'}^\alpha$, $\psi_{fs'}^\beta$ and $\psi_{rs'}^\beta$ are $n_{s'}\mathrm{x}1$.

9. Another set of n_r equations can be obtained by writing the force equilibrium equations at the interface, where the rigid-body degrees of freedom of the β component are constrained. The total reaction force at the 'n_r' degrees of freedom of the β component is the sum of the reaction forces due to the external force F^β and the reaction forces $\lambda_{s'}^\beta$ at the n_s' interface degrees of freedom. The same can be written as

$$\lambda_r^\beta = \mathbf{R}_{\mathbf{Ir}}^\beta . \lambda_{s'}^\beta + \mathbf{r}_\mathbf{f}^\beta \tag{2.49}$$

where the dimension of $\mathbf{R}_{Ir}^\beta$ is $n_r \times n_{s'}$ and the dimension of λ_r^β and $\mathbf{r}_f^\beta$ is $\mathbf{n_r x 1}$. Note that the reaction forces of components α and β at the interface degrees of freedom are equal in magnitude and opposite in direction, so that the following expression can be written as

$$\begin{Bmatrix} \lambda_r^\alpha \\ \lambda_{s'}^\alpha \end{Bmatrix} = -\begin{Bmatrix} \lambda_r^\beta \\ \lambda_{s'}^\beta \end{Bmatrix} \tag{2.50}$$

With Eq. (2.50), Eqs. (2.48) and (2.49) are simplified as

$$\left[\Psi_{Is'}^\alpha + \Psi_{Is'}^\beta - \Psi_{rs'}^\beta\right] \begin{Bmatrix} \lambda_r^\alpha \\ \lambda_{s'}^\alpha \end{Bmatrix} = \left\{\psi_{fs'}^\beta - \psi_{fs'}^\alpha + \psi_{rs'}^\beta\right\} \tag{2.51}$$

and

$$[\mathbf{I} \quad -\mathbf{R}_{Is'}^\beta] \begin{Bmatrix} \lambda_r^\alpha \\ \lambda_{s'}^\alpha \end{Bmatrix} = -\left\{\mathbf{r}_f^\beta\right\} \tag{2.52}$$

where Eqs. (2.51) and (2.52) have n_s' and n_r equations, respectively. After Eqs. (2.50)-(2.52) have been solved for the unknowns λ_r^α, $\lambda_{s'}^\alpha$, λ_r^β, and $\lambda_{s'}^\beta$, the displacement of the subassembly under the external forces F^α and F^β can be obtained from Eqs. (2.46) and (2.47).

If none of the components in the subassembly have rigid-body degrees of freedom, then the above procedure will be simplified such that the rigid-body displacement Ψ_r^β and the reaction forces λ_r^α and λ_r^β at the constrained rigid-body degrees of freedom are dropped from the equations.

2.9 Numerical Examples

Two numerical examples are presented in this chapter to demonstrate component mode synthesis based on the residual-attachment-mode set. The examples considered here are

1. A multilevel fixed-fixed beam.
2. A simplified model of an engine cradle.

The first example demonstrates two capabilities of the proposed component mode synthesis method: its ability to handle components with rigid-body degrees of freedom and the multilevel component mode synthesis. In the second example, issues related to the accuracy of the method are studied (e.g., the number of modes and the use of the M_{ss}^{*} terms in the generalized mass matrix).

2.9.1 Multilevel Fixed-Fixed Beam

A fixed-fixed beam shown in Fig. 2.3 is assembled in a multilevel process from two identical cantilever beams: α and two identical free-free beams β. In the first level, components α and β are assembled to form two identical cantilever beams "a" and "b." In the second level, the two cantilever beams are assembled to form a symmetric fixed-fixed beam.

Both components α and β are modeled with two nodes and 4-degree-of-freedom beam elements. The finite-element discretization of both the components is shown in Fig. 2.4. Component α is discretized into eight elements, and component β is discretized into six elements; hence, they have 16 and 14 degrees of freedom, respectively. When all components are assembled together, as shown in Fig. 2.3, the global structure has a total of 54 degrees of freedom.

The material properties (Young's modulus–30 000 kgf/cm^2; shear modulus–13 500 kgf/cm^2; and mass density–0.0024093 kg/cm^3) are assumed to be the same for both of

components. The geometrical properties are given in Fig. 2.4. As shown in this figure, both α and β components have a uniform rectangular cross section of 2×4 cm^2.

Eigenmodes of each component are obtained by performing a normal mode analysis, whereas attachment modes are obtained by applying one unit force at a time at each of the interface degrees of freedom. Because component β is unconstrained, the attachment modes are obtained by constraining the rigid-body degrees of freedom at one end and applying the unit forces at the other end. The corresponding reaction forces at the constrained degrees of freedom are also needed for the components with rigid-body degrees of freedom.

First Level

At the first level, component mode synthesis was performed to obtain the eigenvalues and eigenvectors of subassemblies "a" and "b"; beams α and β are considered as the components. For the component mode synthesis, two different cases were considered in which the number of eigenmodes for each component was four and two, respectively. In addition to the eigenmodes, two attachment modes of each component were considered as part of the basis vectors in the eigenvector approximation. Because component β is unconstrained, its first two eigenmodes are rigid-body modes.

The computed eigenvalues of subassembly "a" are given in Tables 2.1 and 2.2. The results for subassembly "b" are identical to those of "a." The exact eigenvalues and eigenvectors of subassembly "a" were obtained by performing a normal mode analysis of the entire finite-element model of subassembly "a." These are also given in Tables 2.1 and 2.2 for comparison purposes. In Table 2.1, only the first two eigenmodes are computed accurately; however, when the number of modes considered for each component is increased in Table 2.2, a greater number of higher order modes agree with the exact values. The increase in the number of modes also improved the accuracy of the lower order modes.

Second Level

In the second level, subassemblies "a" and "b," which are the cantilever beams, are assembled to form the global structure (i.e., the fixed-fixed beam). Therefore, the eigenvalues and the eigenvectors of the fixed-fixed beam can be obtained by component mode synthesis, with subassemblies "a" and "b" as components. Eigenmodes of the subassemblies "a" and "b" computed in the first-level component mode synthesis were used directly as the basis vectors for the eigenvector approximation. However, the exact attachment modes of these subassemblies were obtained with the static substructuring technique explained in section 2.8.

The computed eigenvalues of the global structure are given in Tables 2.3 and 2.4 with the exact values. The exact eigenvalues and eigenvectors of the fixed-fixed beam were obtained by normal mode analysis of its finite-element model. In Table 2.3, only the first two eigenmodes are computed accurately. Again, similar to the observation made in the first level, as the number of modes for each component is increased, more higher order modes are computed accurately. Note that in the second level the approximate eigenmodes of the subassemblies (obtained in the first level by component mode synthesis) were used.

2.9.2 Simplified Model of Engine Cradle

A simplified model of an engine cradle is shown in Fig. 2.5. The topology of the structure clearly lends itself to division into four components. These components are discretized with circular-tube elements. Each of the tube elements has 2 nodes and 6 degrees of freedom at each node. Components 1 and 2 are discretized into 8 and 9 elements, respectively, whereas components 3 and 4 are both discretized into 10 elements. Because, components 1 and 2 are unconstrained, these components have 54 degrees of freedom and 60 degrees of freedom, respectively. However, components 3 and 4 are

constrained at two nodes; hence, they have 54 degrees of freedom each. When the components are assembled, the global structure has a total of 198 degrees of freedom.

The material properties (Young's modulus–1207×10^3 kgf/cm^2; Shear modulus –362.1×10^3 kgf/cm^2; mass density–7.8×10^{-6} kg/cm^3) are assumed to be the same for all components.

The eigenmodes and static modes of each component are obtained as explained in the previous example. Because components 1 and 2 are unconstrained, the attachment modes are obtained by constraining the rigid-body degrees of freedom at one end and applying the unit forces at the other end. In this example, all components are assembled in one level to form the global structure. Therefore, component mode synthesis is performed only once to obtain the eigenvalues and eigenvectors of the global structure, unlike the first example in which the analysis was done in two levels.

The computed eigenvalues of the engine cradle are shown in Tables 2.5, 2.6, and 2.7. The number of eigenmodes considered for each of the four components are listed in the table. In addition to these eigenmodes, six attachment modes for each component were also included in the eigenvector expansion of the global structure. In Table 2.5, the computed eigenvalues are not very accurate. However, similar to the observation made in the previous example, as the number of modes retained is increased, the error in the computed values was reduced (see Table 2.6).

As explained in section 2.4, the M^*_{ss} terms in the generalized mass matrix of Eq. (2.33) are simply the product of $\Psi^{i^T}_{ra} M^i \Psi^i_{ra}$. These values are small in comparison with unity; hence, they can be neglected without incurring a large error in the computed results. To validate this claim, the eigenvalues of the engine cradle were computed with and without these terms. The results are shown in Table 2.7. This table shows that neglecting the M^*_{ss} terms does not incur a large error in the computed eigenvalues; in fact, this effect is hardly noticeable, especially in the lower order modes.

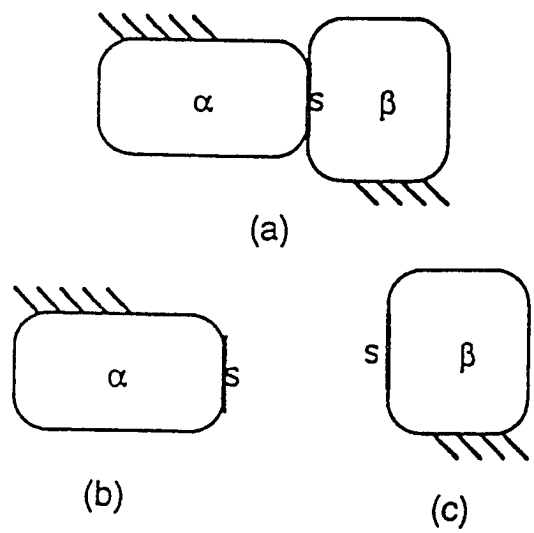

Figure 2.1 (a) Global structure. (b) Component α. (c) Component β.

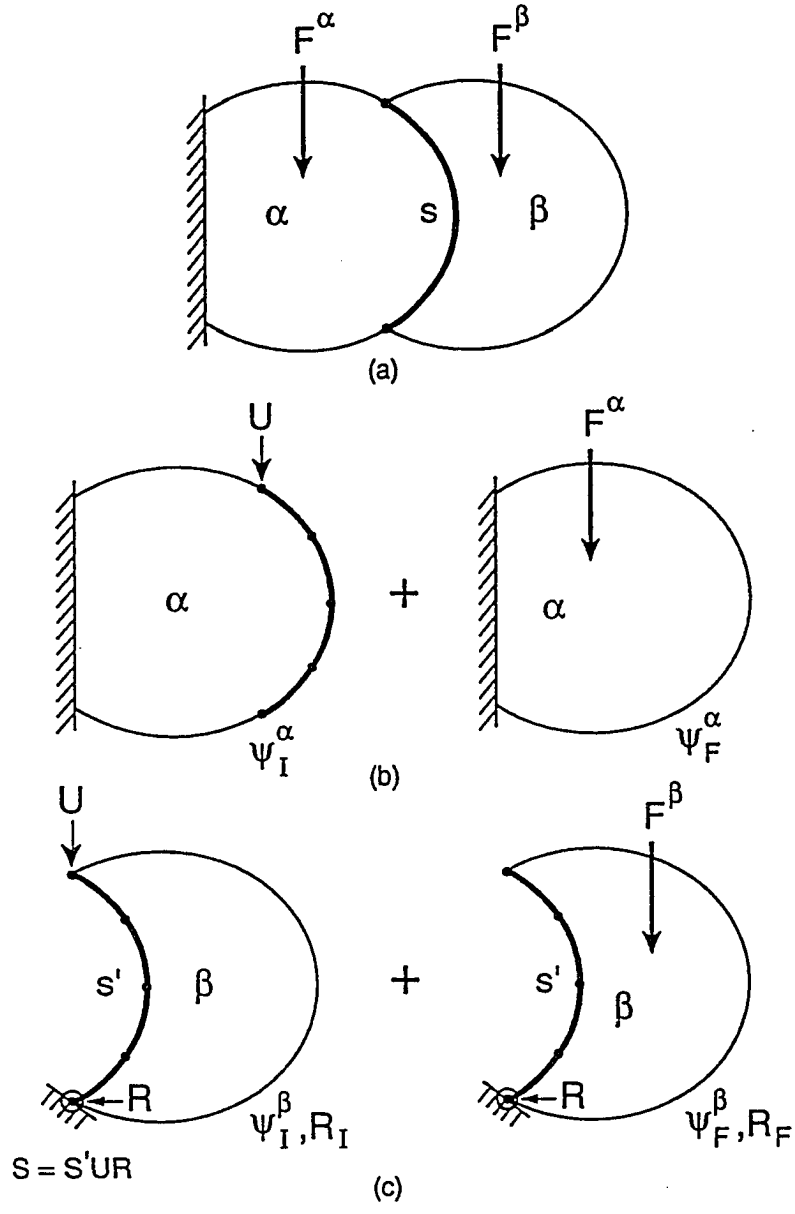

Figure 2.2 Static substructuring

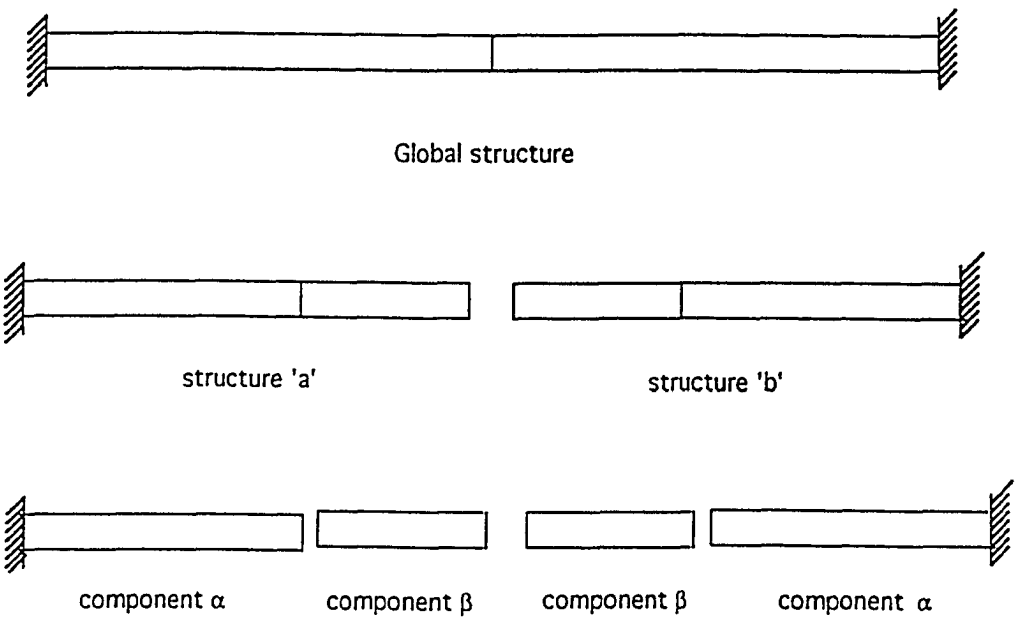

Figure 2.3 Fixed-fixed beam

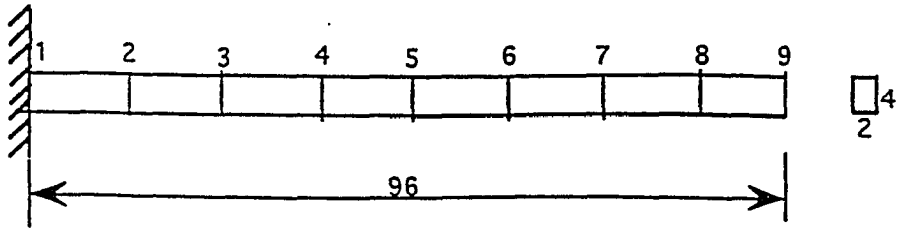

Component α

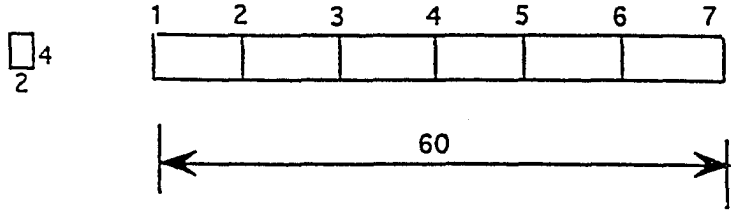

Component β

Figure 2.4 Finite-element discretization

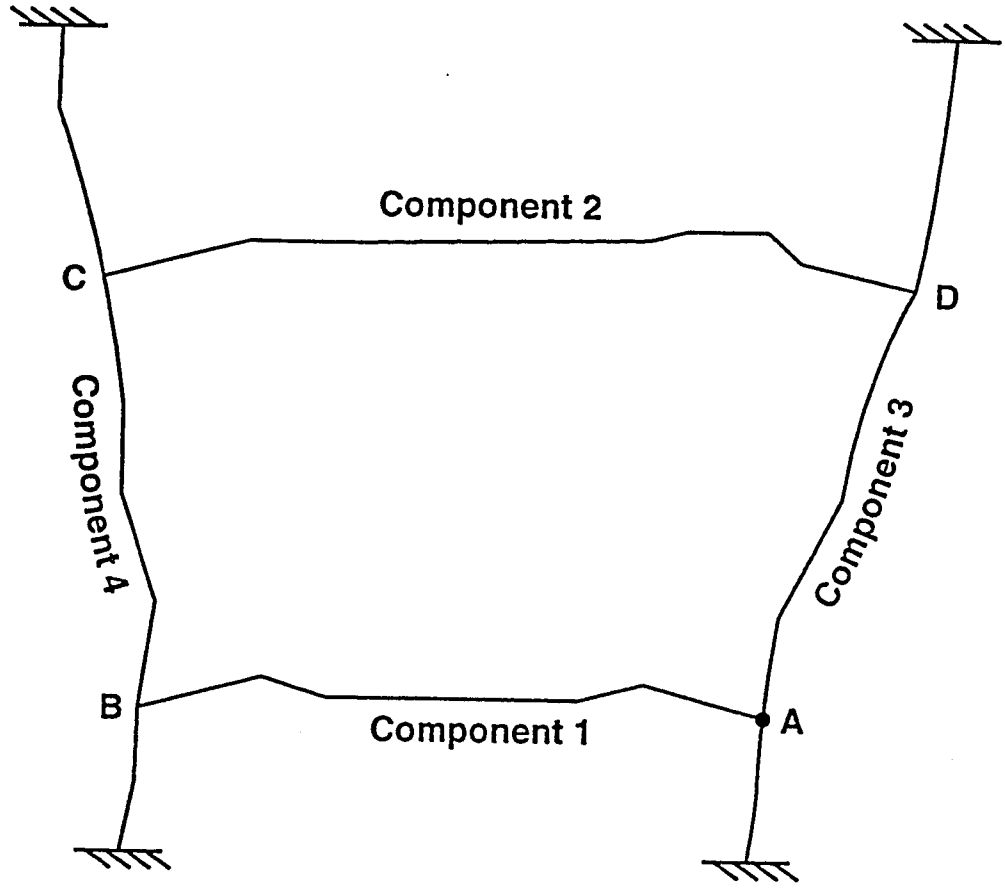

Figure 2.5 Simplified model of engine cradle

Table 2.1 Eigenvalues of Cantilever Beam "a"

(with 2 Eigenmodes for Each Component)

Eigenmode no.	Computed	Exact	% error
1	0.344381	0.344269	0.0325
2	13.358456	13.272335	0.6489
3	109.240154	100.720191	8.4590
4	1045.851050	374.512423	279.2570

Table 2.2 Eigenvalues of Cantilever Beam "a"

(with 4 Eigenmodes for Each Component)

Eigenmode no.	Computed	Exact	% error
1	0.344274	0.344269	0.0014
2	13.274837	13.272335	0.0189
3	100.832641	100.720191	0.1116
4	375.135402	374.512423	0.1663
5	991.099042	975.980845	1.5490
6	2075.214936	2064.884072	0.5003
7	4972.120367	3837.257472	129.5748
8	76419.775900	6325.022908	1208.2134

Table 2.3 Eigenvalues of Fixed-Fixed Beam

(With 2 Eigenmodes for Each Component in Both Levels)

Eigenmode no.	Computed	Exact	% error
1	0.876799	0.874996	0.206
2	6.686553	6.630984	0.838
3	26.926142	25.361507	6.169
4	175.488455	68.434796	256.432

Table 2.4 Eigenvalues of Fixed-Fixed Beam

(With 4 Eigenmodes for Each Component in Both Levels)

Eigenmode no.	Computed	Exact	% error
1	0.875068	0.874996	0.008
2	6.632265	6.630984	0.019
3	25.416308	25.361507	0.216
4	68.572038	68.434796	0.201
5	153.475557	151.149354	1.539
6	295.673015	292.318954	1.147
7	565.372673	507.572605	11.388
8	3097.086261	821.137606	377.170

Table 2.5 Eigenvalues of Engine Cradle

$(ne_1 = 9, ne_2 = 10, ne_3 = 5, ne_4 = 5)$

Eigenmode no.	Computed	Exact	% error
1	16222.8529	15087.4786	7.52
2	32299.1070	29158.2649	10.77
3	43955.1313	33236.5053	32.24
4	59219.9949	36274.4406	63.26
5	64378.8180	41613.1581	54.71
6	72465.1126	54886.3679	32.02
7	129165.2393	75086.3132	72.02
8	138091.5285	117514.4083	17.51
9	149514.7586	126419.0107	18.27
10	202265.4159	134789.5861	50.06

Table 2.6 Eigenvalues of Engine Cradle

$(ne_1 = 9, ne_2 = 10, ne_3 = 10, ne_4 = 10)$

Eigenmode no.	Computed	Exact	% error
1	15773.9212	15087.4786	4.55
2	31732.2031	29158.2649	8.83
3	41511.7815	33236.5053	24.89
4	47769.5795	36274.4406	31.69
5	49389.1219	41613.1581	18.69
6	69934.5729	54886.3679	27.42
7	94449.9811	75086.3132	25.78
8	126297.7357	117514.4083	7.47
9	132357.7821	126419.0107	4.69
10	153933.2359	134789.5861	14.20

Table 2.7 Eigenvalues of Engine Cradle With and Without Inclusion of M_{ss}^{*} Terms

$(ne_1 = 9, ne_2 = 10, ne_3 = 5, ne_4 = 5)$

Eigenmode no.	Without M_{ss}^{*} terms	With M_{ss}^{*} terms	% deviation
1	16222.8529	16211.1549	0.072
2	32299.1070	32257.4448	0.129
3	43955.1313	43718.9265	0.540
4	59219.9949	58457.7154	1.304
5	64378.8180	63236.5014	1.806
6	72465.1126	70712.7899	2.478
7	129165.2393	127674.4651	1.168
8	138091.5285	136330.1646	1.292
9	149514.7586	146026.8097	2.389
10	202265.4159	176890.1094	14.345

Chapter 3

SENSITIVITY ANALYSIS

3.1 Introduction

In the previous chapter, component mode synthesis was explained in detail. Here, we will discuss how the responses of the global structure can be expressed in terms of individual component responses. This expression enables the individual component to be treated as a design entity by using its structural responses (i.e., the eigenvalues, eigenvector components, and static-mode components) as its representative variables.

By employing the free-interface eigenmodes and the residual-attachment-mode set, the coefficient matrices of the reduced eigenproblem in Eq. (2.16) are reduced to a considerably simpler form. The reduced eigenproblem of an isolated component i, which is obtained by employing this particular combination of component modes, can be written as follows:

$$\begin{bmatrix} \mathbf{\Lambda}^i & 0 \\ 0 & \mathbf{K}_s^i \end{bmatrix} \begin{Bmatrix} \mathbf{a}_e^i \\ \mathbf{a}_s^i \end{Bmatrix} = \lambda^i \begin{bmatrix} \mathbf{I} & 0 \\ 0 & \mathbf{M}_s^i \end{bmatrix} \begin{Bmatrix} \mathbf{a}_e^i \\ \mathbf{a}_s^i \end{Bmatrix} + \begin{Bmatrix} \mathbf{f}_e^i \\ \mathbf{f}_s^i \end{Bmatrix} \tag{3.1}$$

where $\mathbf{\Lambda}^i$ is a diagonal matrix that contains the eigenvalues of the individual components, $\mathbf{I}$ is the identity matrix, and $\mathbf{K}_s^i$ is the boundary partition of the residual attachment modes. As mentioned in chapter 2, the values of the matrix $\mathbf{M}_s^i$ are small in comparison with unity; hence, $\mathbf{M}_s^i$ can even be neglected without incurring a large error. The generalized internal forces $\mathbf{f}_e^i$ and $\mathbf{f}_s^i$ are the constraint forces at the interface degrees of freedom. The modal coefficients $\mathbf{a}_e^i$ and $\mathbf{a}_s^i$ are associated with the eigenmodes and static modes, respectively, of component i.

Equation (3.1) can be combined with other components to form a reduced eigenproblem of the entire structure (as a collection of uncoupled components) (Eq. (2.16)) and may be written as

$$\bar{\mathbf{K}}\mathbf{a} = \lambda^g \bar{\mathbf{M}}\mathbf{a} + \mathbf{f} \tag{3.2}$$

The assembly of these coefficients forms the vector **a** in the above equation. However, all components of **a** are not independent and must satisfy the compatibility conditions between components. Symbolically, the compatibility condition can be written in matrix form as

$$\mathbf{C}\,\mathbf{a} = 0 \tag{3.3}$$

where the rectangular matrix **C** is a function of the interface degrees of freedom of the basis vectors. This relationship can be used to choose the independent modal coefficients **p** of the assembled structure as

$$\mathbf{a} = \mathbf{B}\left(\mathbf{\Phi}_s^i, \mathbf{\Psi}_{s_{ra}}^i\right)\mathbf{p} \tag{3.4}$$

where the matrices $\mathbf{\Phi}_s^i$ and $\mathbf{\Psi}_{s_{ra}}^i$ are the matrices of the interface degrees of freedom of the eigenmodes and the static modes of individual components, respectively. Because this compatibility condition is imposed, the eigenproblem in Eq. (3.2) can be further reduced to Eq. (2.41), which is rewritten as

$$\mathbf{K}^*\mathbf{p} = \lambda^g \mathbf{M}^*\mathbf{p} \tag{3.5}$$

and

$$\mathbf{P}^T\mathbf{M}^*\mathbf{P} = 1 \tag{3.6}$$

where $\mathbf{K}^* = \mathbf{B}^T\bar{\mathbf{K}}\mathbf{B}$ and $\mathbf{M}^* = \mathbf{B}^T\bar{\mathbf{M}}\mathbf{B}$. The internal forces **f** in Eq. (3.2) cancel each other out because they must satisfy the force-equilibrium equation $\mathbf{B}^T\mathbf{f} = 0$. Finally, Eq. (3.5) can be solved to obtain the eigenvalues λ^g and the eigenvectors **p** of the reduced eigenproblem.

Note that $\mathbf{K}_s^i$ in Eq. (3.1) can be written in terms of the eigenvalues $\mathbf{\Lambda}^i$ and the interface degrees of freedom of both the static modes $\mathbf{\Psi}_s^i$ and the eigenmodes $\mathbf{\Phi}_s^i$, as shown in Eq. (2.32); this statement is reproduced here by writing the product $\mathbf{\Phi}_{sk}\mathbf{\Lambda}_k^{-1}\mathbf{\Phi}_{sk}$ in the summation form

$$\mathbf{K}_s^i = \mathbf{\Psi}_s^i - \sum_{k=1}^{n_e^i} \phi_{sk}^i \left(\lambda_k^i\right)^{-1} \phi_{sk}^{i^{\mathrm{T}}} \tag{3.7}$$

where $\mathbf{\Psi}_s^i$ are the interface degrees of freedom of the attachment modes and n_e^i is the number of eigenmodes kept for component i in the basis vectors.

If the $\mathbf{M}_s^i$ terms are neglected in Eq. (3.1), then the generalized stiffness and mass matrices $\bar{\mathbf{K}}$ and $\bar{\mathbf{M}}$ in Eq. (3.2) can be expressed as functions of λ^i, $\mathbf{\Phi}_s^i$, and $\mathbf{\Psi}_s^i$. Consequently, $\mathbf{K}^*$ and $\mathbf{M}^*$ in Eq. (3.5) can be expressed as functions of λ^i, $\mathbf{\Phi}_s^i$, and $\mathbf{\Psi}_s^i$, and Eq. (3.5) can be rewritten as

$$\mathbf{K}^*\left(\lambda^i, \mathbf{\Phi}_s^i, \mathbf{\Psi}_s^i\right)\mathbf{p} = \lambda^g\, \mathbf{M}^*\left(\lambda^i, \mathbf{\Phi}_s^i, \mathbf{\Psi}_s^i\right)\mathbf{p} \tag{3.8}$$

Hence, the global eigenvalues and eigenvectors are also functions of these individual component responses. Therefore, Eq. (3.8) helps fulfill our primary objective to quantitatively define the functional relationship between the global responses u_g and the responses of the individual components (i.e., λ^i, $\mathbf{\Phi}_s^i$, and $\mathbf{\Psi}_s^i$). Each of these individual components can be treated as a design entity by using its structural responses (such as the eigenvalues λ^i, the eigenvector components $\mathbf{\Phi}_s^i$, and the static-mode components $\mathbf{\Psi}_s^i$) as the design variables. Throughout the remainder of this dissertation, these component responses (λ^i, $\mathbf{\Phi}_s^i$, and $\mathbf{\Psi}_s^i$) are referred to as the intermediate variables u_i.

In general, if components can exhibit rigid-body motion, then the resulting reaction forces at the constraint degrees of freedom also must be considered as part of the intermediate variables. However, in this study only the statically determinate structures are considered as components, for which the reaction forces are dependent only on the geometry of the structure. Hence, as long as the geometry of the component does not

change, the reaction forces remain constant. For this reason, the reaction forces are not considered as part of the intermediate variables in the rest of this study.

The sensitivity derivatives of the global responses u_g with respect to the component responses u_i are required to quantify the contribution of each component to the global responses. These sensitivity derivatives have many applications in the structural modification techniques proposed in the later chapters. In the next section, detailed mathematical formulations are given for computing the sensitivity derivatives of the eigenvalues and eigenvectors of the assembled structure with respect to the intermediate variables of the individual components.

3.2 Mathematical Formulation

The reduced eigenproblem in Eq. (3.8), which relates the responses of the global structure to the component responses, is the basis for the structural modification and synthesis techniques proposed in this study. The solution to the above eigenproblem gives the eigenvalues λ^g and the eigenvectors $\mathbf{p}$ of the reduced eigenproblem. The true eigenvectors of the assembled structure are obtained by back substitution with Eqs. (2.40) and (2.4):

$$\begin{aligned} \mathbf{x} &= \mathbf{A}\,\mathbf{a} \\ &= \mathbf{A}\,\mathbf{B}\,\mathbf{p} \end{aligned} \tag{3.9}$$

The sensitivity derivatives of the eigenvectors of the assembled structure $\mathbf{x}$ with respect to any intermediate variable u_i can be obtained by differentiating Eq. (3.9) as

$$\frac{\mathrm{d}\mathbf{x}}{\mathrm{d}u_i} = \frac{\mathrm{d}\mathbf{A}}{\mathrm{d}u_i}\mathbf{B}\mathbf{p} + \mathbf{A}\frac{\mathrm{d}\mathbf{B}}{\mathrm{d}u_i}\mathbf{p} + \mathbf{A}\mathbf{B}\frac{\mathrm{d}\mathbf{p}}{\mathrm{d}u_i} \tag{3.10}$$

The sensitivity derivatives of the eigenvector $\mathbf{p}$ and the corresponding eigenvalue λ^g can be obtained by differentiating Eqs. (3.5) and (3.6) and solving the following system of equations [29–33]:

$$\begin{bmatrix} \mathbf{K}^* - \lambda\mathbf{M}^* & -\mathbf{M}^*\mathbf{p} \\ -\mathbf{p}^T\mathbf{M}^* & 0 \end{bmatrix} \begin{Bmatrix} \frac{\mathrm{d}\mathbf{p}}{\mathrm{d}u_i} \\ \frac{\mathrm{d}\lambda}{\mathrm{d}u_i} \end{Bmatrix} = \begin{Bmatrix} -\frac{\mathrm{d}\mathbf{K}^*}{\mathrm{d}u_i}\mathbf{p} + \lambda\frac{\mathrm{d}\mathbf{M}^*}{\mathrm{d}u_i}\mathbf{p} \\ \frac{1}{2}\mathbf{p}^T\frac{\mathrm{d}\mathbf{M}^*}{\mathrm{d}u_i}\mathbf{p} \end{Bmatrix} \tag{3.11}$$

In the above equation, the derivatives of matrices $\mathbf{K}^*$ and $\mathbf{M}^*$ with respect to the intermediate variables are required. These derivatives can be obtained by using the definitions of these matrices given in Eq. (3.5). With the product rule, these derivatives can be written as

$$\frac{d\mathbf{K}^*}{du_i} = \frac{d\mathbf{B}^T}{du_i}\bar{\mathbf{K}}\mathbf{B} + \mathbf{B}^T\frac{d\bar{\mathbf{K}}}{du_i}\mathbf{B} + \mathbf{B}^T\bar{\mathbf{K}}\frac{d\mathbf{B}}{du_i} \tag{3.12}$$

and

$$\frac{\mathrm{d}\mathbf{M}^*}{\mathrm{d}u_i} = \frac{\mathrm{d}\mathbf{B}^T}{\mathrm{d}u_i}\bar{\mathbf{M}}\mathbf{B} + \mathbf{B}^T\frac{\mathrm{d}\bar{\mathbf{M}}}{\mathrm{d}u_i}\mathbf{B} + \mathbf{B}^T\bar{\mathbf{M}}\frac{\mathrm{d}\mathbf{B}}{\mathrm{d}u_i} \tag{3.13}$$

in which the derivatives of the generalized stiffness matrix $\bar{\mathbf{K}}$, the generalized mass matrix $\bar{\mathbf{M}}$, and the compatibility matrix $\mathbf{B}$ must be calculated.

Matrix $\mathbf{B}$, which enforces the compatibility condition at the interface degrees of freedom between the components, is obtained as shown in section 2.5 and is defined by Eq. (2.40). With this definition, the derivatives of $\mathbf{B}$ with respect to the intermediate variable u_i can be written as

$$\frac{\mathrm{d}\mathbf{B}}{\mathrm{d}u_i} = \begin{bmatrix} -\frac{\mathrm{d}(\mathbf{C}_1^{-1})}{\mathrm{d}u_i}\mathbf{C}_2 - \mathbf{C}_1^{-1}\frac{\mathrm{d}\mathbf{C}_2}{\mathrm{d}u_i} \\ 0 \end{bmatrix} \tag{3.14}$$

The derivative of the inverse of the $\mathbf{C}_1$ matrix can be written in terms of the derivative of the $\mathbf{C}_1$ matrix as

$$\frac{\mathrm{d}(\mathbf{C}_1^{-1})}{\mathrm{d}u_i} = -\mathbf{C}_1^{-1}\frac{\mathrm{d}\mathbf{C}_1}{\mathrm{d}u_i}\mathbf{C}_1^{-1} \tag{3.15}$$

Because the matrices $\mathbf{C}_1$ and $\mathbf{C}_2$ are part of the matrix $\mathbf{C}$, after the derivatives of the $\mathbf{C}$ matrix are known, then the derivatives of the matrix $\mathbf{B}$ can be obtained from Eq. (3.14) and (3.15).

If the $\mathbf{M}_s^i$ terms in Eq. (3.1) are neglected, then the generalized mass matrix $\bar{\mathbf{M}}$ in Eq. (3.2) remains constant. Therefore, its derivative with respect to any intermediate variable u_i will be equal to 0. That is,

$$\frac{\mathrm{d}\bar{\mathbf{M}}}{\mathrm{d}u_i} = 0 \tag{3.16}$$

The computation of the derivatives of the eigenvalue λ^g and the eigenvector $\mathbf{x}$ of the global structure requires in addition to Eqs. (3.10)–(3.16) the derivatives of the generalized stiffness matrix $\bar{\mathbf{K}}$, the eigenvector expansion matrix $\mathbf{A}$, and the compatibility matrix $\mathbf{C}$ with respect to the intermediate variables.

In the following, the generalized stiffness matrix $\bar{\mathbf{K}}$ and the transformation matrices $\mathbf{A}$ and $\mathbf{C}$ are defined explicitly in terms of the intermediate variables u_i of component i (i.e., the eigenvalues λ^i, the interface degrees of freedom of the eigenvectors Φ_s^i, and the static modes Ψ_s^i).

In deriving the expressions for the derivatives of the generalized stiffness matrix $\bar{\mathbf{K}}$ in Eq. (3.2) with respect to any intermediate variable of a particular component i, only the part of this matrix that is related to the particular component (i.e., $\bar{\mathbf{K}}^i$) given in Eq. (3.1) must be considered.

The derivative of the generalized stiffness matrix of component i (i.e., $\bar{\mathbf{K}}^i$) with respect to any intermediate variable u_i can be written as follows by differentiating Eq. (3.1):

$$\frac{\mathrm{d}\bar{\mathbf{K}}^i}{\mathrm{d}u_i} = \begin{bmatrix} \frac{\mathrm{d}\Lambda^i}{\mathrm{d}u_i} & 0 \\ 0 & \frac{\mathrm{d}\mathbf{K}_s^i}{\mathrm{d}u_i} \end{bmatrix} \tag{3.17}$$

where the derivative of $\mathbf{K}_s^i$ can be written based upon its definition from Eq. (3.7) as

$$\frac{\mathrm{d}\mathbf{K}_s^i}{\mathrm{d}u_i} = \frac{\mathrm{d}\mathbf{K}_s^i}{\mathrm{d}\Lambda^i} \cdot \frac{\mathrm{d}\Lambda^i}{\mathrm{d}u_i} + \frac{\mathrm{d}\mathbf{K}_s^i}{\mathrm{d}\Psi_s^i} \cdot \frac{\mathrm{d}\Psi_s^i}{\mathrm{d}u_i} + \frac{\mathrm{d}\mathbf{K}_s^i}{\mathrm{d}\phi_{sk}^i} \cdot \frac{\mathrm{d}\phi_{sk}^i}{\mathrm{d}u_i} \tag{3.18}$$

In the above derivative, Λ^i is the diagonal matrix of the eigenvalues of component i. From Eq. (3.7), the derivative of $\mathbf{K}_s^i$ with respect to a component in Λ^i (the jth eigenvalue λ_j^i) (i.e., $\frac{\mathrm{d}\mathbf{K}_s^i}{\mathrm{d}\lambda_j^i}$) can be written as

$$\frac{\mathrm{d}\mathbf{K}_s^i}{\mathrm{d}\lambda_j^i} = \phi_{sj}^i (\lambda_j^i)^{-2} \phi_{sj}^{iT} \tag{3.19}$$

In the second term of Eq. (3.18), the derivative of matrix $\mathbf{K}_s^i$ with respect to ψ_{lj}^i (i.e., the lth interface degree of freedom of the jth attachment mode) can be written as

$$\frac{\mathrm{d}\mathbf{K}_s^i}{\mathrm{d}\psi_{lj}^i} = \frac{\mathrm{d}\boldsymbol{\Psi}_s}{\mathrm{d}\psi_{lj}^i} \tag{3.20}$$

where $\frac{\mathrm{d}\boldsymbol{\Psi}_s}{\mathrm{d}\psi_{lj}}$ is a matrix of dimension $n_s \times n_s$ with unit value at the (l, j)th location and the remainder of its terms equal to 0. Finally, the derivative of the $\mathbf{K}_s^i$ matrix with respect to ϕ_{lj}^i (i.e., the lth interface degree of freedom of the jth eigenmode) can be written as

$$\frac{\mathrm{d}\mathbf{K}_s^i}{\mathrm{d}\phi_{lj}^i} = -\frac{\mathrm{d}\left(\phi_{sj}^i\right)}{\mathrm{d}\phi_{sj}^i}(\lambda_j^i)^{-1}\phi_{sj}^{i^T} - \phi_{sj}^i(\lambda_j^i)^{-1}\frac{\mathrm{d}\left(\phi_{sj}^i\right)^T}{\mathrm{d}\phi_{sj}^i} \tag{3.21}$$

where $\frac{\mathrm{d}(\phi_{sj}^i)}{\mathrm{d}\phi_{lj}}$ is a vector with a dimension equal to that of ϕ_{sj}^i. (Its lth element is unity and the remaining terms are equal to 0).

The eigenvector expansion matrix **A**, as defined in Eq. (2.4), has the eigenmodes and the residual attachment modes of all components as part of its columns. For example, for a two component structure, it has the form

$$\mathbf{A} = \begin{bmatrix} \boldsymbol{\Phi}^\alpha & \boldsymbol{\Psi}_{ra}^\alpha & 0 & 0 \\ 0 & 0 & \boldsymbol{\Phi}^\beta & \boldsymbol{\Psi}_{ra}^\beta \end{bmatrix} \tag{3.22}$$

The coefficient matrix **C** defined in Eq. (3.3) contains only the information related to the interface degrees of freedom of the eigenmodes $\boldsymbol{\Phi}_s^i$ and the interface degrees of freedom of the residual attachment modes $\boldsymbol{\Psi}_{s_{ra}}^i$ of all components. For a two component structure, the **C** matrix has the form

$$\mathbf{C} = \begin{bmatrix} \boldsymbol{\Phi}_s^\alpha & \boldsymbol{\Psi}_{s_{ra}}^\alpha & -\boldsymbol{\Phi}_s^\beta & -\boldsymbol{\Psi}_{s_{ra}}^\beta \end{bmatrix} \tag{3.23}$$

The matrix **B** is simply a function of the matrix **C**; this relationship is defined in Eqs. (2.39) and (2.40). With the above definitions for matrices **A**, **B**, and **C**, their derivatives with respect to the intermediate variable u_i can be written as

$$\frac{\mathrm{d}\mathbf{A}}{\mathrm{d}u_i} = \frac{\mathrm{d}\mathbf{A}}{\mathrm{d}\boldsymbol{\Phi}^i} \cdot \frac{\mathrm{d}\boldsymbol{\Phi}^i}{\mathrm{d}u_i} + \frac{\mathrm{d}\mathbf{A}}{\mathrm{d}\boldsymbol{\Psi}_{ra}^i} \cdot \frac{\mathrm{d}\boldsymbol{\Psi}_{ra}^i}{\mathrm{d}u_i} \tag{3.24}$$

$$\frac{\mathrm{dC}}{\mathrm{d}u_i} = \frac{\mathrm{dC}}{\mathrm{d}\Phi_s^i} \cdot \frac{\mathrm{d}\Phi_s^i}{\mathrm{d}u_i} + \frac{\mathrm{dC}}{\mathrm{d}\Psi_{s_{ra}}^i} \frac{\mathrm{d}\Psi_{s_{ra}}^i}{\mathrm{d}u_i} \tag{3.25}$$

and

$$\frac{\mathrm{dB}}{\mathrm{d}u_i} = \frac{\mathrm{dB}}{\mathrm{dC}_1} \cdot \frac{\mathrm{dC}_1}{\mathrm{d}u_i} + \frac{\mathrm{dB}}{\mathrm{dC}_2} \cdot \frac{\mathrm{dC}_2}{\mathrm{d}u_i} \tag{3.26}$$

In Eq. (3.24), the derivative of matrix **A** with respect to ϕ_{lj}^i (i.e., the *l*th degree of freedom of the *j*th eigenmode) is a matrix that has the same dimensions as matrix **A** with a unit value at the *lj*th location and the remaining terms equal to 0. The derivative of matrix **A** with respect to $(\psi_{ra}^i)_{lj}$ (i.e., the *l*th degree of freedom of the *j*th residual attachment mode) for the second term can be obtained in a similar manner.

In Eq. (3.25), the derivatives of the **C** matrix with respect to the interface degrees of freedom of the eigenmodes $\frac{\mathrm{dC}}{\mathrm{d}\Phi_s}$ and the residual attachment modes $\frac{\mathrm{dC}}{\mathrm{d}\Phi_{s_{ra}}}$ can be obtained in a manner similar to that in which the derivatives of matrix **A** were obtained.

After the derivatives of matrix **C** (i.e., $\frac{\mathrm{dC}}{\mathrm{d}u_i}$) are obtained, then $\frac{\mathrm{dC}_1}{\mathrm{d}u_i}$ and $\frac{\mathrm{dC}_2}{\mathrm{d}u_i}$ can be calculated because $\mathbf{C}_1$ and $\mathbf{C}_2$ are part of the **C** matrix (shown in Eq. (2.37)).

To complete the computation of the derivatives of the generalized stiffness matrix $\bar{\mathbf{K}}$ and the transformation matrices **A** and **C** with respect to the various intermediate variables of component *i* (i.e., the eigenvalues λ^i, the interface degrees of freedom of the eigenvectors Φ_s^i, and the static modes Ψ_s^i), the remaining derivative terms in Eqs. (3.18) and (3.24)–(3.25) with respect to the various intermediate variables are required (e.g., the derivatives of $\Lambda^i, \Phi^i, \Phi_s^i, \Psi_s^i, \Psi_{ra}^i$, and $\Psi_{s_{ra}}^i$). The procedures for obtaining these derivatives are discussed in sections 3.2.1, 3.2.2, and 3.2.3.

3.2.1 Differentiation With Respect to Eigenvalues (Λ^i)

If k eigenmodes of component *i* are used in the eigenvector expansion, then k eigenvalues are part of the intermediate variables. In Eq. (3.18), the derivative of the eigenvalue matrix Λ^i with respect to the *j*th eigenvalue λ_j^i is a matrix with a dimension

equal to that of Λ^i; the jth diagonal element is unity and the remaining terms are 0. That is,

$$\frac{d\Lambda^i}{d\lambda_j^i} = \begin{bmatrix} 0 & & & & \\ & \ddots & & & \\ & & 1 & & \\ & & & \ddots & \\ & & & & 0 \end{bmatrix} \tag{3.27}$$

The attachment modes Ψ_a^i and the eigenmodes Φ^i are independent of the eigenvalue; hence, their derivatives with respect to the eigenvalue λ_j^i are equal to 0. That is,

$$\frac{d\Psi_a^i}{d\lambda_j^i} = 0 \quad \text{and} \quad \frac{d\Phi^i}{d\lambda_j^i} = 0 \tag{3.28}$$

The submatrices Ψ_s^i and Φ_s^i and the vector ϕ_{sk}^i are part of Ψ_a^i and Φ^i; hence, their derivatives with respect to the eigenvalues are also equal to 0; that is,

$$\frac{d\Psi_s^i}{d\lambda_j^i} = 0 \tag{3.29}$$

and

$$\frac{d\Phi_s^i}{d\lambda_j^i} = 0 \text{ and } \frac{d\phi_{sk}^i}{d\lambda_j^i} = 0 \tag{3.30}$$

However, the derivative of the residual attachment mode Ψ_{ra}^i with respect to the eigenvalue λ_j^i is not equal to 0 because, given the definition of the residual attachment mode Ψ_{ra}^i in Eq. (2.27), it is a function of the eigenvalues Λ^i that correspond to the kept eigenmodes. Therefore, the derivative of the residual attachment mode Ψ_{ra}^i with respect to the eigenvalue λ_j^i can be obtained by differentiating Eq. (2.27) this step can be shown as

$$\frac{d\Psi_{ra}^i}{d\lambda_j^i} = \frac{d\Psi_a^i}{d\lambda_j^i} - \sum \phi_k^i \frac{d(\lambda_k^i)^{-1}}{d\lambda_j^i} \phi_{sk}^{i^T} \tag{3.31}$$

where the derivative $\frac{d\Psi_a^i}{d\lambda_j^i}$ is equal to 0, as given in Eq. (3.28). Then, the second term in the equation can be simplified to obtain the derivative of the residual attachment mode as

$$\frac{d\Psi_{ra}^i}{d\lambda_j^i} = \phi_j^i (\lambda_j^i)^{-2} \phi_{sj}^{i^T} \tag{3.32}$$

Because $\Psi_{s_{ra}}^i$ is a subset of Ψ_{ra}^i, its derivative can be written with Eq. (3.32) as

$$\frac{d\Psi_{s_{ra}}^i}{d\lambda_j^i} = \phi_{sj}^i (\lambda_j^i)^{-2} \phi_{sj}^{i^T} \tag{3.33}$$

3.2.2 Differentiation With Respect to Eigenvector Components (Φ_s^i)

If k eigenmodes of component *i* are used in the eigenvector expansion, then the Φ_s^i matrix has a dimension of $n_s \times k$, where n_s is the number of interface degrees of freedom. Therefore, $n_s \times k$ intermediate variables result from the eigenvector components.

The derivatives of the eigenvalue matrix Λ^i and the attachment modes Ψ_a^i with respect to the eigenmode component ϕ_{lj}^i (i.e., the *l*th interface degree of freedom of the *j*th eigenmode) are equal to 0. That is,

$$\frac{d\Lambda^i}{d\phi_{lj}^i} = 0 \text{ and } \frac{d\Psi_a^i}{d\phi_{lj}^i} = 0 \tag{3.34}$$

Because the matrix Ψ_s^i is a subset of the attachment-mode matrix Ψ_a^i, its derivative with respect to the eigenmode component ϕ_{lj}^i is also 0. That is,

$$\frac{d\Psi_s^i}{d\phi_{lj}^i} = 0 \tag{3.35}$$

The derivative of the eigenmode matrix Φ^i with respect to the eigenmode component ϕ_{lj}^i is a matrix with the same dimensions as Φ^i; its (*l*, *j*)th element is unity and the remainder of the terms are 0. The derivatives of its subset matrix Φ_s^i make up the boundary partition of the matrix $\frac{d\Phi^i}{d\phi_{lj}^i}$. Similarly, the derivative of the vectors ϕ_{sk}^i with respect to ϕ_{lj}^i equal 0 for all eigenmodes, except the *j*th eigenmode ϕ_{sj}^i. In this case,

the derivative has the *l*th element as unity, and the remainder of the terms are equal to 0. That is,

$$\frac{d\phi_{sj}^{i}}{d\phi_{lj}^{i}} = \begin{Bmatrix} 0 \\ . \\ . \\ 1 \\ 0 \\ . \end{Bmatrix} \tag{3.36}$$

The derivative of the residual attachment mode Ψ_{ra} with respect to the eigenmode component ϕ_{lj}^{i} (i.e., $\frac{d\Psi_{ra}^{i}}{d\phi_{lj}^{i}}$) can be obtained by differentiating the definition given in Eq. (2.27) as

$$\frac{d\Psi_{ra}^{i}}{d\phi_{lj}^{i}} = \frac{d\Psi_{a}^{i}}{d\phi_{lj}^{i}} - \frac{d\phi_{j}^{i}}{d\phi_{lj}^{i}}(\lambda_{j}^{i})^{-1}\phi_{sj}^{i^{T}} - \phi_{j}^{i}(\lambda_{j}^{i})^{-1}\frac{d\phi_{sj}^{i^{T}}}{d\phi_{lj}^{i}} \tag{3.37}$$

In the above equation, $\frac{d\Psi_{a}^{i}}{d\phi_{lj}^{i}} = 0$, and the derivatives $\frac{d\phi_{sj}^{i}}{d\phi_{lj}^{i}}$ and $\frac{d\phi_{j}^{i}}{d\phi_{lj}^{i}}$ can be obtained from the derivative $\frac{d\Phi^{i}}{d\phi_{lj}^{i}}$ because these vectors are part of the eigenmode matrix Φ^{i}. Consequently, Eq. (3.37) can be simplified as

$$\frac{d\Psi_{ra}^{i}}{d\phi_{lj}^{i}} = -\frac{d\phi_{j}^{i}}{d\phi_{lj}^{i}}(\lambda_{j}^{i})^{-1}\phi_{sj}^{i^{T}} - \phi_{j}^{i}(\lambda_{j}^{i})^{-1}\frac{d\phi_{sj}^{i^{T}}}{d\phi_{lj}^{i}} \tag{3.38}$$

Because $\Psi_{s_{ra}}^{i}$ is part of Ψ_{ra}^{i}, its derivative can be obtained from the above expression.

3.2.3 Differentiation With Respect to Static-Mode Components (Ψ_{s}^{i})

In general, the number of attachment modes is equal to the number of interface degrees of freedom n_s, although this equality is not required. The dimension of Ψ_{s}^{i}, which represents the interface degrees of freedom of all attachment modes, is $n_s \times n_s$. Note that the matrix Ψ_{s}^{i} is part of the flexibility matrix that corresponds to the interface degrees of freedom; hence, the matrix Ψ_{s}^{i} is a symmetric matrix. Therefore, among the $n_s \times n_s$ intermediate variables, only $\frac{n_s(n_s+1)}{2}$ terms are treated as independent intermediate variables.

The eigenvalues $\mathbf{\Lambda}^i$ and the eigenmodes $\mathbf{\Phi}^i$ are independent of the attachment mode components ψ_{lj}^i. Therefore, their derivatives are equal to 0. That is,

$$\frac{\mathrm{d}\mathbf{\Lambda}^i}{\mathrm{d}\psi_{lj}^i} = 0 \text{ and } \frac{\mathrm{d}\mathbf{\Phi}^i}{\mathrm{d}\psi_{lj}^i} = 0 \tag{3.39}$$

Because the matrix $\mathbf{\Phi}_s^i$ and the vector ϕ_{sk}^i are subsets of the matrix $\mathbf{\Phi}^i$, their derivatives with respect to the ψ_{lj}^i terms are also equal to 0. That is,

$$\frac{\mathrm{d}\mathbf{\Phi}_s^i}{\mathrm{d}\psi_{lj}^i} = 0 \text{ and } \frac{\mathrm{d}\phi_{sk}^i}{\mathrm{d}\psi_{lj}^i} = 0 \tag{3.40}$$

Furthermore, the derivative of the attachment mode $\mathbf{\Psi}_a^i$ with respect to ψ_{lj}^i is a matrix with the same dimensions as $\mathbf{\Psi}_a^i$ and with a unit value at the location (l, j); the remainder of the terms equal 0. The derivative of the matrix, $\mathbf{\Psi}_s^i$ (i.e., $\frac{\mathrm{d}\mathbf{\Psi}_s^i}{\mathrm{d}\psi_{lj}^i}$) can be obtained as part of the derivative $\frac{\mathrm{d}\mathbf{\Psi}_a^i}{\mathrm{d}\psi_{lj}^i}$.

As defined in Eq. (2.27), the residual attachment mode $\mathbf{\Psi}_{ra}$ is obtained by subtracting the contribution of the kept eigenmodes from the attachment modes. Hence, $\mathbf{\Psi}_{ra}$ is a function of the attachment modes. By using Eq. (2.27), the derivative of the residual attachment modes $\mathbf{\Psi}_{ra}^i$ with respect to the static-mode components ψ_{lj}^i can be written as

$$\frac{\mathrm{d}\mathbf{\Psi}_{ra}^i}{\mathrm{d}\psi_{lj}^i} = \frac{\mathrm{d}\mathbf{\Psi}_a^i}{\mathrm{d}\psi_{lj}^i} - \frac{\mathrm{d}}{\mathrm{d}\psi_{lj}^i}\left(\sum_k \phi_k^i \left(\lambda_k^i\right)^{-1} \phi_{sk}^{i^T}\right) \tag{3.41}$$

The derivative of the second term is equal to 0. Therefore, Eq. (3.41) can be simplified to

$$\frac{\mathrm{d}\mathbf{\Psi}_{ra}^i}{\mathrm{d}\psi_{lj}^i} = \frac{\mathrm{d}\mathbf{\Psi}_a^i}{d\psi_{lj}^i} \tag{3.42}$$

The above equation clearly shows that the derivatives of $\mathbf{\Psi}_s^i$ and $\mathbf{\Psi}_{s_{ra}}^i$ with respect to ψ_{lj}^i are the same and can be obtained as part of the derivatives of $\mathbf{\Psi}_a^i$ and $\mathbf{\Psi}_{ra}^i$.

3.2.4 Sensitivity Analysis in Multilevel Component Mode Synthesis

As explained in section 2.7, in the first level of component mode synthesis the eigenmodes and the static modes of the components are obtained with finite-element analysis. Then, component mode synthesis is performed to obtain the eigenmodes of the subassemblies. These eigenmodes will be used directly as the basis vectors in the next level of component mode synthesis, along with the attachment modes of the subassemblies, which are also obtained by performing the static substructuring procedure given in section 2.7.

The sensitivity derivatives of both the eigenvalues and the eigenvectors of the subassemblies with respect to the component responses are calculated at each level of the component mode synthesis. Hence, to obtain the sensitivity derivatives of the eigenvalues and the eigenvectors of the global structure with respect to the responses of the individual components at the lowest level, the chain rule of differentiation is used.

For example, if the global structure "g" has a subassembly "a" as a component that in turn has a structure α as a component, then the derivatives of the eigenvalues λ^g of the global structure "g" with respect to the responses λ^α, $\mathbf{\Phi}^\alpha$, and $\mathbf{\Psi}^\alpha$ of component α can be written as

$$\begin{Bmatrix} \frac{d\lambda^g}{d\lambda^\alpha} \\ \frac{d\lambda^g}{d\Phi_s^\alpha} \\ \frac{d\lambda^g}{d\Psi_s^\alpha} \end{Bmatrix} = \begin{bmatrix} \frac{\partial\lambda^a}{\partial\lambda^\alpha} & \frac{\partial\Phi_s^a}{\partial\lambda^\alpha} & \frac{\partial\Psi_s^a}{\partial\lambda^\alpha} \\ \frac{\partial\lambda^a}{\partial\Phi_s^\alpha} & \frac{\partial\Phi_s^a}{\partial\Phi_s^\alpha} & \frac{\partial\Psi_s^a}{\partial\Phi_s^\alpha} \\ \frac{\partial\lambda^a}{\partial\Psi_s^\alpha} & \frac{\partial\Phi_s^a}{\partial\Psi_s^\alpha} & \frac{\partial\Psi_s^a}{\partial\Psi_s^\alpha} \end{bmatrix} \begin{Bmatrix} \frac{\partial\lambda^g}{\partial\lambda^\alpha} \\ \frac{\partial\lambda^g}{\partial\Phi_s^\alpha} \\ \frac{\partial\lambda^g}{\partial\Psi_s^\alpha} \end{Bmatrix} \tag{3.43}$$

Expressions for the derivatives of the eigenvectors of the global structure can be written in a similar manner.

Note that in Eq. (3.43) the derivatives of the eigenvalues λ^a and the eigenvector $\mathbf{\Phi}_s^a$ with respect to the responses of component α, which are shown in the first two columns in the Jacobian matrix, are obtained with the procedures discussed earlier in this chapter. The derivatives of the attachment-mode terms $\mathbf{\Psi}_s^a$ with respect to the eigenvalues $\frac{\partial\Psi_s^a}{\partial\lambda^\alpha}$ and the eigenvectors $\frac{\partial\Psi_s^a}{\partial\Phi_s^\alpha}$ are equal to 0 because the static mode of subassembly "a" is

obtained by performing static substructuring, which at the lowest level involves neither the eigenvalues nor the eigenvectors of the components.

However, the derivative of attachment mode Ψ_s^a, with respect to the attachment-mode terms of component α (i.e., $\frac{d\Psi_s^a}{d\Psi_s^\alpha}$), is not equal to 0. This derivative term can be obtained by differentiating the attachment mode obtained in Eqs. (2.46) and (2.47) as a result of the static substructuring technique. In the following discussion, the procedure to obtain the derivative $\frac{d\Psi_s^a}{d\Psi_s^\alpha}$ is given.

If the displacements x^α and x^β in Eqs. (2.46) and (2.47) are differentiated with respect to Ψ_s^α (i.e., the interface degrees of freedom of Ψ_I^α) (which is referred to as Ψ_{Is}^α in section 2.8 for clarity), then the following derivatives can be obtained:

$$\frac{dx^\alpha}{d\Psi_s^\alpha} = \left[\frac{d\Psi_I^\alpha}{d\Psi_s^\alpha}\right]\begin{Bmatrix}\lambda_r^\alpha\\ \lambda_{s'}^\alpha\end{Bmatrix} + [\Psi_I^\alpha]\begin{Bmatrix}\frac{d\lambda_r^\alpha}{d\Psi_s^\alpha}\\ \frac{d\lambda_{s'}^\alpha}{d\Psi_s^\alpha}\end{Bmatrix} + \begin{Bmatrix}\frac{d\psi_f^\alpha}{d\Psi_s^\alpha}\end{Bmatrix} \tag{3.44}$$

and

$$\begin{aligned}\frac{dx^\beta}{d\Psi_s^\alpha} = &\left[\frac{d\Psi_I^\alpha}{d\Psi_s^\alpha}\right]\begin{Bmatrix}\lambda_r^\beta\\ \lambda_{s'}^\beta\end{Bmatrix} + [\Psi_I^\alpha]\begin{Bmatrix}\frac{d\lambda_r^\beta}{d\Psi_s^\alpha}\\ \frac{d\lambda_{s'}^\beta}{d\Psi_s^\alpha}\end{Bmatrix}\\ &+ \begin{Bmatrix}\frac{d\psi_f^\beta}{d\Psi_s^\alpha}\end{Bmatrix} + \left[\frac{d\Psi_r^\beta}{d\Psi_s^\alpha}\right]\begin{Bmatrix}\lambda_r^\alpha\\ \lambda_{s'}^\alpha\end{Bmatrix} + \left[\Psi_r^\beta\right]\begin{Bmatrix}\frac{d\lambda_r^\alpha}{d\Psi_s^\alpha}\\ \frac{d\lambda_{s'}^\alpha}{d\Psi_s^\alpha}\end{Bmatrix}\end{aligned} \tag{3.45}$$

Note that in Eqs. (3.44) and (3.45), the derivatives of the reaction forces $\begin{Bmatrix}\lambda_r^\alpha\\ \lambda_{s'}^\alpha\end{Bmatrix}$ and $\begin{Bmatrix}\lambda_r^\beta\\ \lambda_{s'}^\beta\end{Bmatrix}$ are obtained by differentiating Eqs. (2.48) and (2.49) and using Eq. (2.50). The derivatives $\begin{Bmatrix}\frac{d\psi_f^\alpha}{d\Psi_s^\alpha}\end{Bmatrix}$ and $\begin{Bmatrix}\frac{d\psi_f^\beta}{d\Psi_s^\alpha}\end{Bmatrix}$ in Eqs. (3.44) and (3.45) are equal to 0 because the calculation of the displacement vectors ψ_f^α and ψ_f^β do not depend on the Ψ_s^α terms.

3.3 Numerical Examples

By using the presented derivations, the analytical sensitivity derivatives have been calculated for the same two sample problems discussed in chapter 2: the fixed-fixed beam and the simplified model of an engine cradle. These derivatives have been compared with those calculated with the finite-difference method.

3.3.1 Multilevel Fixed-Fixed Beam

The fixed-fixed beam is assembled in a multilevel manner as explained in the previous chapter. Hence, the derivatives of the eigenvalues and eigenvectors of the global structure with respect to the responses λ^{α}, Φ_s^{α}, and Ψ_s^{α} of component α and λ^{β}, Φ_s^{β}, and Ψ_s^{β} of component β are calculated with the chain rule of differentiation given in Eq. (3.43).

At the first level, the derivatives of the responses of structures "a" and "b" with respect to the responses of components α and β are calculated; at the second level, the derivatives of the responses of the global structure "g" with respect to the responses of structures "a" and "b" are calculated. The derivatives of the global responses with respect to the responses of components α and β are then calculated with Eq. (3.43).

All sensitivity derivatives were calculated using four eigenmodes and two attachment modes of both components at each level of the component mode synthesis. The various intermediate variables of components α and β, as well as of structures "a" and "b" are listed in the Table 3.1. Note that among the four eigenmodes used in the eigenvector expansion for component β, the first two are rigid-body modes; hence, their corresponding eigenvalues are equal to 0. Therefore, only the two eigenvalues that correspond to the flexible modes can be considered as part of the intermediate variables.

Because each component considered has two interface degrees of freedom, eight intermediate variables (from the four eigenmodes) result from the eigenvector components for each component. At each level, two attachment modes are considered for each component in the eigenvector expansion. Four intermediate variables represent the static-mode terms (which result from the two interface degrees of freedom). The interface degrees of freedom of the attachment modes are simply the part of the flexibility matrix that corresponds to those degrees of freedom; hence, it is a symmetric matrix. Therefore, among these four static-mode terms, only three are treated as part of the intermediate variables.

For structure "a," the derivatives of the first four eigenvalues λ^a with respect to the responses λ, Φ_s, and Ψ_s of both components α and β are listed in Tables 3.2–3.7. The derivatives of the eigenvector components Φ_s^a of only the first two modes with respect to the responses of the component α are listed in Tables 3.8–3.10. For the global structure "g," only the derivatives of the eigenvalues with respect to the responses of the component α are listed in Tables 3.11–3.13.

In these tables, the derivatives calculated with the finite-difference method are also listed with the analytical sensitivity derivatives. Notice that these all agree well, although the error between the analytical and the finite-difference derivatives increases in those cases in which the derivative value is small. This result can be attributed to the inappropriate step size used in calculating the finite-difference derivatives. In such cases, determination of the correct step size is difficult, which is a primary disadvantage to using the finite-difference derivatives.

These tables show that the derivatives of the eigenvalues of the structure "a" and the global structure "g" with respect to the static-mode components are more sensitive by several orders of magnitude than those with respect to the eigenvalues and eigenmode components of both components α and β. This difference can be attributed to the fact that the values of the static-mode components are smaller by several orders of magnitude than the eigenvalues and the eigenvector components.

3.3.2 Simplified Model of Engine Cradle

The simplified model of an engine cradle is shown in Fig. 2.5. As explained in the previous chapter, this structure was assembled from four components in one level. The number of eigenmodes and attachment modes used as the basis vectors in the component mode synthesis are given in Table 3.14. This table also lists the various intermediate variables for each component.

Because components 1 and 2 are unconstrained, the first six eigenmodes of these two components are rigid-body modes. Hence, among the respective 9 and 10 eigenvalues considered, only 3 and 4, respectively, can be treated as intermediate variables. Each component has 2 interfaces; each interface has 6 degrees of freedom. Therefore, each component has 12 interface degrees of freedom. The total number of eigenmode components for each component is given in Table 3.14. These totals are the product of the number of eigenmodes and the 12 interface degrees of freedom.

Although 12 interface degrees of freedom exist, only 6 attachment modes of each component are considered as basis vectors in the component mode synthesis. Because components 1 and 2 are unconstrained, their attachment modes are obtained by constraining the nodes at A and D and applying unit forces at nodes B and C, respectively. Therefore, the values of the attachment modes that correspond to nodes B and C are treated as the intermediate variables. As mentioned earlier, the 6×6 matrix of the interface degrees of freedom of the attachment modes is simply the part of flexibility matrix that corresponds to those interface degrees of freedom. Therefore, among the 37 components, only 21 are treated as independent variables (see Table 3.14). For components 3 and 4, the six attachment modes were obtained by applying the unit forces at nodes A and B. Therefore, of the 37 components of the attachment modes that correspond to these nodes only 21 are treated as intermediate variables. In addition, 36 components from the 6 interface degrees of freedom of the 6 attachment modes also must be considered as intermediate variables.

The derivatives of the eigenvalues and eigenvectors of the global structure with respect to each variable have been computed. However, not all of the derivatives are shown here. Only the derivatives of the first two eigenvalues of the global structure with respect to a selected few intermediate variables are listed in Tables 3.15, 3.16, 3.17, and 3.18 for the four components, respectively. The intermediate variables considered for each component are the first three elastic eigenvalues, the 6 interface degrees of freedom

of the first eigenmode, and the 6 interface degrees of freedom of the first attachment mode. The derivatives computed with finite differences are also listed with the analytical derivatives. Note that the analytical derivatives agree well with those calculated with the finite differences.

Table 3.1 Number of Intermediate Variables
of Various Components of Fixed-Fixed Beam

Component	No. of eigen-modes	No. of attachment modes	No. of intermediate variables: Eigenvalues λ^i	Eigenvector compo-nents Φ_s^i	Static-mode components Ψ_s^i	Total
α	4	2	4	8	3	15
β	4	2	2	8	3	13
"a"	4	2	4	8	3	15
"b"	4	2	4	8	3	15

Table 3.2 Derivatives of Eigenvalues of Structure
"a" With Respect to Eigenvalues of Component α

Intermediate variable	$\frac{\partial\lambda_1^a}{\partial\lambda^\alpha}$	$\frac{\partial\lambda_2^a}{\partial\lambda^\alpha}$	$\frac{\partial\lambda_3^a}{\partial\lambda^\alpha}$	$\frac{\partial\lambda_4^a}{\partial\lambda^\alpha}$
Analytical				
λ_1^α	3.532057 E–02	-1.120160 E+01	-6.160168 E+01	-2.409820 E+03
λ_2^α	1.770000 E–06	1.963397 E–02	4.991824 E–01	-2.127472 E+00
λ_3^α	8.7 E–09	9.464000 E–05	1.507820 E–03	2.708106 E–01
λ_4^α	3.0 E–10	3.685800 E–06	8.543920 E–05	1.986837 E–03
Finite difference				
λ_1^α	3.531646 E–02	-1.120161 E+01	-6.160213 E+01	-2.409842 E+03
λ_2^α	1.670000 E–06	1.963306 E–02	4.991833 E–01	-2.127468 E+00
λ_3^α	1.91 E–08	9.467000 E–05	1.508150 E–03	2.708100 E–01
λ_4^α	2.5 E–10	3.632600 E–06	8.547400 E–05	1.986772 E–03

Table 3.3(a) Derivatives of Eigenvalues of Structure "a" With Respect to Eigenvector of Component α (Analytical)

Intermediate variable	$\frac{\partial\lambda_1^a}{\partial\Phi_s^\alpha}$	$\frac{\partial\lambda_2^a}{\partial\Phi_s^\alpha}$	$\frac{\partial\lambda_3^a}{\partial\Phi_s^\alpha}$	$\frac{\partial\lambda_4^a}{\partial\Phi_s^\alpha}$
$\Phi_s^\alpha(1,1)$	6.044009 E–02	9.847118 E–07	2.242507 E–09	2.300111 E–11
$\Phi_s^\alpha(2,1)$	6.617114 E–04	–2.265993 E–08	–2.080772 E–10	–9.540830 E–12
$\Phi_s^\alpha(1,2)$	–7.839118 E–01	1.432091 E–03	4.732553 E–06	1.559575 E–07
$\Phi_s^\alpha(2,2)$	–3.652602 E–02	5.189506 E–05	1.646373 E–07	5.152688 E–09
$\Phi_s^\alpha(1,3)$	1.474008 E–00	–2.287280 E–03	5.221901 E–05	2.178695 E–06
$\Phi_s^\alpha(2,3)$	7.757073 E–02	–3.211285 E–05	2.884335 E–06	1.211914 E–07
$\Phi_s^\alpha(1,4)$	–3.348313 E–00	1.725768 E–03	4.873722 E–04	–6.547771 E–06
$\Phi_s^\alpha(2,4)$	–3.850829 E–01	2.119741 E–06	5.662088 E–05	–3.544489 E–07

Table 3.3(b) Derivatives of Eigenvalues of Structure "a" With Respect to Eigenvector of Component α (Finite Difference)

Intermediate variable	$\frac{\partial\lambda_1^a}{\partial\Phi_s^\alpha}$	$\frac{\partial\lambda_2^a}{\partial\Phi_s^\alpha}$	$\frac{\partial\lambda_3^a}{\partial\Phi_s^\alpha}$	$\frac{\partial\lambda_4^a}{\partial\Phi_s^\alpha}$
$\Phi_s^\alpha(1,1)$	6.043943 E–02	9.851257 E–07	1.632942 E–09	1.535553 E–11
$\Phi_s^\alpha(2,1)$	6.617036 E–04	–2.264716 E–08	–2.265637 E–10	–9.881390 E–12
$\Phi_s^\alpha(1,2)$	–7.839069 E–01	1.432073 E–03	4.733012 E–06	1.562369 E–07
$\Phi_s^\alpha(2,2)$	–3.652552 E–02	5.189441 E–05	1.646413 E–07	5.155551 E–09
$\Phi_s^\alpha(1,3)$	1.474070 E–00	–2.287229 E–03	5.221844 E–05	2.178472 E–06
$\Phi_s^\alpha(2,3)$	7.757367 E–02	–3.211023 E–05	2.884299 E–06	1.211836 E–07
$\Phi_s^\alpha(1,4)$	–3.349934 E–00	1.725691 E–03	4.873710 E–04	–6.547651 E–06
$\Phi_s^\alpha(2,4)$	–3.852124 E–01	2.114862 E–06	5.662066 E–05	–3.544438 E–07

Table 3.4 Derivatives of Eigenvalues of Structure "a"
With Respect to Static-Mode Terms of Component α

Intermediate Variable	$\frac{\partial\lambda_1^a}{\partial\Psi_s^\alpha}$	$\frac{\partial\lambda_2^a}{\partial\Psi_s^\alpha}$	$\frac{\partial\lambda_3^a}{\partial\Psi_s^\alpha}$	$\frac{\partial\lambda_4^a}{\partial\Psi_s^\alpha}$
Analytical				
$\Psi_s^\alpha(1,1)$	–1.139885 E–01	–5.738754 E+01	–4.519597 E+02	–1.370554 E+05
$\Psi_s^\alpha(2,1)$	–7.716251 E 00	–1.074535 E+03	2.731049 E+04	–6.484738 E+05
$\Psi_s^\alpha(2,2)$	–1.305845 E+02	–5.029949 E+04	–4.125718 E+05	–7.670589 E+05
Finite difference				
$\Psi_s^\alpha(1,1)$	–1.139882 E–01	–5.738833 E+01	–4.520026 E+02	–1.368832 E+05
$\Psi_s^\alpha(2,1)$	–7.716233 E+00	–1.074553 E+03	2.731083 E+04	–6.482575 E+05
$\Psi_s^\alpha(2,2)$	–1.305845 E+02	–5.029895 E+04	–4.125615 E+05	–7.670379 E+05

Table 3.5 Derivatives of Eigenvalues of Structure
"a" With Respect to Eigenvalues of Component β

Intermediate variable	$\frac{\partial\lambda_1^a}{\partial\lambda^\beta}$	$\frac{\partial\lambda_2^a}{\partial\lambda^\beta}$	$\frac{\partial\lambda_3^a}{\partial\lambda^\beta}$	$\frac{\partial\lambda_4^a}{\partial\lambda^\beta}$
Analytical				
λ_3^β	8.589653 E–07	1.949861 E–04	2.874077 E–02	2.990145 E–01
λ_4^β	3.712000 E–10	5.558907 E–06	3.533315 E–04	5.117361 E–04
Finite difference				
λ_3^β	8.589923 E–07	1.949464 E–04	2.873601 E–02	2.989911 E–01
λ_4^β	3.849000 E–10	5.557384 E–06	3.532444 E–04	5.115890 E–04

Table 3.6(a) Derivatives of Eigenvalues of Structure "a" With Respect to Eigenvector Terms of Component β (Analytical)

Intermediate variable	$\frac{\partial\lambda_1^a}{\partial\Phi_s^\beta}$	$\frac{\partial\lambda_2^a}{\partial\Phi_s^\beta}$	$\frac{\partial\lambda_3^a}{\partial\Phi_s^\beta}$	$\frac{\partial\lambda_4^a}{\partial\Phi_s^\beta}$
$\Phi_s^\beta(1,1)$	5.925223 E–01	1.498954 E–00	–4.854015 E+00	1.086451 E–00
$\Phi_s^\beta(2,1)$	2.009327 E+01	1.839794 E+02	5.088226 E+01	1.31395 E+01
$\Phi_s^\beta(1,2)$	–2.002073 E–01	2.291677 E–00	–5.454496 E+01	–1.178137 E+01
$\Phi_s^\beta(2,2)$	–6.7896 E+00	2.557804 E+02	1.095266 E+03	–1.347831 E+02
$\Phi_s^\beta(1,3)$	–2.7012 E–04	2.487325 E–02	-5.50617 E–00	–8.557840 E+01
$\Phi_s^\beta(2,3)$	–5.7941 E–04	6.337824 E–01	5.374667 E+01	–3.919670 E+02
$\Phi_s^\beta(1,4)$	–4.9475 E–06	5.124522 E–03	9.284865 E–01	3.0209225 E–00
$\Phi_s^\beta(2,4)$	–1.2688 E–05	–3.09376 E–02	–6.60923 E–01	4.240216 E–00

Table 3.6(b) Derivatives of Eigenvalues of Structure "a" With Respect to Eigenvector Terms of Component β (Finite Difference)

Intermediate variable	$\frac{\partial\lambda_1^a}{\partial\Phi_s^\beta}$	$\frac{\partial\lambda_2^a}{\partial\Phi_s^\beta}$	$\frac{\partial\lambda_3^a}{\partial\Phi_s^\beta}$	$\frac{\partial\lambda_4^a}{\partial\Phi_s^\beta}$
$\Phi_s^\beta(1,1)$	5.931926 E–01	1.509513 E–00	–4.855410 E+00	1.086684 E–00
$\Phi_s^\beta(2,1)$	2.009335 E+01	1.839801 E+02	5.088146 E+01	1.313799 E+01
$\Phi_s^\beta(1,2)$	–2.002058 E–01	2.291683 E–00	–5.454113 E+01	–1.174945 E+01
$\Phi_s^\beta(2,2)$	–6.789600 E+00	2.557763 E+02	1.095249 E+03	–1.347997 E+02
$\Phi_s^\beta(1,3)$	–2.700820 E–04	2.487636 E–02	–5.506303 E–00	–8.557882 E+01
$\Phi_s^\beta(2,3)$	–5.928990 E–04	6.338568 E–01	5.374700 E+01	–3.919643 E+02
$\Phi_s^\beta(1,4)$	–4.099800 E–06	5.128111 E–03	9.284900 E–01	3.020980 E–00
$\Phi_s^\beta(2,4)$	–8.925800 E–06	–3.091684 E–02	–6.609030 E–01	4.240214 E–00

Table 3.7 Derivatives of Eigenvalues of Structure "a"
With Respect to Static Mode Terms of Component β

Intermediate variable	$\frac{\partial \lambda_1^a}{\partial \Psi_s^\beta}$	$\frac{\partial \lambda_2^a}{\partial \Psi_s^\beta}$	$\frac{\partial \lambda_3^a}{\partial \Psi_s^\beta}$	$\frac{\partial \lambda_4^a}{\partial \Psi_s^\beta}$
Analytical				
$\Psi_s^\beta(1,1)$	−8.546972 E−02	−1.088662 E+01	2.672391 E+02	−6.830298 E+02
$\Psi_s^\beta(2,1)$	−7.210331 E+00	−1.477204 E+03	1.179341 E+04	−3.893229 E+04
$\Psi_s^\beta(2,2)$	−1.303280 E+02	−4.924907 E+04	−2.750050 E+05	−1.901346 E+05
Finite difference				
$\Psi_s^\beta(1,1)$	−8.546938 E−02	−1.088667 E+01	2.672046 E+02	−6.832358 E+02
$\Psi_s^\beta(2,1)$	−7.210203 E+00	−1.477210 E+03	1.179479 E+04	−3.892493 E+04
$\Psi_s^\beta(2,2)$	−1.303226 E+02	−4.924877 E+04	−2.750018 E+05	−1.901340 E+05

Table 3.8 Derivatives of Eigenvector Components of Structure "a" With Respect to Eigenvalues of Component α

Intermediate variable	$\frac{\partial \Phi_s^a(1,1)}{\partial \lambda^\alpha}$	$\frac{\partial \Phi_s^a(2,1)}{\partial \lambda^\alpha}$	$\frac{\partial \Phi_s^a(1,2)}{\partial \lambda^\alpha}$	$\frac{\partial \Phi_s^a(2,2)}{\partial \lambda^\alpha}$
Analytical				
λ_1^α	6.044009 E–02	6.617114 E–04	-7.839118 E–01	-3.652602 E–02
λ_2^α	9.847118 E–07	–2.26599 E–08	1.432090 E–03	5.189506 E–05
λ_3^α	2.242500 E–09	-2.081000 E–10	4.732553 E–06	1.646373 E–07
λ_4^α	2.30000 E–11	-9.500000 E–12	1.559575 E–07	5.152700 E–09
Finite difference				
λ_1^α	6.043942 E–02	6.617036 E–04	–7.839069 E–01	–3.652552 E–02
λ_2^α	9.851257 E–07	–2.264720 E–08	1.432073 E–03	5.189441 E–05
λ_3^α	1.632900 E–09	-2.266000 E–10	4.733012 E–06	1.646413 E–07
λ_4^α	1.540000 E–11	-9.900000 E–12	1.562369 E–07	5.155600 E–09

Table 3.9 Derivatives of Eigenmode Components of Structure "a" With Respect to Eigenmode Terms of Component α

Intermediate variable	$\frac{\partial \Phi_s^a(1,1)}{\partial \Phi_s^a}$	$\frac{\partial \Phi_s^a(2,1)}{\partial \Phi_s^a}$	$\frac{\partial \Phi_s^a(1,2)}{\partial \Phi_s^a}$	$\frac{\partial \Phi_s^a(2,2)}{\partial \Phi_s^a}$
Analytical				
$\Phi_s^\alpha(1,1)$	-6.888392 E-02	-1.133962 E-03	2.124441 E+00	1.031761 E-01
$\Phi_s^\alpha(2,1)$	-9.350915 E-01	1.492655 E-02	3.188079 E+01	1.911615 E+00
$\Phi_s^\alpha(1,2)$	5.202530 E-05	6.248000 E-07	2.752054 E-02	1.147562 E-03
$\Phi_s^\alpha(2,2)$	1.849556 E-04	-3.901530 E-05	9.621387 E-01	3.247800 E-02
Finite difference				
$\Phi_s^\alpha(1,1)$	-6.888432 E-02	-1.133972 E-03	2.124438 E+00	1.031759 E-01
$\Phi_s^\alpha(2,1)$	-9.350801 E-01	1.492718 E-02	3.188110 E+01	1.911622 E+00
$\Phi_s^\alpha(1,2)$	5.152590 E-05	6.079000 E-07	2.751913 E-02	1.147560 E-03
$\Phi_s^\alpha(2,2)$	1.836818 E-04	-3.902680 E-05	9.620819 E-01	3.247703 E-02

Table 3.10 Derivatives of Eigenmode Components of Structure "a" With Respect to Static-Mode Terms of Component α

Intermediate variable	$\frac{\partial \Phi_s^a(1,1)}{\partial \Psi_s^\alpha}$	$\frac{\partial \Phi_s^a(2,1)}{\partial \Psi_s^\alpha}$	$\frac{\partial \Phi_s^a(1,2)}{\partial \Psi_s^\alpha}$	$\frac{\partial \Phi_s^a(2,2)}{\partial \Psi_s^\alpha}$
Analytical				
$\Psi_s^\alpha(1,1)$	–4.153998 E–02	–3.323766 E–03	–9.448765 E–01	–4.435696 E–02
$\Psi_s^\alpha(2,1)$	6.141835 E–00	1.168296 E–01	–8.252026 E+01	–3.925563 E–00
$\Psi_s^\alpha(2,2)$	2.554581 E+02	7.761585 E–00	5.920813 E+02	2.293785 E+01
Finite difference				
$\Psi_s^\alpha(1,1)$	–4.154025 E–02	–3.323698 E–03	–9.450594 E–01	–4.436457 E–02
$\Psi_s^\alpha(2,1)$	6.141586 E–00	1.168254 E–01	–8.251317 E+01	–3.925083 E–00
$\Psi_s^\alpha(2,2)$	2.554552 E+02	7.761514 E–00	5.919300 E+02	2.293280 E+01

Table 3.11 Derivatives of Eigenvalues of Structure "g" With Respect to Eigenvalues of Component α

Intermediate variable	$\frac{\partial\lambda_1^g}{\partial\lambda^\alpha}$	$\frac{\partial\lambda_2^g}{\partial\lambda^\alpha}$	$\frac{\partial\lambda_3^g}{\partial\lambda^\alpha}$	$\frac{\partial\lambda_4^g}{\partial\lambda^\alpha}$
Analytical				
λ_1^α	6.328365 E–02	5.588829 E–07	–1.002730 E–08	1.123700 E–09
λ_2^α	6.474562 E–01	1.454832 E–03	9.153085 E–06	3.972362 E–07
λ_3^α	–2.509079 E+01	3.941295 E–02	7.197233 E–05	3.338799 E–06
λ_4^α	–5.728619 E+01	2.055320 E–01	–4.007656 E–05	2.170278 E–06
Finite difference				
λ_1^α	6.327800 E–02	5.587554 E–07	–1.008060 E–08	1.133500 E–09
λ_2^α	6.473540 E–01	1.454550 E–03	9.157439 E–06	4.033748 E–07
λ_3^α	–2.508893 E+01	3.940768 E–02	7.195915 E–05	3.341011 E–06
λ_4^α	–5.728810 E+01	2.055202 E–01	–3.987281 E–05	2.384566 E–06

Table 3.12(a) Derivatives of Eigenvalues of Structure "g"
With Respect to Eigenvector Terms of Component α (Analytical)

Intermediate variable	$\frac{\partial\lambda_1^g}{\partial\Phi_s^\alpha}$	$\frac{\partial\lambda_2^g}{\partial\Phi_s^\alpha}$	$\frac{\partial\lambda_3^g}{\partial\Phi_s^\alpha}$	$\frac{\partial\lambda_4^g}{\partial\Phi_s^\alpha}$
$\Phi_s^\alpha(1,1)$	−1.411695 E−01	−5.822620 E−02	7.253010 E+01	2.295159 E+02
$\Phi_s^\alpha(2,1)$	4.276940 E−00	3.317886 E+02	1.270823 E+03	−2.534124 E+03
$\Phi_s^\alpha(1,2)$	−7.103160 E−05	−3.246840 E−04	1.075163 E−00	1.074896 E+01
$\Phi_s^\alpha(2,2)$	1.897514 E−03	1.680189 E−00	1.857646 E+01	−1.194501 E+02
$\Phi_s^\alpha(1,3)$	−1.042070 E−05	−4.090610 E−05	1.073423 E−02	−1.937798 E−02
$\Phi_s^\alpha(2,3)$	1.936337 E−04	4.960991 E−02	4.3130840 E−01	2.703940 E−01
$\Phi_s^\alpha(1,4)$	−2.953000 E−07	5.827000 E−07	1.990533 E−03	−4.359099 E−03
$\Phi_s^\alpha(2,4)$	1.673850 E−05	5.438180 E−03	3.252901 E−02	5.534037 E−02

Table 3.12(b) Derivatives of Eigenvalues of Structure "g" With
Respect to Eigenvector Terms of Component α (Finite difference)

Intermediate variable	$\frac{\partial\lambda_1^g}{\partial\Phi_s^\alpha}$	$\frac{\partial\lambda_2^g}{\partial\Phi_s^\alpha}$	$\frac{\partial\lambda_3^g}{\partial\Phi_s^\alpha}$	$\frac{\partial\lambda_4^g}{\partial\Phi_s^\alpha}$
$\Phi_s^\alpha(1,1)$	−1.411695 E−01	−5.819430 E−02	7.253010 E+01	2.295159 E+02
$\Phi_s^\alpha(2,1)$	4.276893 E−00	3.317844 E+02	1.270823 E+03	−2.534124 E+03
$\Phi_s^\alpha(1,2)$	−7.070650 E−05	−2.486184 E−04	1.075163 E−00	1.074896 E+01
$\Phi_s^\alpha(2,2)$	1.901284 E−03	1.680162 E−00	1.857646 E+01	−1.194501 E+02
$\Phi_s^\alpha(1,3)$	−1.070230 E-05	−4.090610 E-05	1.073423 E-02	−1.937798 E-02
$\Phi_s^\alpha(2,3)$	1.944564 E−04	4.960991 E−02	4.313084 E−01	2.703940 E−01
$\Phi_s^\alpha(1,4)$	−1.418000 E−07	5.827000 E−07	1.990533 E−03	−4.359099 E−03
$\Phi_s^\alpha(2,4)$	1.629280 E−05	5.438180 E−03	3.252901 E−02	5.534037 E−02

Table 3.13 Derivatives of Eigenvalues of Structure "g"
With Respect to Static-Mode Terms of Component α

Intermediate variable	$\frac{\partial \lambda_1^g}{\partial \Psi_s^\alpha}$	$\frac{\partial \lambda_2^g}{\partial \Psi_s^\alpha}$	$\frac{\partial \lambda_3^g}{\partial \Psi_s^\alpha}$	$\frac{\partial \lambda_4^g}{\partial \Psi_s^\alpha}$
Analytical				
$\Psi_s^\alpha(1,1)$	–3.459955 E–01	5.480197 E–04	–4.256311 E+01	–2.140266 E+02
$\Psi_s^\alpha(2,1)$	2.095946 E+01	4.157938 E+03	–1.503743 E+03	4.728299 E+03
$\Psi_s^\alpha(2,2)$	–3.175394 E+02	–1.216943 E+04	–1.281498 E+04	–2.619165 E+04
Finite difference				
$\Psi_s^\alpha(1,1)$	–3.459994 E–01	5.690741 E–04	–4.256395 E+01	–2.140301 E+02
$\Psi_s^\alpha(2,1)$	2.095959 E+01	4.162427 E+03	–1.503711 E+03	4.728587 E+03
$\Psi_s^\alpha(2,2)$	–3.175376 E+02	–1.216898 E+04	–1.281469 E+04	–2.618014 E+04

Table 3.14 Number of Intermediate Variables
of Various Components of the Engine Cradle

Component	No. of eigen-modes	No. of attachment modes	No. of intermediate variables: Eigenvalues λ^i	Eigenvector compo-nents Φ_s^i	Static-mode components Ψ_s^i	Total
1	9	6	3	108	21	132
2	10	6	4	120	21	145
3	5	6	5	60	57	122
4	5	6	5	60	57	122

Table 3.15 Derivatives of Eigenvalues of Structure "g"
With Respect to Intermediate Variables of Component 1

Intermediate variable	Analytical		Finite difference	
	$\frac{\partial \lambda_1^g}{\partial u}$	$\frac{\partial \lambda_2^g}{\partial u}$	$\frac{\partial \lambda_1^g}{\partial u}$	$\frac{\partial \lambda_2^g}{\partial u}$
λ_1^1	2.505095 E–02	2.067049 E–04	2.502283 E–02	2.064552 E–04
λ_2^1	6.353675 E–04	6.372510 E–05	6.351703 E–04	6.371020 E–05
λ_3^1	1.557000 E–06	1.261442 E–03	1.556800 E–06	1.261246 E–03
$\Phi_s^1(1,1)$	–2.009724 E+03	1.714023 E+03	–2.009594 E+03	1.713927 E+03
$\Phi_s^1(2,1)$	–1.049337 E+03	–1.317352 E+04	–1.049484 E+03	–1.317310 E+04
$\Phi_s^1(3,1)$	–2.301483 E+03	–8.027234 E+03	–2.301384 E+03	–8.027191 E+03
$\Phi_s^1(4,1)$	–1.820771 E+05	–4.811228 E+04	–1.820863 E+05	–4.816586 E+04
$\Phi_s^1(5,1)$	–1.937102 E+05	1.120235 E+06	–1.937125 E+05	1.120220 E+06
$\Phi_s^1(6,1)$	2.264321 E+05	–1.543757 E+06	2.264028 E+05	–1.543461 E+06
$\Psi_s^1(1,1)$	–9.265113 E+01	–5.418250 E+00	–9.265750 E+01	–5.440020 E+00
$\Psi_s^1(2,1)$	–2.275218 E+03	7.038891 E+03	–2.275210 E+03	7.038863 E+03
$\Psi_s^1(3,1)$	–4.813875 E+01	3.834089 E+03	–4.811324 E+01	3.834254 E+03
$\Psi_s^1(4,1)$	–9.870524 E+04	–1.863407 E+03	–9.873360 E+04	–1.831024 E+03
$\Psi_s^1(5,1)$	–3.968004 E+04	–3.472378 E+05	–3.968110 E+04	–3.472324 E+05
$\Psi_s^1(6,1)$	1.556020 E+05	4.393213 E+05	1.555981 E+05	4.393126 E+05

Table 3.16 Derivatives of Eigenvalues of Structure "g"
With Respect to Intermediate Variables of Component 2

Intermediate variable	Analytical		Finite difference	
	$\frac{\partial \lambda_1^g}{\partial u}$	$\frac{\partial \lambda_2^g}{\partial u}$	$\frac{\partial \lambda_1^g}{\partial u}$	$\frac{\partial \lambda_2^g}{\partial u}$
λ_1^2	2.076989 E–03	6.072601 E–02	2.072721 E–03	6.072081 E–02
λ_2^2	1.428901 E–03	1.062410 E–05	1.428797 E–03	1.061990 E–05
λ_3^2	7.811620 E–05	1.109410 E–04	7.808410 E–05	1.109243 E–04
$\Phi_s^2(1,1)$	7.245859 E+02	–3.184401 E+03	7.241642 E+02	–3.183047 E+03
$\Phi_s^2(2,1)$	4.486467 E+02	1.026709 E+03	4.486775 E+02	1.026807 E+03
$\Phi_s^2(3,1)$	1.553872 E+03	–1.415626 E+03	1.553781 E+03	–1.414782 E+03
$\Phi_s^2(4,1)$	–3.915090 E+05	5.478491 E+05	–3.909638 E+05	5.506580 E+05
$\Phi_s^2(5,1)$	–1.303657 E+05	-2.812268 E+05	–1.306137 E+05	–2.811797 E+05
$\Phi_s^2(6,1)$	–4.732038 E+05	6.746980 E+05	–4.731151 E+05	6.745690 E+05
$\Psi_s^2(1,1)$	1.441807 E+01	–2.193288 E+03	1.444059 E+01	–2.193339 E+03
$\Psi_s^2(2,1)$	–1.116013 E+03	1.135318 E+03	–1.115474 E+03	1.135289 E+03
$\Psi_s^2(3,1)$	–9.494662 E+01	1.147178 E+03	–9.246952 E+01	1.149739 E+03
$\Psi_s^2(4,1)$	1.288568 E+06	1.643423 E+06	1.287729 E+06	1.643021 E+06
$\Psi_s^2(5,1)$	–1.288423 E+05	–3.616315 E+05	–1.28753 E+05	–3.614096 E+05
$\Psi_s^2(6,1)$	7.483640 E+05	1.629961 E+06	7.48372 E+05	1.630005 E+06

Table 3.17 Derivatives of Eigenvalues of Structure "g"
With Respect to Intermediate Variables of Component 3

Intermediate variable	Analytical		Finite difference	
	$\frac{\partial \lambda_1^g}{\partial u}$	$\frac{\partial \lambda_2^g}{\partial u}$	$\frac{\partial \lambda_1^g}{\partial u}$	$\frac{\partial \lambda_2^g}{\partial u}$
λ_1^3	8.591723 E–02	8.603888 E–02	8.590769 E–02	8.602732 E–02
λ_2^3	8.492919 E–02	1.750348 E–01	8.492765 E–02	1.750342 E–01
λ_3^3	3.837318 E–03	8.571574 E–03	3.837130 E–03	8.571335 E–03
$\Phi_s^3(1,1)$	4.946359 E+03	–2.371328 E+03	4.946507 E+03	–2.37167 E+03
$\Phi_s^3(2,1)$	7.806596 E+01	–2.894245 E+04	7.797756 E+01	–2.894239 E+04
$\Phi_s^3(3,1)$	1.296364 E+04	2.385785 E+04	1.296372 E+04	2.385803 E+04
$\Phi_s^3(4,1)$	–1.515845 E+05	4.029027 E+05	–1.515770 E+05	4.028921 E+05
$\Phi_s^3(5,1)$	5.682340 E+05	–2.615997 E+06	5.682454 E+05	–2.616004 E+06
$\Phi_s^3(6,1)$	5.257354 E+05	–4.172757 E+06	5.257375 E+05	–4.172746 E+06
$\Psi_s^3(1,1)$	–2.421489 E+03	2.813842 E+02	–2.421221 E+03	2.804946 E+02
$\Psi_s^3(2,1)$	8.700186 E+02	–1.511053 E+03	8.706181 E+02	–1.51004 E+03
$\Psi_s^3(3,1)$	–8.621950 E+03	–7.281814 E+02	–8.621793 E+03	–7.283691 E+02
$\Psi_s^3(4,1)$	2.32692 E+05	–5.336094 E+04	2.327195 E+05	–5.332817 E+04
$\Psi_s^3(5,1)$	–4.366611 E+05	–2.772801 E+04	–4.366823 E+05	–2.762827 E+04
$\Psi_s^3(6,1)$	–4.093099 E+05	–5.864896 E+02	–4.095516 E+05	–5.245383 E+02

Table 3.18 Derivatives of Eigenvalues of Structure "g"
With Respect to Intermediate Variables of Component 4

Intermediate variable	Analytical		Finite difference	
	$\frac{\partial \lambda_1^g}{\partial u}$	$\frac{\partial \lambda_2^g}{\partial u}$	$\frac{\partial \lambda_1^g}{\partial u}$	$\frac{\partial \lambda_2^g}{\partial u}$
λ_1^4	8.150269 E–02	9.718820 E–02	8.149349 E–02	9.717429 E–02
λ_2^4	8.322837 E–02	1.788511 E–01	8.322677 E–02	1.788503 E–01
λ_3^4	4.457674 E–03	9.997060 E–03	4.457493 E–03	9.996758 E–03
$\Phi_s^4(1,1)$	–4.865338 E+03	6.523793 E+03	–4.865244 E+03	6.525877 E+03
$\Phi_s^4(2,1)$	5.020728 E+02	–3.247714 E+04	5.020858 E+02	–3.247719 E+04
$\Phi_s^4(3,1)$	–1.250571 E+04	–2.860694 E+04	–1.250572 E+04	–2.860683 E+04
$\Phi_s^4(4,1)$	–1.705342 E+05	1.155843 E+05	–1.70528 E+05	1.155814 E+05
$\Phi_s^4(5,1)$	–5.053949 E+05	3.206715 E+06	–5.053892 E+05	3.206709 E+06
$\Phi_s^4(6,1)$	5.563555 E+05	–4.649758 E+06	5.563539 E+05	–4.649748 E+06
$\Psi_s^4(1,1)$	–2.358877 E+03	2.399448 E+02	–2.358799 E+03	2.396128 E+02
$\Psi_s^4(2,1)$	–9.799586 E+02	4.095777 E+03	–9.808720 E+02	4.094903 E+03
$\Psi_s^4(3,1)$	–7.686265 E+03	3.155581 E+02	–7.685818 E+03	3.158380 E+02
$\Psi_s^4(4,1)$	–2.936333 E+05	7.455590 E+04	–2.934578 E+05	7.439130 E+04
$\Psi_s^4(5,1)$	–3.887053 E+05	–2.336486 E+05	–3.886026 E+05	–2.339284 E+05
$\Psi_s^4(6,1)$	4.452265 E+05	2.680198 E+05	4.451937 E+05	2.672992 E+05

Chapter 4

STRUCTURAL SYNTHESIS

4.1 Introduction

In many engineering applications, the selection of components for assembly into a useful structure is a more important design decision than modification of the detailed dimensions of individual members in a component. Examples in the auto industry include the selection of stiffeners to provide greater resistance to buckling in the roof of a van or the placement of engine support members in the chassis of a truck to reduce vibration. In these problems, the design variables are the components themselves, rather than the geometric details of the components.

Design optimization techniques, particularly those that are incorporated with mathematical programming techniques, have been successfully applied to the detailed design of structural components. In fact, finite-element codes are commercially available that can perform detailed structural design optimization. In these codes, the design variables represent parameters such as thickness or shape that describe the detailed dimensions of the finite elements. However, these design optimization techniques were essentially developed for the modification of existing structures to achieve better structural performance.

In a practical design environment such as the auto industry, an entirely new structure must be built for each new automobile model. Usually, this new structure is built by assembling the components of various structural members from existing models. However, no systematic way has been devised so far to determine the optimal combination that will produce responses closest to the desired performance. Desired performance is usually obtained by trial and error. By choosing from the available choices for

different components and then testing the possible combinations, engineers come up with a structure that produces responses closest to the desired characteristics. Existing design optimization techniques cannot be applied to this type of structural synthesis problem for two reasons. First, existing methods are unable to treat each individual component as a design entity. Second, the design variables are simply the various choices available for each component; hence, they are integers, whereas existing design optimization techniques can only handle continuous variables.

In this chapter, a structural synthesis tool is developed by incorporating the component mode synthesis technique with a genetic algorithm. As discussed in previous chapters, the method of component mode synthesis enables individual components to be treated as design entities. Hence, this technique is used here as the reanalysis tool for vibration analysis of the assembled structure, in which various component members are represented by their responses. A genetic algorithm [34] is used as an integer programming technique to handle the various component choices as design variables. The next section discusses how the component mode synthesis technique can be used as a fast reanalysis technique in conjunction with the genetic algorithm. The basic procedure for genetic algorithms is reviewed briefly in section 4.3. Section 4.4 discusses the proposed structural synthesis technique in detail. In section 4.5, the proposed method is applied to determine the optimal cross members and their locations in a simplified model of an engine cradle.

4.2 Component Mode Synthesis as Reanalysis Technique

Previous chapters have discussed how an individual component can be successfully characterized as a design entity with the component mode synthesis technique. This eliminates the major difficulty in solving the structural synthesis problem stated above. The reduced eigenvalue problem given in Eq. (2.41) states the relationship between the global responses (e.g., eigenvalues and eigenvectors) and the individual component

responses because the generalized stiffness and mass matrices in Eq. (2.41) are functions of the responses of the components that comprise the assembled structure.

After the candidate components have been analyzed independently for the required responses, the eigenvalues and eigenvectors for each possible assembly of the global structure can be obtained repetitively by solving a new reduced eigenvalue problem (i.e., Eq. (2.41)). Furthermore, as discussed in section 2.4, the constituent terms of the coefficient matrices of the reduced eigenvalue problem can be reduced to a simpler form. As a result, the required component responses can be obtained by testing the respective components. In the auto industry, test data for existing components of various structural members are typically available.

This repetitive calculation of the global structure responses can be viewed as an efficient reanalysis technique for two reasons. First, the individual components are analyzed once for the required responses, and the same responses are used whenever this particular component is chosen as a part of an assembly. Second, if a particular component in the assembly is replaced by a different selection, then only the responses that belong to that particular component in Eq. (2.41) must be replaced by new values to produce a new reduced eigenvalue problem. This reduced eigenvalue problem is solved to obtain a new set of global eigenvalues and eigenvectors without the reanalysis of the other components in the assembly.

4.3 Genetic Algorithm

A genetic algorithm is a numerical procedure that produces a set of better designs based on the process of natural evolution (i.e., Darwin's theory of the survival of the fittest) [34]. The process of evolution primarily relies on the random generation of new designs, from which only the superior designs will survive to participate in future reproduction processes. Initially, a set of designs called the "population" of designs for this algorithm is generated randomly. The designs are then evaluated and ranked

according to certain design criteria before the reproduction process begins. The designs in this population will then be randomly selected, with favor given to the superior designs, to mate (called "crossover" in genetic algorithm terminology) and produce a new set of designs. The new designs are again randomly selected to undergo other reproductive mechanisms such as mutation and permutation, which are commonly found in the process of evolution.

Genetic algorithms have been applied to many engineering design optimization problems and have proved effective for both nonconvex and nondifferentiable types of problems. The most attractive feature of such algorithms is that they have the ability to locate the global minimum, whereas gradient-based algorithms are susceptible to convergence to a local minimum. Because genetic algorithms work on Darwin's theory, the good chromosomes, called "schema," which are attributed to the good characteristics of the design, will be preserved and will accumulate throughout the reproduction process to eventually lead to the best global design.

A string of integers is usually used in a genetic algorithm to symbolically represent an individual design. The integers play the role of the chromosomes in biology. The determination of the correspondence between the integers and the numerical values of the physical design variables is called the coding process. For example, a design alternative for a 10-bar truss can be represented by a string of 10 integers. If each integer ranges from 1 to 4, then each truss member has up to four possibilities in its properties and size.

The reproduction process is performed by manipulating the chromosomes (i.e., the integers in a genetic algorithm) of the parent designs. Three major operations are implemented in this study for this manipulation: crossover, mutation, and permutation. The determination of whether any of these operations will be activated to modify the designs is, again, a random process.

The crossover is simply a mating process in biological terms. In this operation, chromosomes from a pair of parent designs will be exchanged to produce child designs.

The crossover points are determined randomly. The mutation is modeled after the sudden change in chromosomes in biology. Any integer in a design string can be selected to undergo a random change. Again, the integer selected for change is also determined randomly. The permutation operation reverses the order of the chromosomes in a design string.

After the child designs have been populated, a genetic algorithm will evaluate, rank, and select some to produce the next generation. The life cycle continues until no improvement is realized within a certain predetermined number of consecutive generations. The computational flow chart of a basic genetic algorithm is shown in Fig. 4.1.

Even though genetic algorithms are simple to implement, the result depends primarily on certain input parameters, such as the size of the population and the parameters that control the occurrence of certain reproductive processes. A smaller population may not produce better designs. On the other hand, a larger population may require a larger number of function evaluations; hence, more computational time is required. In general, a population size equal to three times the length of the integer string is recommended. In addition, during the reproduction process, a high probability should be assigned to the crossover and permutation processes, and a low possibility should be assigned to mutation process.

A genetic algorithm ranks the performance of each design by evaluating a single-valued function. Hence, it can be directly applied to an unconstrained minimization problem. To solve the constrained minimization problem, the problem must be converted into an equivalent unconstrained minimization problem by using the penalty function method. For example, a typical constrained minimization problem can be stated as

$$\min_{b} \quad F(b) \tag{P4.1}$$

subject to

$$g_i(b) < 0 \qquad (i = 1, 2, ...p)$$

$$h_j(b) = 0 \qquad (j = 1, 2, ...q)$$

where *F(b)* is the objective function, b are the design variables, and g and h are the inequality and equality constraints, respectively. This constrained minimization problem can be converted to an equivalent unconstrained minimization problem by using a penalty function. For example, by using an exterior penalty function the problem can be written as

$$\min_b \quad \Psi(b) = F(b) + r\sum_{i=1}^{p}(g_i + |g_i|) + s\sum_{j=1}^{q}|h_j| \qquad \text{(P4.2)}$$

where r and s are the penalty coefficients that are used to penalize those designs that violate the constraints. Now, the single-valued merit function Ψ can be directly used to rank various designs in the population.

4.4 Proposed Methodology

When a new structure must be synthesized, the performance criteria that must be satisfied by the structure should be defined. For example, the first eigenvalue of the structure must be as high as possible. Then, the possible topology of the structure must be defined, based on considerations such as spatial requirements. After the topology has been identified, the possible choices for various components of the global structure can be selected from the available set of components. The selected components must be analyzed independently for the required vibration and static responses. The responses of the respective components are stored in a data bank for future use in component mode synthesis. The required responses of the components can be obtained either by actually testing the components or by a numerical simulation (e.g., finite-element analysis). Usually, in the auto industry, the test data for the different components of various structural members of existing models is readily available. After the required data

for the individual components are available, component mode synthesis can be performed to efficiently obtain the global responses (e.g., the eigenvalues and eigenvectors) of any possible structure that is composed of the available components.

The problem of selecting components from the available choices to form the global structure can be translated into an integer programming problem by defining the length of the design string to be equal to the number of actual components in the structure. If some components are specified a priori, then the length of the string will be equal to only the number of components that must be selected. For each of these components, many choices may be available. For example, let m be the number of available choices. These choices are numbered from 1 to m, respectively, so that the particular selection of components for a design can be represented in the design string by the corresponding number.

A flowchart for structural synthesis is shown in Fig. 4.2. Notice from this chart that the initial population of designs for the global structure, which is a set of possible combinations of various available components, is randomly generated by the genetic algorithm in this study. These global structure assemblies are analyzed by using component mode synthesis, which utilizes the responses from the various components that are available in the data bank, as the fast reanalysis technique (FRT). The resulting responses of the global structures are supplied to the genetic algorithm. The genetic algorithm ranks the various designs based on the predetermined performance criteria and generates a new set of designs that simulates the natural reproduction processes described in section 4.3. These new global structure designs are evaluated again by the FRT, and the responses are supplied back to the genetic algorithm. The loop between the genetic algorithm and the FRT continues until no improvement is found in the performance of the optimal structure within a predetermined number of successive generations.

4.5 Numerical Example

The procedure for structural synthesis discussed above has been applied to a simplified model of an engine cradle to determine the particular set of engine support members and their location such that the vibration of the engine cradle is minimized.

As shown in Fig. 4.3, the structure has a total of four components. Components 3 and 4 are predetermined; components 1 and 2 are the cross members that must be selected by the genetic algorithm. For convenience, the two cross members are referred to as cm_1 and cm_2, respectively. Each cross member has four possible locations (Fig. 4.3), namely, l_{11}, l_{12}, l_{13}, and l_{14} for cm_1 and l_{21}, l_{22}, l_{23}, and l_{24} for cm_2, respectively. Each of these members can be made from four possible materials, namely, mt_1, mt_2, mt_3, and mt_4. Young's modulus and the shear modulus of the four materials considered are given in Table 4.1. For generating random numbers, the subroutine DRNUNF from IMSL Fortran libraries [35] is used.

4.5.1 Problem Statement

The structural synthesis problem is to determine the optimal location and material for each cross member of the engine cradle, such that the first eigenvalue of the structure is maximized while the second eigenvalue is maintained within a tolerance of 10 percent of the specified value λ_2^0. (For this problem, the λ_2^0 value was taken as 32251). Mathematically, this problem can be written as

$$\max \qquad \lambda_1 \tag{P4.3}$$

subject to

$$g = \left| \frac{\lambda_2 - \lambda_2^0}{\lambda_2^0} \right| - 0.1 < 0$$

4.5.2 Genetic Representation

The genetic representation for this problem is a design string that is four units long, as shown in Fig. 4.4. The first two integers in the design string correspond to the location and the type of material for the first cross member; the other two integers correspond to the location and type of material for the second cross member. Because four possible values exist for these variables, the integer values will vary from 1 to 4; the total number of possible combinations is $4^4 = 256$.

4.5.3 Solution Procedure

As mentioned in section 4.4, the selected components are analyzed for the required vibration and static responses (i.e., eigenvalues, eigenvectors, and the static modes). Components 3 and 4, which are predetermined, are also analyzed to obtain the required responses. All component responses are computed with finite-element analysis. The eigenmodes of each component are obtained by performing a normal mode analysis; the static modes (i.e., attachment modes) are obtained in the usual manner by applying a unit force at each of the interface degrees of freedom. Because both cross members are not constrained, the attachment modes of these members are obtained by constraining the rigid-body degrees of freedom at one end and applying the unit force at the other end. The responses obtained for the components are stored in the data bank for future use in component mode synthesis.

As discussed in section 4.4, the constrained minimization problem must be converted into a single-valued unconstrained minimization problem to solve this problem with the genetic algorithm. With the penalty-function method, the constrained minimization problem described in (P4.1) can be rewritten as an unconstrained minimization problem

$$\max \qquad \frac{\lambda_1}{\lambda_1^0} - r\,(g + |g|) \tag{P4.4}$$

where λ_1^0 is used to normalize the first eigenvalue and r is the penalty coefficient, which is equal to 500 in this sample problem. Notice in the above problem that the objective function will be penalized only when the constraint is violated.

4.5.4 Results

Figure 4.5 shows the optimal 20 designs (among 256 total possible design combinations) in ascending order of the first eigenvalue. This figure also shows the corresponding second eigenvalues. The designs with constraint violation (i.e., the designs whose second eigenvalues are not within the specified limits) are marked with "o" in Fig. 4.5. These designs are not considered to be the best possible designs, although the first eigenvalues have a higher value. Table 4.2 lists the values of the first and second eigenvalues of the optimal five designs. As confirmed by Fig. 4.5, the values of the first three best designs listed in Table 4.2 are close to one another. Table 4.2 also lists the location and material properties of the two cross members for the 5 best possible designs.

Because genetic algorithms are random in nature, we need to examine the consistency and the efficiency of the proposed methodology in finding the best design. To this end, a parametric study was done by changing the population size and the maximum number of successive iterations allowed without improvement (NSTOP).

The population sizes considered in this study were 8, 10, 12, and 14, and the number of successive iterations allowed without improvement was varied between 5 and 10. Furthermore, each case was run 20 times with a new initial population of designs for each new run. Table 4.3 lists the percentage of occurrence for the best three designs among the 256 possible design combinations. Table 4.3 also lists the range of analyses required to obtain a particular design.

The table clearly shows that as the size of the population is increased the probability that the genetic algorithm will find the optimal designs is increased. However, the number of analyses required to find the optimal designs is also increased. In fact, for

a population size of 14 with 10 successive iterations allowed without improvement, the proposed method can find one of the best three designs within 140 to 252 analyses. Experience shows that the appropriate population size is approximately three times the number of design variables. As shown in this study, a population size of 12 with 10 successive iterations allowed without improvement was the optimal combination to produce a population of best designs. For this case, the percentage of occurrence of the best three designs reached 90 percent, and the number of analyses required varied from 120 to 192. However, within this number of analyses, the last ten generations did not improve the design at all; therefore, in actuality the number of analyses required to determine the best design ranged only from 12 to 84.

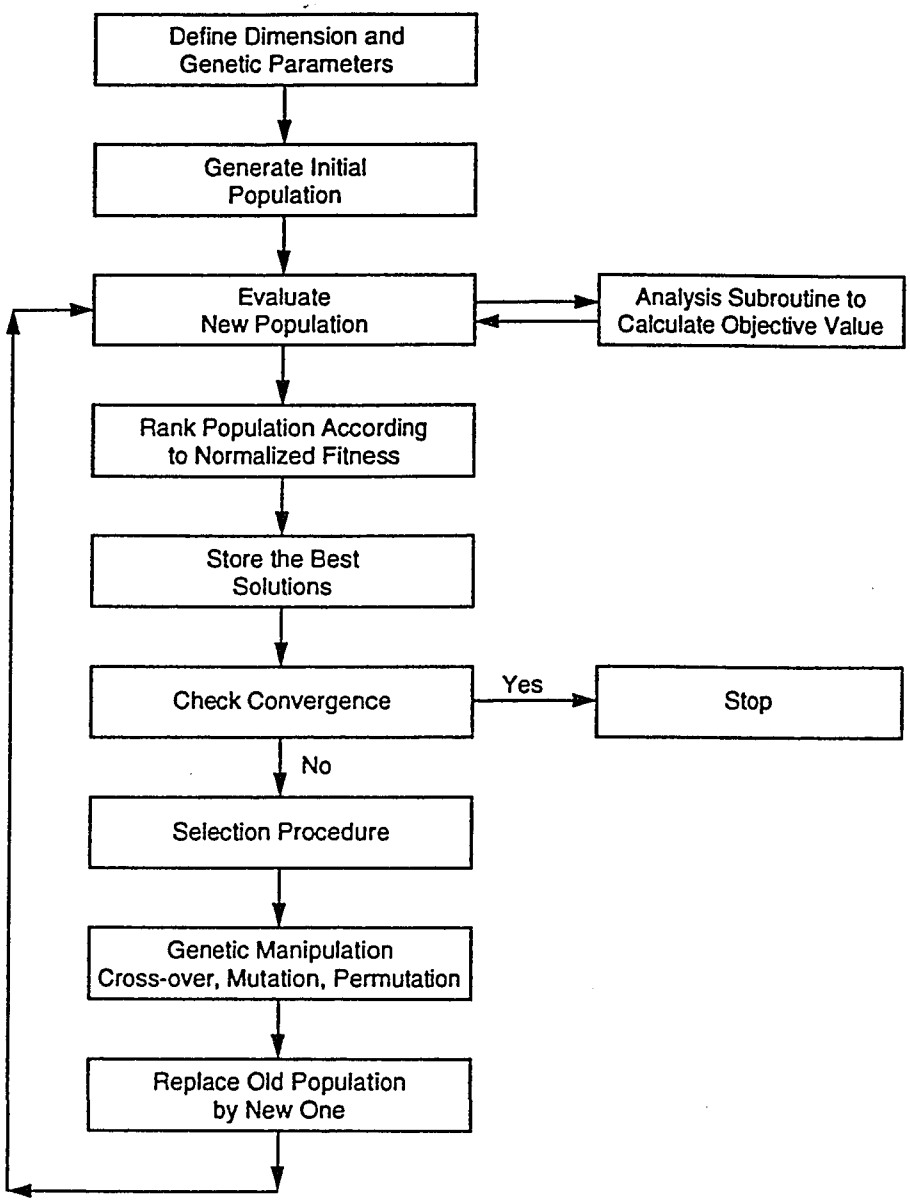

Figure 4.1 Flow chart for genetic algorithm

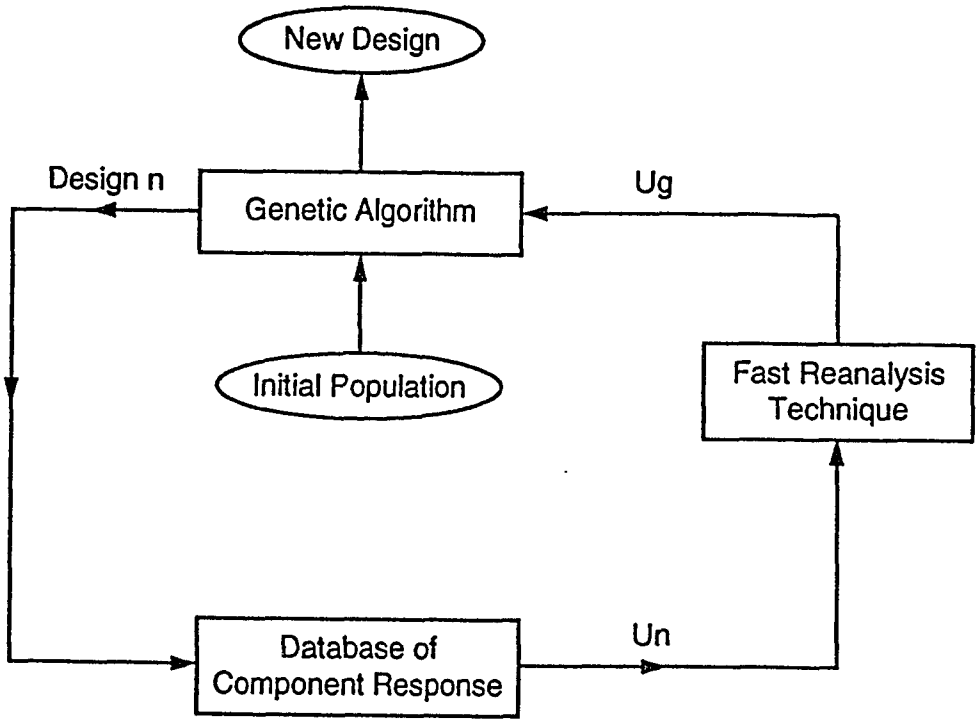

Figure 4.2 Proposed structural synthesis methodology

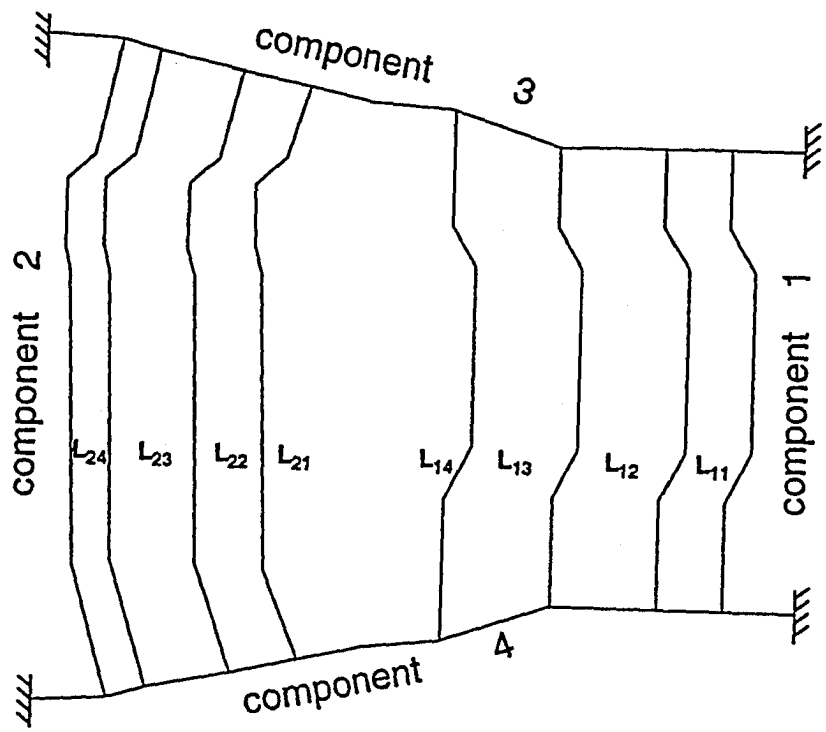

Figure 4.3 Various possible locations of cross members

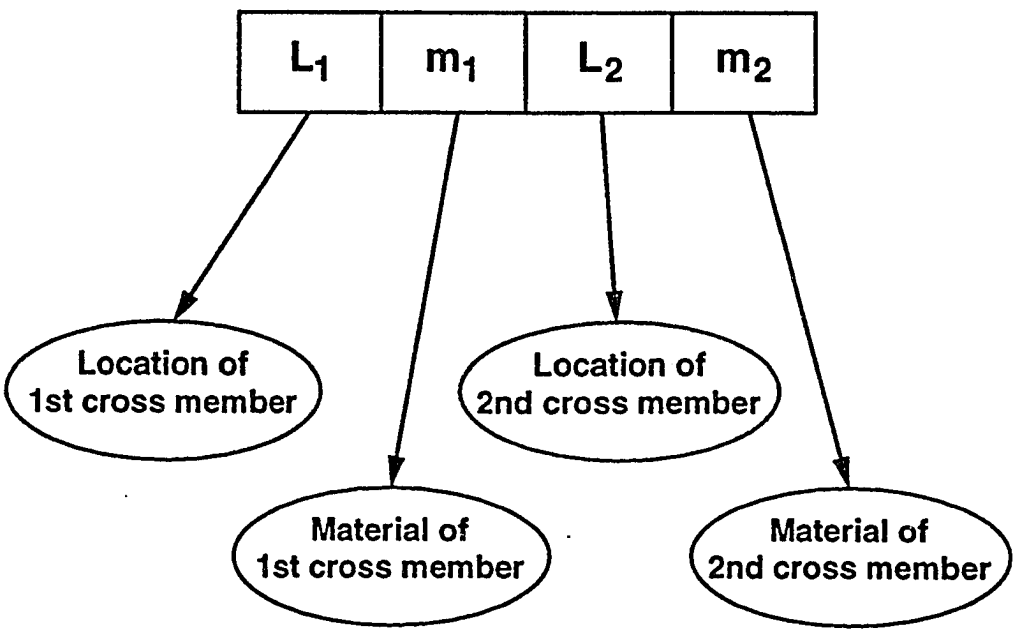

Figure 4.4 Genetic representation of design of global structure

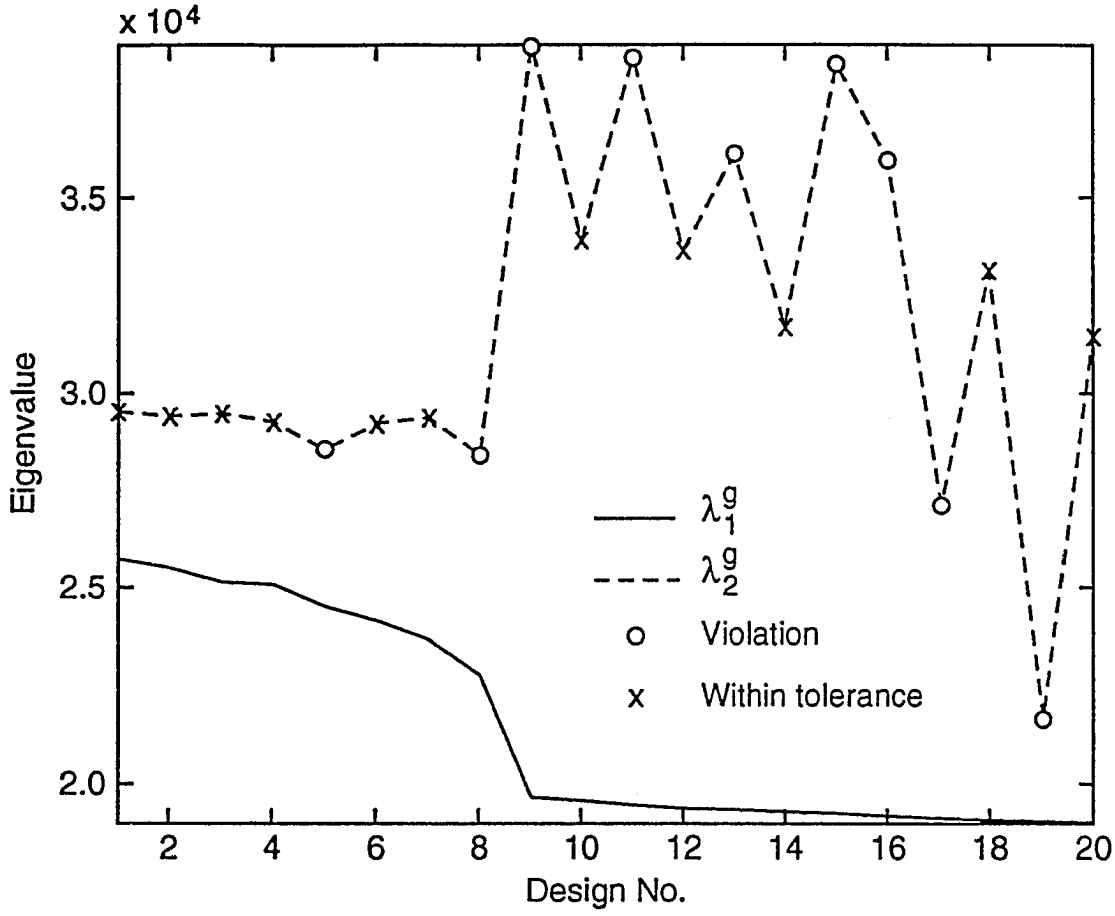

Figure 4.5 Optimal 20 first eigenvalues and corresponding second eigenvalues

Table 4.1 Different Material Properties Considered for Cross Members

Material	Young's modulus (kg/cm^2)	Shear modulus (kg/cm^2)
mt_1	1.2070 E+06	3.6210 E+05
mt_2	1.0863 E+06	3.2589 E+05
mt_3	0.9656 E+06	2.8968 E+05
mt_4	0.6035 E+06	1.8105 E+05

Table 4.2 Optimal Five Possible Designs

Design	Location of cm_1	Material of cm_1	Location of cm_2	Material of cm_2	λ_1^g	λ_2^g
1	l_{11}	mt_2	l_{24}	mt_1	25 759	29 541
2	l_{11}	mt_1	l_{24}	mt_2	25 484	29 408
3	l_{11}	mt_3	l_{24}	mt_1	25 134	29 495
4	l_{11}	mt_2	l_{24}	mt_2	25 071	29 260
5	l_{11}	mt_2	l_{23}	mt_3	24 103	29 210

Table 4.3 Number of Occurrences of Top Three Designs and Number of Analyses for Various Population Sizes

		First best design		Second best design		Third best design	
Population size	NSTOP	Percentage of occurernce	Number of analyses (range)	Percentage of occurrence	Number of analyses (range)	Percentage of occurrence	Number of analyses (range)
	5	15	40–80	10	40–56	0	–
8	8	40	64–168	15	64–64	15	64–72
	10	40	80–168	20	80–152	10	88–120
	5	25	50–110	15	50–60	10	50–60
10	8	40	80–190	10	90–150	15	100–100
	10	65	100–220	10	120–120	5	110–110
	5	45	60–120	15	60–84	5	96–96
12	8	65	96–192	5	96–96	10	108–120
	10	75	120–192	10	120–144	5	120–120
	5	60	70–168	10	70–98	10	70–70
14	8	70	112–224	15	182–196	0	–
	10	90	140–252	5	140–140	5	140–140

Chapter 5

LOCAL VIBRATION TARGETING

Local vibration targeting is the determination of optimal values for the responses of the individual components so that the desired change in the performance of the global structure is achieved. Then, inverse design can be performed to change the local design variables of the individual components to achieve those target values. In this study, local vibration targeting is formulated as a design optimization problem in which any conventional gradient-based optimization [36] or linear programming technique [35] can be utilized to determine the target values for the individual components of the structure.

Local vibration targeting can be effectively used for design modification in many engineering applications. For example, the reduction of noise due to acoustical vibration of a structure by modifying only a few significant parts of the structure is a common engineering challenge faced by structural engineers. Local vibration targeting addresses this problem by identifying the most significant components and setting the target values for the responses of those selected components. Sensitivity derivatives of the global responses with respect to the component responses can be used in selecting the components for modification, and any optimization technique can be utilized to determine the optimal target values for the individual components of the structure. Finally, traditional design modification techniques can be used to modify the design variables (e.g., the elemental thicknesses of the individual components) to achieve the target values for the respective component responses.

In summary, local vibration targeting can be used to accomplish the following three objectives:

1. Identify the components for the modification.
2. Set the target values for the responses of those selected components.
3. If necessary, perform the local design modification to achieve the target values.

The procedures for achieving these three above objectives are explained in detail in sections 5.1, 5.2, and 5.3, respectively.

5.1 Identification of Components for Modification

Finite-element-analysis-based design optimization methods consider the elemental properties, such as cross-sectional areas and thicknesses, as the design variables. As a consequence, in the process of design optimization the design variables of many different elements that belong to various components or subcomponents may need to be changed. However, from a manufacturing point of view, such a redesign would require changes to the entire manufacturing process. On the other hand, if the change were limited to a few significant components in the structure, then the redesign would be limited to only the manufacturing processes that pertain to the modified components.

This manufacturing consideration can be incorporated into existing procedures; the design variables related to only certain components are allowed to change during the design optimization of the structure. However, in this case the main question is how to select the components for modification because existing procedures cannot calculate the performance of the assembled structure by treating individual components as entities; as mentioned earlier, these codes can only calculate the performance of the structure in terms of its elemental properties.

In previous chapters, we have explained how the performance of the assembled structure can be expressed in terms of the responses of the individual components by

adopting the component mode synthesis technique for vibration analysis of the assembled structure. In this way, each individual component can be treated as a design entity that is characterized by its structural responses (i.e., eigenvalues, eigenvectors, and static modes) as the representative variables.

Many factors, such as the cost of manufacturing and materials, can be considered in the selection of the components to be modified. However, if the selection of components to be modified is based only on, for example, the vibration characteristics of the various components in the structure, then the components for modification can be selected in such a way that the desired change in the performance of the global structure can be achieved with a limited change in the responses of those selected components. The primary reason for such a selection of components is the ease with which the required target values for the responses of the selected components can be achieved if the change in those responses is small. However, to accomplish this task a quantitative measure is necessary to evaluate the significance of each component in terms of its contribution to the vibration of the assembled structure.

Sensitivity derivatives of the eigenvalues and the eigenvectors of the global structure with respect to the individual component responses are calculated in chapter 3. This sensitivity information can be directly utilized to rank the components in terms of their contribution to the global performance. Three different categories of responses exist, namely, the eigenvalues λ, the eigenvector components Φ_s, and the static-mode components Ψ_s, which describe the contribution of each component. Therefore, a single quantitative measure is necessary in determining the significance of each component. For this purpose, a comparison study can be made to determine those variables that can be used as the criteria for comparing various components. One possible method for accomplishing this task is to calculate the average change in the global responses for a fixed percentage of change in each of these variables. This average can be easily computed from the sensitivity derivatives of the global responses with respect to the

corresponding component responses; this average can be written mathematically. For example, for a fixed percentage of change ϵ, the average change in λ_1^g is written as

$$\begin{aligned}(\Delta\lambda_1^g)_{av} &= \left(\sum \frac{\partial\lambda_1^g}{\partial u_i}.\Delta u_i\right)/N \\ &= \left(\sum \frac{\partial\lambda_1^g}{\partial u_i}.\epsilon u_i\right)/N \\ &= \epsilon.\left(\sum \frac{\partial\lambda_1^g}{\partial u_i}.u_i\right)/N\end{aligned} \tag{5.1}$$

In Eq. (5.1), N is the number of component responses in the corresponding category, and the summation is done over those many responses. Then, the average change $(\Delta\lambda_1^g)_{av}$ for the three different responses can be compared for each individual component to determine which component responses should be treated as the criteria by which to compare various components.

Another possibility in determining the significance of a component is to compare the values of the derivatives of the first eigenvalue of the assembled structure with the first eigenvalue of the individual components. This procedure is suggested based upon the observation that the first eigenvalue for any structure is the fundamental representation of its vibration characteristics and that any small change in the structural properties of any component will be immediately reflected in the fundamental mode of the structure. Based on the two suggested criteria, one can select the components for modification, depending on the particular problem. For example, if the objective is to increase the first eigenvalue with a minimal change in the current design, then highly sensitive components can be selected for the modification. On the other hand, if the objective is to reduce the weight of the structure with a minimal deviation in its vibration performance, then less significant components might be chosen for modification so that the changes in those components will not effect the fundamental modes of the global structure. Later, both approaches mentioned above will be applied to two different sample problems.

5.2 Setting Target Values for Individual Components

After a set of components has been selected for the design modification, the next step is to determine the target values for the component responses so that the desired change in the response of the assembled structure is achieved. As mentioned earlier, the component responses $\lambda, \mathbf{\Phi}_s$ and $\mathbf{\Psi}_s$ are referred to as the intermediate variables u_i.

The target values can be set by solving an optimization problem and treating the intermediate variables as design variables in solving the optimization problem. The objective function and constraints are defined as functions of the global responses u_g (i.e., eigenvalues and eigenvectors) in such a way that they define the desired structural performance. For example, a typical optimization problem could be the maximization of the first global eigenvalue with a minimal change in the component responses. Mathematically, this problem can be written as

$$\min_{u_i} \qquad \psi_0(u_i, u_g) \tag{P5.1}$$

subject to

$$\mathbf{R}(u_i, u_g) = 0$$

$$\mathbf{G}_j(u_g) \leq 0 \qquad (j = 1, 2, ...p)$$

where $\mathbf{R} = 0$ is the state equation in the form of Eq. (2.41), which represents the reduced eigenvalue problem of the global structure obtained as a result of component mode synthesis. The above optimization problem can be solved by any standard gradient-based design optimization technique. The sensitivity derivatives of the global responses u_g with respect to the intermediate variables $\frac{\partial u_g}{\partial u_i}$ that were computed in chapter 3 can be utilized to calculate the derivatives of the objective function and the constraints with respect to the intermediate variables. The optimal solution for the above design problem (P5.1) will provide the optimal intermediate variables u_i^* for achieving the desired global performance of the structure. These optimal intermediate variables are the target values for the responses of the selected components.

Note that the intermediate variables u_i in design optimization problem (P5.1) can be referred to as either a single component or a group of components selected for the modification. Correspondingly, in solving the optimization problem (P5.1) only the intermediate variables that pertain to those selected components will be treated as design variables.

If the desired change in the global structural performance is small, then the target values can be set more effectively by solving a linear programming problem. For example, a typical design modification problem may be to minimize the change in the second eigenvalue while the first eigenvalue is increased by at least 10 percent. Mathematically, this problem can be written in the form of a linear programming problem as

$$\min_{u_i} \quad \sum_{i=1}^{m} \frac{\partial \psi}{\partial u_i} \Delta u_i \tag{P5.2}$$

subject to

$$\sum_{i=1}^{m} \frac{\partial \mathbf{G}_j}{\partial u_i} \Delta u_i \leq \epsilon_j \qquad (j = 1, 2, ...p)$$

$$|\Delta u_i| \leq \varepsilon_i \qquad (i = 1, 2, ...m)$$

where the derivatives $\frac{\partial \psi}{\partial u_i}$ and $\frac{\partial \mathbf{G}_j}{\partial u_i}$ are calculated for the current design u_i^0. The constant m is the number of intermediate variables. The constraints on Δu_i are imposed to keep the approximation in a linear range. Again, the solution to the above optimization problem (P5.2) will give the approximate optimal intermediate variables u_i^*.

If the number of intermediate variables m is equal to 1, then the target values can be determined by expanding the global performance functions (i.e, eigenvalues and eigenvectors) as a first-order Taylor-series approximation for the current design. For a $\Delta\lambda^g$ change in the global eigenvalue, the required change in the intermediate variables Δu_i can be found as follows:

$$\Delta u_i = \frac{\Delta \lambda^g}{\frac{\partial \lambda^g}{\partial u_i}} \tag{P5.3}$$

Note that the sensitivity derivatives of the global responses with respect to the intermediate variables are important in the entire process of local vibration targeting. In addition to helping in the identification of the components to be modified, they also determine the approximate magnitude of the change required in the intermediate variables to achieve the desired global structural performance.

5.3 Local Design Modification

After the target values for the intermediate variables (i.e., the responses λ, $\mathbf{\Phi}_s$, and $\mathbf{\Psi}_s$ of the individual components) have been determined, then the individual components can be modified to achieve those target values. This process can again be formulated as a design optimization problem for each component of interest. However, in this design optimization problem the elemental properties, such as thickness and cross-sectional area, are treated as design variables. The objective function and the constraints are defined as functions of the component responses λ, $\mathbf{\Phi}_s$, and $\mathbf{\Psi}_s$ and their target values. For example, a typical optimization problem for the local design modification may be to minimize the error between the target values u_i^* and the current design u_i^0, while the volume remains less than the initial value. Mathematically, this problem can be written as

$$\min_{\mathbf{b}} \quad \phi_0(u_i, u_i^*) = \sum_{i=1}^{m^*} (u_i - u_i^*)^2 \tag{P5.4}$$

subject to

$$\mathbf{r}(u_i, \mathbf{b}) = 0$$

$$\mathbf{g}_k(u_i^*, u_i, \mathbf{b}) \leq 0 \qquad (k = 1, 2, ...q)$$

where m^* is a subset of intermediate variables and the remainder of the targeting of intermediate variables is represented in the general form of the constraints $\mathbf{g}_k$ as a function of both u_i and the target values u_i^*. For example, some constraints in $\mathbf{g}_k$ can be in the form $|u_i - u_i^*| < \epsilon_i$ so that some intermediate variables are targeted within a certain tolerance. Accurate targeting cannot be ensured for the intermediate variables that remain in the

objective function; however, the accuracy of the targeting can be controlled by placing them in the constraints.

An optimal solution to the above problem will produce a new component design, which will produce the responses closest to the target values. These component responses, in turn, will generate global structural responses that are close to the desired values. Note that the number of local design modification problems (P5.4) will be the same as the number of components selected for the modification.

The procedures involved in local vibration targeting are depicted in the form of a flowchart in Fig. 5.1. In the next section, these procedures will be explained in more detail with numerical examples.

5.4 Numerical Examples

The above-developed procedures for local vibration targeting have been applied to two problems to demonstrate the applicability of the methodology. In the first example, a simple fixed-fixed beam assembled in a multilevel fashion is presented. For this example, the three procedures in local vibration targeting (i.e., identifying the components, setting the target values, and modifying the local design) are demonstrated. In the second example, a simplified model of an engine cradle is presented. For this sample problem, the components are identified and the target values are set for those components.

5.4.1 A Multilevel Fixed-Fixed Beam

The developed method has been applied to the fixed-fixed beam, shown in Fig. 2.3. The beam is assembled from two identical cantilever beams "a" and "b," which in turn are assembled from two components α and β. The geometrical properties and finite-element discretization are the same as given in chapter 2.

The design modification problem is set up to increase the first eigenvalue of the global structure by modifying either component α or β while the volume of the structure is kept at less than the initial value.

5.4.1.1 Analysis. Before the design modification is performed, component mode synthesis must be performed to obtain the responses of the global structure. As explained in chapter 2, the component mode synthesis was performed in two levels to obtain the eigenvalues of the fixed-fixed beam. Four eigenmodes and two static modes of each component are considered as basis vectors. Of the four eigenmodes of component β, the first two are rigid-body modes, and the other two are elastic modes. The results of the eigenvalue analysis of the fixed-fixed beam have been reported in chapter 2.

5.4.1.2 Sensitivity Analysis. After the analysis has been completed, the next step is to compute the sensitivity derivatives of the global responses with respect to the responses of each component. Because the analysis is performed in a multilevel fashion, the sensitivity derivatives of the eigenvalues and eigenvectors of the subassemblies with respect to the responses of its components are calculated at each level. The required sensitivity derivatives of the global eigenvalues and eigenvectors with respect to the individual component responses are calculated with the chain rule of differentiation. For a typical component α in subassembly "a," the global derivatives can be written as

$$\begin{Bmatrix} \frac{d\lambda^g}{d\lambda_s^\alpha} \\ \frac{d\lambda^g}{d\Phi_s^\alpha} \\ \frac{d\lambda^g}{d\Psi_s^\alpha} \end{Bmatrix} = \begin{bmatrix} \frac{\partial\lambda^a}{\partial\lambda_s^\alpha} & \frac{\partial\Phi_s^a}{\partial\lambda_s^\alpha} & \frac{\partial\Psi_s^a}{\partial\lambda_s^\alpha} \\ \frac{\partial\lambda^a}{\partial\Phi_s^\alpha} & \frac{\partial\Phi_s^a}{\partial\Phi_s^\alpha} & \frac{\partial\Psi_s^a}{\partial\Phi_s^\alpha} \\ \frac{\partial\lambda^a}{\partial\Psi_s^\alpha} & \frac{\partial\Phi_s^a}{\partial\Psi_s^\alpha} & \frac{\partial\Psi_s^a}{\partial\Psi_s^\alpha} \end{bmatrix} \begin{Bmatrix} \frac{\partial\lambda^g}{\partial\lambda_s^a} \\ \frac{\partial\lambda^g}{\partial\Phi_s^a} \\ \frac{\partial\lambda^g}{\partial\Psi_s^a} \end{Bmatrix} \tag{5.2}$$

The expressions for the derivatives of the eigenvalues and the eigenvectors of the global structure with respect to the responses of component β can be written in a similar manner. Because the structure is symmetric with respect to the α and β components, the sensitivity derivatives are calculated with respect to only one of the components.

5.4.1.3 Design Modification. The first step in the design modification process is to select the most significant component in the assembly for modification. This step is accomplished primarily by comparing the sensitivity derivatives of the global responses with the responses of various components in the assembly. In this study, the derivatives of the first eigenvalue of the fixed-fixed beam λ_1^g with respect to the first eigenvalue

of the individual components α and β are used to determine the significance of each component. Because component β has rigid-body modes, the first two eigenvalues are 0. Hence, the derivative of the global eigenvalue with respect to the first elastic mode (i.e., the third eigenvalue) is considered for determining the significance of the components. These sensitivity derivatives are listed in Tables 3.2 and 3.5. The tables clearly show that component α is more sensitive than component β. Therefore, component α is chosen for the modification.

Table 2.3 shows that even with two eigenmodes for each component, the first two eigenvalues of the global structure were computed accurately. Therefore, in performing the design optimization, only two eigenmodes and two static modes for each component are considered. Nevertheless, for the purpose of selecting the component for modification, four eigenmodes of each component were used because the first two eigenmodes of component β are zero.

After the component is selected for modification, the next step is to determine the optimal target values for the intermediate variables (i.e., the component responses λ^{α}, Φ_s^{α}, and Ψ_s^{α}) in such a way that these responses will achieve the required 10-percent increase in the first eigenvalue of the global structure. As discussed in section 5.2, this step can be accomplished by performing the optimization or by solving a linear programming problem. However, here we simply fix the quantities Φ_s^{α} and Ψ_s^{α} and change only the first eigenvalue of the α component λ_1^{α}. If we assume that the changes in both α components are identical, then the required change in λ_1^{α} is determined by expanding λ_1^{g} in a Taylor-series approximation as shown:

$$\begin{aligned} \Delta\lambda_1^{\alpha} &= \frac{\Delta\lambda_1^{g}}{\left(2\frac{\partial\lambda_1^{g}}{\partial\lambda_1^{\alpha}}\right)} \\ &= \frac{0.1 * 0.8768}{(2 * 0.06512016)} \\ &= 0.67321697 \end{aligned} \tag{5.3}$$

Hence, the desired first eigenvalue of component α is

$$\begin{aligned} \lambda_1^{\alpha^*} &= \lambda_1^{\alpha} + \Delta\lambda_1^{\alpha} \\ \lambda_1^{\alpha^*} &= 2.366471 + 0.67321697 \\ &= 3.03968796 \end{aligned} \tag{5.4}$$

In Eq. (5.3), the sensitivity derivatives $\frac{\partial\lambda_1^g}{\partial\lambda_1^{\alpha}}$ in the denominator have been doubled because both α components are modified identically. To check the accuracy of the linear approximation that was assumed in finding the target values, the analysis was repeated with the above-calculated value for λ_1^{α} and the same values for the other intermediate variables. This exercise resulted in an improvement of only 8.2 percent in the first eigenvalue of the global structure over its initial value, instead of the expected 10-percent improvement.

After the target values are determined for the intermediate variables, then local design optimization is performed for the α component to achieve the target values. The optimization problem can be formulated in many ways, depending on the type of problem. For this problem, the width b^i and the height h_i of element i (i = 1–8) are treated as design variables:

$$\min_{b_i,h_i} \quad \sum \left(\Phi_s^{\alpha} - \Phi_s^{\alpha^*}\right)^2 \tag{P5.5}$$

subject to

$$\begin{gathered} \lambda_1^{\alpha} > \lambda_1^{\alpha^*} \\ \left(\frac{\Psi_s^{\alpha} - \Psi_s^{\alpha^*}}{\Psi_s^{\alpha^*}}\right) < \epsilon \\ W < W_0 \end{gathered}$$

The above problem is set up in such a way that the first eigenvalue of the α component must be greater than the desired value and the weight of the component must be less than the initial value. The boundary terms of the static modes Ψ_s^{α} are targeted within a certain percent of allowable error ϵ with their respective target values $\Psi_s^{\alpha^*}$; the deviation

between the eigenmode components Φ_s^α and their target values $\Phi_s^{\alpha^*}$ is minimized because the sensitivity derivatives of the global eigenvalues with respect to the static-mode components are much larger than with respect to the eigenmode components, which can be clearly seen in Table 5.1. Hence, the static-mode components must be targeted more accurately than the eigenmode components. On the other hand, the eigenmode components can be kept in the constraints. However, such an arrangement imposes stringent constraints and does not yield the required change in the global eigenvalue.

In the above design optimization problem, 16 design variables result from 2 variables for each of 8 elements. Nine intermediate variables must be targeted; these result from the 2 eigenvalues and 2 boundary degrees of freedom for each of 2 eigenmodes and 2 static modes used in the component mode synthesis. Among the four components of Ψ_s^α, only three are independent because Ψ_s^α is a symmetric matrix that represents the boundary partition of the flexibility matrix.

The constrained minimization algorithm in MATLAB [37] was used to solve this optimization problem. The optimal solution was obtained for various values of ϵ. By experimenting with ϵ, the first eigenvalue of the global structure was improved to 7.5 percent of the initial value. Table 5.2 shows the percent improvement in the global eigenvalue for various values of ϵ. The optimal solution obtained for $\epsilon = 0.03$ is listed in Table 5.3. The initial and final shapes of the fixed-fixed beam are shown in Fig. 5.2. Notice that exactly targeting $\Psi_s^{\alpha^*}$ results in little improvement in the value of the first eigenvalue because of the large error in the Φ_s^α terms due to the tight constraints. On the other hand, if the allowable error ϵ on the $\Psi_s^{\alpha^*}$ terms is relaxed, the solution improves considerably. For $\epsilon = 0.03$, the improvement is 7.5 percent, which is approximately 91 percent of the improvement with the reanalysis. The initial and final component responses are listed in Table 5.4.

5.4.2 Simplified Model of Engine Cradle

A simplified model of an engine cradle is shown in Fig. 2.5. As seen from the topology of the structure, it can be divided into four components. Information on each component is given in Table 5.5. All components are discretized with two nodes and 12–degree-of-freedom circular-tube beam elements. When the components are assembled together, the global structure has 198 degrees of freedom.

The design modification problem is set up to determine the component for modification and the target values for the responses of the selected component so that a 10-percent increase in the first eigenvalue of the global structure is realized and the change in the second eigenvalue is minimized.

5.4.2.1 Analysis. Eigenmodes and static modes of each component are obtained as explained in the previous example. The number of eigenmodes and static modes considered for each component is also given in Table 5.5. Component mode synthesis was performed with these modes as basis vectors. In this sample problem, the components were assembled in only one level to form the global structure. Therefore, the component mode synthesis was performed only once to obtain the eigenvalues and eigenvectors of the global structure. The results of the eigenvalue analysis have been reported in Table 2.5.

The accuracy of the component mode synthesis increases if the number of modes selected increases, as shown in Table 2.6. However, the increase of the selected modes complicates the task of local vibration targeting. The trade-off between computational effort and the acceptable accuracy of component mode synthesis needs further investigation. In this study, the number of modes (Table 5.5) is used as the basis for validating the proposed design methodology.

5.4.2.2 Sensitivity Analysis. The sensitivity derivatives of the eigenvalues and the eigenvectors of the global structure with respect to the responses λ, Φ_s, and Ψ_s of the four components were computed and are listed in chapter 3. Because the analysis was done in only one level, the sensitivity analysis was also done in one level. With these sensitivity derivatives, the average changes in first eigenvalue of the global structure $(\Delta\lambda_1^g)_{av}$ were calculated for various responses of all four components. These average changes are listed in Table 5.6. Notice that except for component 2, the average change with respect to the eigenvalues of each component is consistently higher than the average change with respect to the eigenmode and the static-mode terms of the corresponding components. Furthermore, Table 5.6 indicates that component 3 is the most significant component because its average change with respect to the eigenvalues of component 3 is the largest.

5.4.2.3 Design Modification. The most significant component in the structure may also be conveniently selected by comparing the sensitivity derivatives of the first eigenvalue of the global structure with respect to the first eigenvalue of the four components. As explained in the earlier sample problem, because components 1 and 2 are unconstrained, the first six eigenvalues of these components are zero; hence, the derivatives with respect to the first elastic mode (i.e., the seventh eigenvalue) are used to rank these components in terms of their contribution to the vibration of the global structure. These sensitivity derivatives are listed in Tables 3.15–3.18. The tables clearly show that component 3 is the most sensitive; hence, it has been selected for modification.

For this case, the component indicated by the above method is also consistent with the selection of the component based on the average changes (shown in Table 5.6); this agreement did not occur in the case of the fixed-fixed beam. As mentioned above, the average change in the eigenvalues is larger in comparison with the rest of the component responses. Hence, the average change with respect to the eigenvalues

of various components can be treated as the criterion for selecting the component for modification. In this case Table 5.6 clearly shows that the third component is the most significant.

Component 3 has 137 intermediate variables. Among these variables are five eigenvalues with 60 eigenvector components as a result of 12 interface degrees of freedom (6 at each of the two interfaces) of 5 eigenmodes considered in the component mode synthesis. A total of 72 (36 at each of the two interfaces) intermediate variables result from the 6 attachment modes; however, only 57 of them are independent. As a result, 36 components that correspond to the degrees of freedom at the interface point A (where the unit forces are applied to calculate the attachment modes) are the partition of the flexibility matrix that corresponds to those degrees of freedom. Therefore, the matrix is symmetric; hence, only 21 of the variables can be treated as independent variables.

Because a greater number of intermediate variables exists, target values for this component are determined by solving a linear programming problem. The problem has been set up such that the change in the second eigenvalue is minimized when subjected to 10-percent increase in the first eigenvalue of the global structure. Mathematically, this problem can be written as

$$\min_{\Delta u_i} \quad \sum \frac{\partial \lambda_2^g}{\partial u_i} \Delta u_i \tag{P5.6}$$

subjected to

$$\sum_{i=1}^{m} \frac{\partial \lambda_1^g}{\partial u_i} \Delta u_i \;>\; 0.1\, \lambda_1^{g^0}$$
$$|\Delta u_i| \;<\; \epsilon\, |u_i|$$

where λ_1^g and λ_2^g are the first and second eigenvalues of the global structure. The constant m is the number of intermediate variables. Constraints on Δu_i are imposed to limit the change in u_i to a certain percentage of its absolute value ϵ, so that the linear approximation assumed in predicting the change in global eigenvalues holds true.

5.4.2.4 Solution Procedure. The simplex algorithm from the IMSL Fortran libraries [35] has been used to solve the above linear programming problem. Because the intermediate variables are composed of terms from different responses, the magnitudes of their values are of different orders. Table 5.7, which contains the initial values of the intermediate variables, shows this problem very clearly. Therefore, these variables are normalized with respect to their initial values to maintain numerical stability in solving the linear programming problem.

Initially, the problem was solved for $\epsilon = 0.1$. However, the improvement in the first eigenvalue was only 6.6 percent, rather than the expected improvement of 10 percent. Nevertheless, the 10-percent improvement in λ_1^g is satisfied in the linear sense in problem (P5.6); it was not true when the analysis was repeated with the new solution for u_i. This result indicates that either the linear approximation was not true in the specified range or that the limits imposed on Δu_i were too tight to yield the desired 10-percent change in λ_1^g. Hence, the above solution procedure must be improved. To this end, the following two approaches were adopted:

1. The limits on Δu_i were increased and the linear programming problem (P5.6) was solved again with the same initial design.

2. The problem (P5.6) was solved by choosing a new initial design u_0^n such that

$$u_0^n = u_0 + (u_1 - u_0) * \alpha \tag{5.5}$$

where u_0 is the initial design, u_1 is the obtained new design, and α is a parameter. Our experience has shown that values for α can be selected between 0.1 and 0.3.

These two approaches must be repeated until the desired change in the global response is achieved.

With the first approach, the limits on Δu_i were increased from 10 to 15 percent (i.e; $\epsilon = 0.15$), and the linear problem (P5.6) was solved with the same initial design. By using the new solution for the intermediate variables u_i, the analysis was repeated to

calculate the new global responses. This exercise successfully resulted in a 10-percent improvement in the first eigenvalue of the global structure.

In regard to the second approach, a new initial design can be calculated with Eq. (5.5). To experiment with the values of parameter α, three values were chosen: $\alpha = 0.1$, 0.2, and 0.3. Three initial designs were obtained to correspond to these three values of α. With these new initial designs as the starting point, the linear programming problem (P5.6) was solved three times, which resulted in three new solutions for the intermediate variables u_i with improvements of 9.3, 11.2, and 11.7 percent in the first eigenvalue of the global structure for the respective values of $\alpha = 0.1$, 0.2, and 0.3.

Although both proposed approaches appear to work well for the problem considered here, the second approach is recommended for two reasons. First, the second approach reaches the desired solution in steps, so that at every iteration the linear expansion of the global responses holds true in that range. On the other hand, the first approach increases the limits on Δu_i, which increases the range in which the linear approximation must hold true. However, the validity of the assumed linear approximation in predicting the change in global responses cannot be ensured in the specified range.

If the second approach cannot yield the desired change in the specified initial limits, then these two approaches can be combined. By first increasing the limits on Δu_i and then adopting the second approach, the desired change can be reached more accurately.

Table 5.8 lists the obtained changes in the eigenvalues of the global structure for the cases discussed above. In the second iteration for $\epsilon = 0.1$, only the results obtained for $\alpha = 0.3$ are listed. The corresponding final solutions obtained for the intermediate variables are given in Tables 5.9 and 5.10. The values shown in these tables are normalized with respect to their initial values, which are given in Table 5.6.

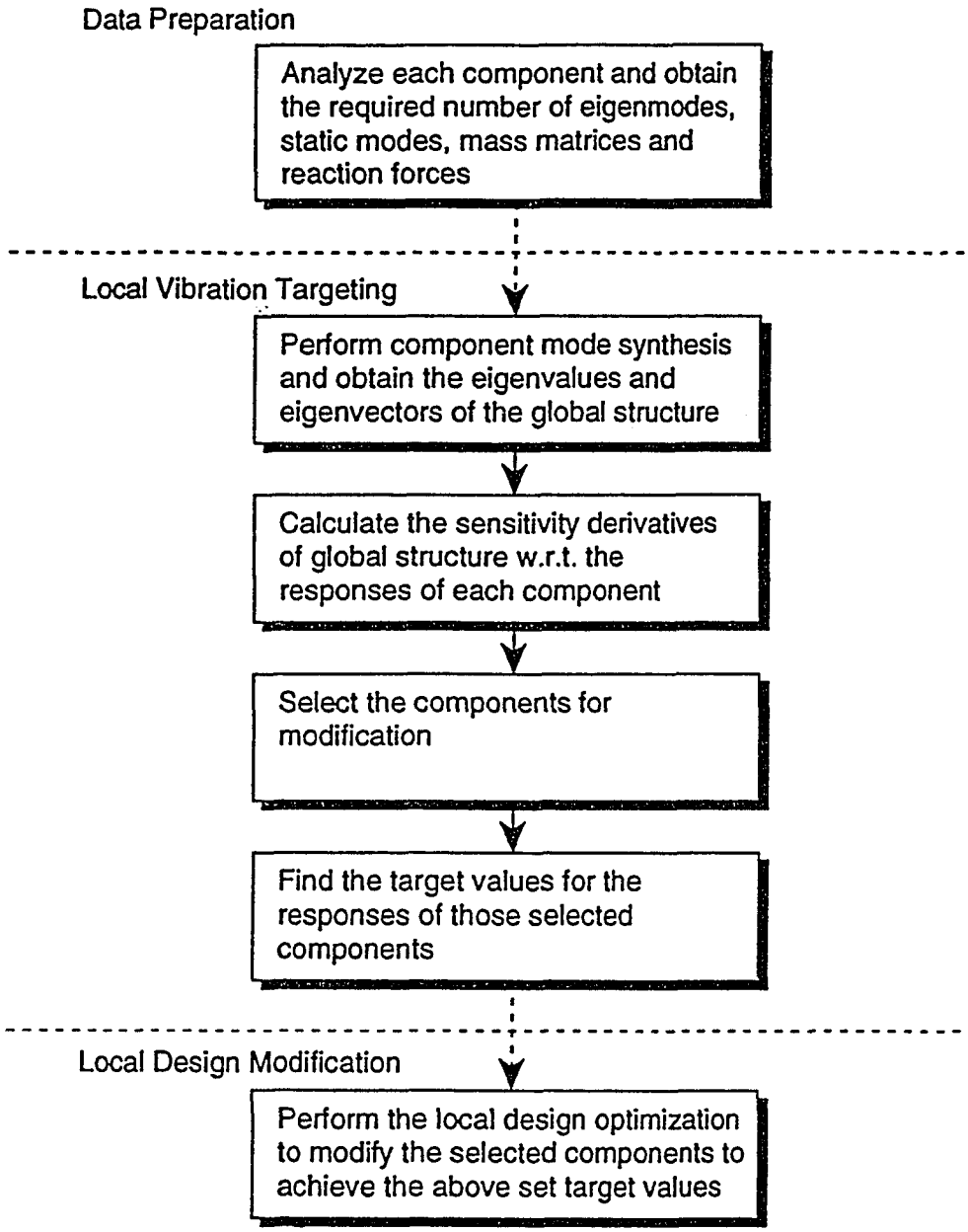

Figure 5.1 Flow chart for local vibration targeting

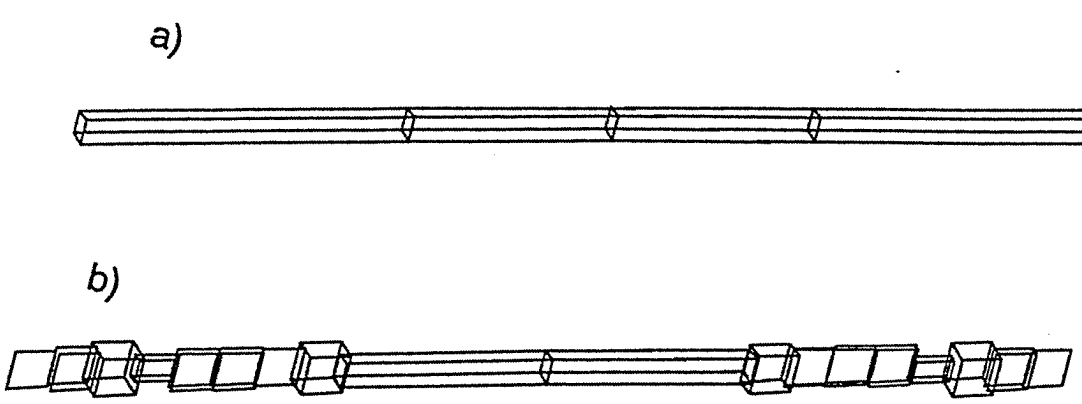

Figure 5.2 Initial and final shapes of fixed-fixed beam

Table 5.1 Average Change in First Eigenvalue of Global Structure

(Multilevel Fixed-Fixed Beam)

Type of variables	$\sum \frac{\partial \lambda_1^g}{\partial u_i}.u_i$	No. of variables	Average change $(\Delta\lambda_1^g)_{av}$
Component α			
λ^α	0.149816	4	0.037454
Φ_s^α	0.295767	8	0.036971
Ψ_s^α	0.715948	3	0.238649
Component β			
λ^β	0.001719	2	0.0008594
Φ_s^β	4.336118	8	0.542015
Ψ_s^β	0.356897	3	0.118966

Table 5.2 Change in First Eigenvalue of Global Structure

(Fixed-Fixed Beam)

	% change	λ_1^g	λ_1^α
Initial	0.0	0.8768	2.3665
Desired	10.0	0.9645	3.0397
Reanalysis	8.2	0.9490	3.0397
Achieved			
$\epsilon = 0$	4.5	0.9177	3.0397
$\epsilon = 0.01$	5.6	0.9261	3.0397
$\epsilon = 0.02$	6.6	0.9346	3.0397
$\epsilon = 0.03$	7.5	0.9423	3.0397

Table 5.3 Design Variables Before and After Modification

(Multilevel Fixed-Fixed Beam)

($0.25 < b_i, d_i > 6.0$)

Element no.	Initial		Final	
	Width (b)	Height (h)	Width (b)	Height (h)
1	2	4	0.3480	6.0000
2	2	4	1.4625	6.0000
3	2	4	4.3686	5.9950
4	2	4	1.5277	3.8683
5	2	4	0.9642	6.0000
6	2	4	0.7876	6.0000
7	2	4	0.2779	5.5083
8	2	4	1.5372	5.8522

Table 5.4 Component Responses Before and After Modification

(Multilevel Fixed-Fixed Beam)

Component response	Initial	Final	% change
λ_1^α	2.366471	3.039900	28.46
λ_2^α	86.496593	66.925989	–22.63
$\Phi_s^\alpha(1,1)$	1.456987	1.619062	11.12
$\Phi_s^\alpha(2,1)$	0.020999	0.022687	8.04
$\Phi_s^\alpha(1,2)$	–1.367577	–1.390534	–1.68
$\Phi_s^\alpha(2,2)$	–0.072152	–0.072249	–0.14
$\Psi_s^\alpha(1,1)$	0.921600	0.893952	–3.00
$\Psi_s^\alpha(2,1)$	0.014400	0.013968	–3.00
$\Psi_s^\alpha(2,2)$	0.000300	0.000309	2.87

Table 5.5 Component Data

(Simplified Model of Engine Cradle)

Component no.	Degrees of freedom.	No. of eigenmodes	No. of static modes	Total no. of modes
1	54	9	6	15
2	60	10	6	16
3	54	5	6	11
4	54	5	6	11

Table 5.6 Average Change in First Eigenvalue of Global Structure
(Simplified Model of Engine Cradle)

Type of variables	$\sum \frac{\partial \lambda_1^g}{\partial u_i}.u_i$	No. of variables	Average change $(\Delta\lambda_1^g)_{av}$
Component 1			
λ^1	2453.5312	3	817.8436
Φ_s^1	32487.7974	108	300.8130
Ψ_s^1	7185.3527	21	342.1597
Component 2			
λ^2	446.8331	4	111.7083
Φ_s^2	30528.3012	120	254.4025
Ψ_s^2	4828.9288	21	229.9490
Component 3			
λ^3	5941.3544	5	1188.2709
Φ_s^3	10247.7410	60	170.7957
Ψ_s^3	5801.1974	57	101.7754
Component 4			
λ^4	5865.0658	5	1173.0132
Φ_s^4	9910.7259	60	165.1788
Ψ_s^4	6128.3770	57	107.5154

Table 5.7(a) Initial Values of Intermediate Variables

(Eigenvalues and Eigenvector Components)

Eigenmode	1	2	3	4	5
Eigenvalue	18368.86	43199.15	159908.70	248882.07	667587.41
Eigenvector at interface C_1	–0.005103	0.036563	–0.003474	0.060643	0.091502
	0.099304	0.030356	–0.224202	0.121270	–0.128283
	–0.067216	0.139054	–0.126558	–0.203080	0.122545
	0.000583	–0.000121	0.002599	0.000511	–0.002518
	–0.000429	0.000848	–0.000528	–0.000354	0.000144
	–0.000668	–0.000244	0.000606	–0.000389	–0.000239
Eigenvector at interface C_3	0.002220	0.064956	0.108784	0.044909	0.096400
	0.174259	0.090198	0.194862	–0.146428	–0.132585
	–0.062987	0.103757	0.090866	0.163931	–0.004457
	0.000763	0.000124	0.002128	–0.000954	–0.001862
	0.000107	–0.000597	–0.000613	0.000029	0.000977
	0.000345	0.000224	–0.000712	0.000390	0.001394

Table 5.7(b) Initial Values of Intermediate Variables

(Static-Mode Components) $\times 10^{-6}$

Static mode	1	2	3	4	5	6
At interface A	0.118878	0.036788	0.095061	–0.000492	0.000999	–0.000143
	0.036788	1.076743	–0.191628	–0.001813	–0.001124	–0.004321
	0.095061	–0.191628	1.068969	–0.004443	0.004553	0.001492
	–0.000492	–0.001813	–0.004443	0.000279	–0.000034	–0.000015
	0.000999	–0.001124	0.004553	–0.000034	0.000044	0.000009
	–0.000143	–0.004321	0.001492	–0.000015	0.000009	0.000044
At interface D	0.081867	–0.057161	0.103388	0.001522	0.000824	–0.000059
	–0.011651	0.718677	–0.388759	0.008798	–0.002742	–0.005819
	0.124204	–0.305747	0.394022	–0.000961	0.002861	0.001795
	–0.000377	0.001212	–0.003083	0.000104	–0.000023	–0.000019
	–0.000466	0.000934	–0.001698	–0.000019	–0.000011	–0.000003
	0.000197	0.002748	–0.000318	–0.000015	–0.000001	–0.000016

Table 5.8 Obtained Improvement in Eigenvalues

	λ_1^g	λ_2^g
Initial	16222.85	32299.10
First iteration		
$\epsilon = 0.10$	17302.67 (6.7%)	35903.22 (11.2%)
Second iteration		
$\epsilon = 0.10$ ($\alpha = 0.3$)	18118.14 (11.7%)	35289.48 (9.3%)
$\epsilon = 0.15$	17845.43 (10.0%)	36779.62 (13.9%)

Table 5.9(a) Final Values of Intermediate Variables for $\epsilon = 0.15$
(Normalized with Respect to Initial Values)

(Eigenvalues and Eigenvector Components)

Eigenmode	1	2	3	4	5
Eigenvalue	1.15	1.15	1.15	1.15	1.15
Eigenvector at interface A	1.15	0.85	1.15	0.85	0.85
	0.85	1.15	0.85	0.85	0.85
	0.85	0.85	0.85	0.85	1.15
	1.15	1.15	1.15	1.15	0.85
	1.15	1.15	0.85	1.15	1.15
	1.15	0.85	1.15	1.15	0.85
Eigenvector at interface D	1.15	0.85	0.85	1.15	0.85
	1.15	0.85	0.85	0.85	1.15
	0.85	0.85	0.85	1.15	1.15
	1.15	0.85	0.85	0.85	1.15
	1.15	1.15	1.15	1.15	0.85
	1.15	0.85	1.15	1.15	0.85

Table 5.9(b) Final Values of Intermediate Variables for $\epsilon = 0.15$
(Normalized with Respect to Initial Values)

(Static-Mode Components)

Static mode	1	2	3	4	5	6
At interface A	1.15					
	0.85	0.85				
	0.85	0.85	0.85			
	1.15	0.85	0.85	1.15		
	0.85	1.15	1.15	0.85	0.85	
	1.15	1.15	1.15	0.85	0.85	0.85
At interface D	1.15	0.85	0.85	0.85	1.15	0.85
	0.85	1.15	1.15	0.85	0.85	0.85
	1.15	0.85	0.85	1.15	1.15	1.15
	0.85	1.15	1.15	0.85	0.85	0.85
	0.85	1.15	1.15	1.15	0.85	0.85
	1.15	1.15	1.15	1.15	0.85	0.85

Table 5.10(a) Final Values of Intermediate Variables with $\epsilon = 0.10$ ($\alpha = 0.3$)
(Normalized with Respect to Initial Values)

(Eigenvalues and Eigenvector Components)

Eigenmode	1	2	3	4	5
Eigenvalue	1.10	1.10	1.10	1.10	1.10
Eigenvector at interface A	0.90	0.90	1.10	0.90	0.90
	0.90	1.10	0.90	1.10	0.90
	0.90	0.90	0.90	0.90	1.10
	1.10	0.90	1.10	1.10	0.90
	1.10	1.10	0.90	1.10	1.10
	1.10	0.90	1.10	1.10	0.90
Eigenvector at interface D	1.10	0.90	0.90	0.90	0.90
	1.10	0.90	1.10	0.90	1.10
	0.90	0.90	0.90	0.90	1.10
	1.10	0.90	0.90	1.10	1.10
	1.10	0.90	0.90	1.10	0.90
	1.10	0.90	1.10	0.90	0.90

Table 5.10(b) Final Values of Intermediate Variables for $\epsilon = 0.10$ ($\alpha = 0.3$)
(Normalized with Respect to Initial Values)

(Static-Mode Components)

Static mode	1	2	3	4	5	6
At interface A	0.90					
	0.90	0.90				
	0.90	0.90	0.90			
	0.90	0.90	0.90	0.90		
	0.90	1.10	1.10	0.90	0.90	
	1.10	1.10	1.10	0.90	0.90	0.90
At interface D	0.90	0.90	0.90	0.90	1.10	0.90
	0.90	1.10	0.90	0.90	0.90	0.90
	0.90	0.90	0.90	0.9141	0.90	1.10
	1.10	1.10	1.10	0.90	1.10	0.90
	0.90	1.10	0.90	1.10	0.90	0.90
	0.90	1.10	1.10	1.10	1.10	0.90

Chapter 6

MULTILEVEL DESIGN OPTIMIZATION FOR LOCAL STRUCTURAL MODIFICATION

6.1 Introduction

Current design practices in design optimization may not be suitable for design modification of complex automobile or aircraft structures because of the computational intensity involved in structural analysis. These complex structures are usually assembled from many different components, which may in turn be assembled from smaller components and each component may be fabricated by a different manufacturing process. Therefore, any structural modification considered should ideally result in a minimal change in the existing manufacturing processes. However, this consideration cannot be easily accommodated by many current design optimization techniques because these techniques only consider the properties of finite elements as design variables and are unable to treat an individual component as a design entity. In the previous chapters, the method of component mode synthesis has been integrated with a multilevel design optimization technique to generate a structural modification procedure that enables structural components to be considered as design entities. This chapter presents the mathematical formulation and discusses the numerical implementation of this newly-developed component-mode-synthesis-based multilevel design optimization technique for local structural modification.

This chapter is organized as follows. Section 6.2 describes the formulation of the problem as a two-stage design optimization problem. In section 6.3, the Kuhn-Tucker necessary conditions for both the single-stage and two-stage optimization problems are derived to establish the relationship between the optimum solutions of these two different formulations. Some numerical considerations that pertain to the implementation of the

proposed multilevel design optimization scheme are discussed in section 6.4. Numerical examples are presented in section 6.5, and concluding remarks are given in section 6.6.

6.2 Design Optimization Problem Formulation

The generalized stiffness and mass matrices $\mathbf{K}^*$ and $\mathbf{M}^*$ of the reduced eigenvalue problem in Eq. (2.41) are functions of the individual component responses λ^i, $\mathbf{\Phi}_s^i$, and $\mathbf{\Psi}_s^i$. Hence, the global eigenvalues and eigenvectors are also functions of these individual component responses. In the proposed methodology, the component responses λ^i, $\mathbf{\Phi}_s^i$, and $\mathbf{\Psi}_s^i$ are treated as intermediate variables u_i, which in turn are functions of the primary design variables **b** (which could be the sizing variables of the structural members). Mathematically, this relationship can be represented as $u_g = u_g(u_i(\mathrm{b}))$.

With the above relationship, component mode synthesis can be viewed as a two-stage analysis method. In the first stage, each component is analyzed independently to obtain the component responses λ^i, $\mathbf{\Phi}^i$,, and $\mathbf{\Psi}^i$, which are then assembled into the reduced eigenvalue problem given in Eq. (2.41). This equation is then solved in the second stage to obtain the eigenvalues and eigenvectors of the global structure. In accordance with the two-stage analysis procedure, the sensitivity derivatives $\frac{\partial u_i}{\partial b}$ and $\frac{\partial u_g}{\partial u_i}$ are computed separately in the first and second stages, respectively. With the chain rule, the direct sensitivities of global responses u_g, such as the eigenvalues and the eigenvectors, with respect to a primary design variable b can be written as

$$\frac{\partial u_g}{\partial b} = \sum_{i=1}^{m} \frac{\partial u_g}{\partial u_i} \frac{\partial u_i}{\partial b} \tag{6.1}$$

where m is the number of intermediate variables.

With the help of the above analysis and sensitivity analysis procedure, a two-stage structural modification technique can be developed. First, in the upper-level, the intermediate variables u_i are treated as design variables, and the design optimization problem is set up to have its objective function and constraints defined as functions

of the global responses, such as eigenvalues and eigenvectors. For example, a typical optimization problem could be stated as the maximization of the first global eigenvalue with a minimal change in the intermediate variables. Mathematically, this problem can be written as

$$\min_{u_i} \qquad \psi_0(u_i, u_g) \tag{P6.1}$$

subject to

$$\mathbf{R}(u_i, u_g) = 0$$

$$\mathbf{G}_j(u_g) \leq 0 \qquad\qquad j = 1, 2, ...p$$

where $\mathbf{R} = 0$ is the state equation in the form of Eq. (2.41), which represents the reduced eigenvalue problem of the global structure obtained by component mode synthesis. The optimal solution of the above design problem (P6.1) will provide the optimal intermediate variables u_i^* for the desired global performance of the structure.

After the optimal intermediate variables for the individual components have been found, then in the second stage (i.e., the lower-level) the individual components are modified to achieve the optimal intermediate variables. These variables are simply the static and dynamic responses of the individual components. This process again involves the formulation of a design optimization problem for each component of concern. In this design optimization problem, elemental thicknesses and cross-sectional areas are treated as the design variables **b**. The objective function and constraints are formulated as functions of component responses, such as eigenvalues, eigenvectors, and static deflections. For example, a typical optimization problem for the lower-level can be stated as the minimization of the error between the target values u_i^* and the current design u_i with the volume kept at less than the initial value. Mathematically, this problem can be written as

$$\min_{\mathbf{b}} \qquad \phi_0(u_i, u_i^*) = \sum_{i=1}^{m} (u_i - u_i^*)^2 \tag{P6.2}$$

subject to

$$\mathbf{r}(u_i, \mathbf{b}) = 0$$

$$\mathrm{g}_k(u_i, \mathbf{b}) \leq 0 \qquad k = 1, 2, ...q$$

Again, u_i^* is the optimal solution of the upper-level design optimization, which is independent of **b**. The equation r = 0 represents the state equation for the component, which includes both the eigenvalue equation and the static equation, and g_k are the constraints on certain quantities, such as the volume of the component. The solution to the above problem results in a new design $\mathbf{b}^*$ for the components involved, which generates the closest possible response to the target values u_i^*, which in turn achieves the desired global performance.

The intermediate variables u_i in design optimization problems (P6.1) and (P6.2) can be referred to as either a single component or a group of components selected for the modification. As a result, the number of lower-level design optimization (P6.1) problems equals the number of selected components. A schematic diagram of the proposed multilevel design optimization is shown in Fig. 6.1; this technique will be discussed in more detail in section 6.4.

6.3 Kuhn-Tucker Necessary Conditions

In this section, the Kuhn-Tucker necessary conditions [29] are derived for the proposed multilevel and conventional single-stage design optimization methods to establish a relationship between the optimal solutions of these two different formulations. The purpose of this exercise is to improve the quality of the optimal solution of the proposed multilevel design optimization method.

6.3.1 Single-Stage Problem

A single-stage optimization problem can be formulated by treating the primary variables **b** (e.g., thicknesses and cross-sectional areas of the finite elements) as the design variables. A typical problem can be stated as the maximization of the first eigenvalue while the volume is kept at less than the initial value. Mathematically, this problem can be written as

$$\min_{\mathbf{b}} \qquad \psi_0(u_i, u_g) \tag{P6.3}$$

subjected to

$$\mathbf{R}(u_i, u_g) = 0$$

$$\mathbf{r}(u_i, \mathbf{b}) = 0$$

$$\mathbf{G}_j(u_g) \leq 0 \qquad\qquad j = 1, 2, ...p$$

$$\mathbf{g}_k(u_i, \mathbf{b}) \leq 0 \qquad\qquad k = 1, 2, ...q$$

in which $\mathbf{R} = 0$ defines the state equation, which is simply the reduced eigenvalue equation (Eq. (2.41)) for the entire structure; $\mathbf{r} = 0$ is the state equation for the local analysis of the individual components, which includes both the eigenvalue and the static equations. The quantities u_g and u_i represent the global and component responses, such as eigenvalues, eigenvectors, and static deflections. Note that in this formulation u_g is considered an implicit function of **b** as $u_g(\mathbf{b}) = u_g[u_i(\mathbf{b})]$. The Kuhn-Tucker necessary conditions can be derived for the above constrained minimization problem by first writing the Lagrangian in terms of the Lagrange multipliers γ, μ, γ_j, and μ_k as

$$\mathbf{L} = \psi_0 + \gamma^{\mathrm{T}}\mathbf{R} + \mu^{\mathrm{T}}\mathbf{r} + \sum_{j=1}^{p} \gamma_j^{\mathrm{T}}\mathbf{G}_j + \sum_{k=1}^{q} \mu_k^{\mathrm{T}}\mathbf{g}_k \tag{6.8}$$

At the optimal solution $\mathbf{b}^*$, the following Kuhn-Tucker necessary conditions exist:

1. $\frac{\partial \mathbf{L}}{\partial b} = 0$ at $\mathbf{b}^*$, where

$$\frac{\partial \mathbf{L}}{\partial b} = \sum_{i=1}^{m} \frac{\partial \psi_0}{\partial u_i}\frac{\partial u_i}{\partial b} + \frac{\partial \psi_0}{\partial u_g}\sum_{i=1}^{m}\frac{\partial u_g}{\partial u_i}\frac{\partial u_i}{\partial b} + \gamma^{\mathrm{T}}\frac{\partial \mathbf{R}}{\partial u_g}\sum_{i=1}^{m}\frac{\partial u_g}{\partial u_i}\frac{\partial u_i}{\partial b}$$
$$+ \gamma^{\mathrm{T}}\sum_{i=1}^{m}\frac{\partial \mathbf{R}}{\partial u_i}\frac{\partial u_i}{\partial b} + \mu^{\mathrm{T}}\frac{\partial \mathbf{r}}{\partial b} + \mu^{\mathrm{T}}\sum_{i=1}^{m}\frac{\partial \mathbf{r}}{\partial u_i}\frac{\partial u_i}{\partial b} \tag{6.9}$$
$$+ \sum_{j=1}^{p}\gamma_j^{\mathrm{T}}\frac{\partial \mathbf{G}_j}{\partial u_g}\sum_{i=1}^{m}\frac{\partial u_g}{\partial u_i}\frac{\partial u_i}{\partial b} + \sum_{k=1}^{q}\mu_k^{\mathrm{T}}\sum_{i=1}^{m}\frac{\partial \mathbf{g}_k}{\partial u_i}\frac{\partial u_i}{\partial b} + \sum_{k=1}^{q}\mu_k^{\mathrm{T}}\frac{\partial \mathbf{g}_k}{\partial b}$$

2. $\mathbf{R}[u_g(\mathbf{b}^*), u_i(\mathbf{b}^*)] = 0$ and $\mathbf{G}_j[u_g(\mathbf{b}^*)] \leq 0$ $(j = 1, 2, ...p)$

   $\mathbf{r}[u_i(\mathbf{b}^*), \mathbf{b}^*] = 0$ and $\mathbf{g}_k[u_i(\mathbf{b}^*), \mathbf{b}^*] \leq 0$ $(k = 1, 2, ...q)$

3. $\gamma_j \geq 0$ and $\gamma_j \mathbf{G}_j[\mathbf{u_g}(\mathbf{b}^*)] = 0$ $(j = 1, 2, ...p)$

4. $\mu_k \geq 0$ and $\mu_k \mathbf{g}_k[u_i(\mathbf{b}^*), \mathbf{b}^*] = 0$ $(k = 1, 2, ...q)$

6.3.2 Two-Stage Problem

A two-stage optimization problem is discussed in section 6.2. Mathematical formulations for the upper and lower-level design optimization problems are given by problems (P6.1) and (P6.2), respectively. In the upper-level, the intermediate variables u_i are treated as design variables, and in the lower-level the primary variables $\mathbf{b}$ are treated as design variables.

For the upper-level design optimization, the Lagrangian is given as

$$\mathbf{L_u} = \psi_0 + \bar{\gamma}^{\mathrm{T}}\mathbf{R} + \sum_{j=1}^{p}\bar{\gamma}_j^{\mathrm{T}}\mathbf{G}_j \tag{6.10}$$

where $\bar{\gamma}$ and $\bar{\gamma}_j$ are Lagrange multipliers. Then, the Kuhn-Tucker necessary conditions at the optimal solution $\bar{u}_i^*$ can be written as follows:

1. $\frac{\partial \mathbf{L}_u}{\partial u_i} = 0$ at $\bar{u}_i^*$, where

$$\frac{\partial \mathbf{L}_u}{\partial u_i} = \frac{\partial \psi_0}{\partial u_i} + \frac{\partial \psi_0}{\partial u_g}\frac{\partial u_g}{\partial u_i} + \bar{\gamma}^{\mathbf{T}}\frac{\partial \mathbf{R}}{\partial u_g}\frac{\partial u_g}{\partial u_i} + \bar{\gamma}^{\mathbf{T}}\frac{\partial \mathbf{R}}{\partial u_i} + \sum_{j=1}^{p}\bar{\gamma}_j{}^{\mathbf{T}}\frac{\partial \mathbf{G}_j}{\partial u_g}\frac{\partial u_g}{\partial u_i} \tag{6.11}$$

2. $\mathbf{R}[u_g(\bar{u}_i^*), \bar{u}_i^*] = 0$ and $\mathbf{G}_j[u_g(\bar{u}_i^*)] \leq 0$ $(j = 1, 2, ...p)$

3. $\bar{\gamma}_j \geq 0$ and $\bar{\gamma}_j \mathbf{G}_j[u_g(\bar{u}_i^*)] = 0$ $(j = 1, 2, ...p)$

Similarly, the Lagrangian for the lower-level can be written as

$$\mathbf{L}_l = \phi_0 + \bar{\mu}^{\mathbf{T}}\mathbf{r} + \sum_{k=1}^{q}\bar{\mu}_k{}^{\mathbf{T}}\mathbf{g}_k \tag{6.12}$$

with the Lagrange multipliers $\bar{\mu}$ and $\bar{\mu}_k$. Then, the Kuhn-Tucker necessary conditions at the optimal solution $\bar{\mathbf{b}}^*$ are

1. $\frac{\partial \mathbf{L}_l}{\partial b} = 0$ at $\bar{\mathbf{b}}^*$, where

$$\frac{\partial \mathbf{L}_l}{\partial b} = \sum_{i=1}^{m}\frac{\partial \phi_0}{\partial u_i}\frac{\partial u_i}{\partial b} + \bar{\mu}^{\mathbf{T}}\sum_{i=1}^{m}\frac{\partial \mathbf{r}}{\partial u_i}\frac{\partial u_i}{\partial b} + \bar{\mu}^{T}\frac{\partial \mathbf{r}}{\partial b} + \sum_{k=1}^{q}\bar{\mu}_k{}^{\mathbf{T}}\sum_{i=1}^{m}\frac{\partial \mathbf{g}_k}{\partial u_i}\frac{\partial u_i}{\partial b} + \sum_{k=1}^{q}\bar{\mu}_k{}^{\mathbf{T}}\frac{\partial \mathbf{g}_k}{\partial b} \tag{6.13}$$

2. $\mathbf{r}[u_i(\bar{\mathbf{b}}^*), \bar{\mathbf{b}}^*] = 0$ and $\mathbf{g}_k[u_i(\bar{\mathbf{b}}^*), \bar{\mathbf{b}}^*] \leq 0$ $(k = 1, 2, ...q)$

3. $\bar{\mu}_k \geq 0$ and $\bar{\mu}_k \mathbf{g}_k[u_i(\bar{\mathbf{b}}^*), \bar{\mathbf{b}}^*] = 0$ $(k = 1, 2, ...q)$

The following steps show that the optimal solutions $\bar{\mathbf{b}}^*$ and $\bar{u}_i^*$ of the two-stage design optimization approach satisfy the Kuhn-Tucker necessary conditions for the single-stage design optimization approach. To this end, let $\bar{\mathbf{b}}^*$ be a possible solution of the single-stage design optimization and let the Lagrange multipliers $\bar{\gamma}, \bar{\mu}, \bar{\gamma}_j$, and $\bar{\mu}_k$ be the corresponding Lagrange multipliers of the single-stage design optimization. If perfect targeting exists in the lower-level design optimization as

$$\begin{aligned} \phi_0 &= \sum_{i=1}^{m} \left[u_i(\bar{\mathbf{b}}^*) - \bar{u}_i^*\right]^2 \\ &= 0 \end{aligned} \tag{6.14}$$

then $u_i(\bar{\mathbf{b}}^*) = \bar{u}_i^*$. As a result, $\bar{\mathbf{b}}^*$ and $\bar{u}_i^*$ or $u_i(\bar{\mathbf{b}}^*)$ (which satisfy the second and the third Kuhn-Tucker necessary conditions of the upper-level and lower-level design optimization) also satisfy the second, third, and fourth Kuhn-Tucker necessary conditions for the single-stage design optimization. The first Kuhn-Tucker necessary condition for the single-stage design optimization is satisfied at $\bar{\mathbf{b}}^*$ and $\bar{u}_i^*$ because

$$\frac{\partial \mathbf{L}}{\partial b} = \sum_{i=1}^{m} \frac{\partial \mathbf{L}_u}{\partial u_i}\frac{\partial u_i}{\partial b} + \frac{\partial \mathbf{L}_l}{\partial b} - \sum_{i=1}^{m} \frac{\partial \phi_0}{\partial u_i}\frac{\partial u_i}{\partial b} \tag{6.15}$$

which is obtained by combining Eqs. (6.11) and (6.13) with Eq. (6.9). Note that the first two terms on the right-hand side of Eq. (6.15) equal 0 because of the Kuhn-Tucker conditions $\frac{\partial \mathbf{L}_l}{\partial b} = 0$ and $\frac{\partial \mathbf{L}_u}{\partial u_i} = 0$ at $\bar{\mathbf{b}}^*$ and $\bar{u}_i^*$, respectively. The last term is also equal to 0 as $\frac{\partial \phi_0}{\partial u_i} = 2\left[u_i(\bar{\mathbf{b}}^*) - \bar{u}_i^*\right] = 0$ for perfect targeting.

In summary, the above derivation has shown that a local minimum of the two-stage approach will satisfy the Kuhn-Tucker conditions for the single-stage approach. As a result, the optimal design obtained by the two-stage approach should also be an optimum design of the single-stage approach, although the opposite may not be true; thus, some optimum designs of the single-stage approach may not be realizable by the two-stage approach. Hence, the conventional single-stage approach may produce a better design than that obtained by the proposed two-stage approach. However, we emphasize that the purpose of the proposed two-stage approach is to divide a complex design problem into many smaller and tractable ones.

6.4 Numerical Considerations

According to the multilevel design optimization method proposed above, once the target values are found for the intermediate variables by the upper-level optimization, local design modification must be performed to achieve these target values. Therefore, the success of the proposed multilevel optimization method depends solely on whether the lower-level optimization can achieve the target values. However, the artificial target values set by the upper-level optimization for the intermediate variables, the static and dynamic responses of the components, may not be realizable in the lower-level design space.

To circumvent this difficulty, an iterative multilevel design optimization scheme has been developed in which the bounds on the intermediate variables are dynamically changed at the upper-level for every new cycle. The primary objective of this scheme is to force the target values in the upper-level to fall within a range that is realizable by the lower-level design space. This objective can only be achieved by imposing the proper bounds on the intermediate variables. However, the extent to which the intermediate variables will vary within the given bounds on the primary design variables is usually not known. In the following paragraphs, a systematic way to specify the bounds for the upper-level design optimization is explained. Hereafter, the term "bounds" will be used to refer to the bounds on the intermediate variables in the upper-level design optimization, unless otherwise stated.

First, an initial set of bounds can be estimated such that the desired global performance is achieved in the upper-level design optimization. Let the optimal solution to the upper-level be u_i^*. Then, the lower-level design optimization can be performed to achieve these target values. As explained earlier, the perfect target values may not be achieved initially. Hence, the optimal solution to the lower-level u_i^a and target values u_i^* will

deviate by a certain amount; this deviation can guide modification of the bounds for the upper-level design optimization. The new bounds for the upper-level can be specified as

$$u_i^{bl} = u_i^a - \Delta u_i$$
$$u_i^{bu} = u_i^a + \Delta u_i \tag{6.16}$$

where $\Delta u_i = \frac{1}{2}|u_i^a - u_i^*|$ and u_i^{bl} and u_u^{bu} are the new sets of lower and upper bounds. The same is depicted in Fig. 6.2. The magnitude of the difference Δu_i occasionally can be either small or large so that they result in either tight or loose bounds. For targeting purposes, neither of these situations is desirable because tight bounds limit the design space available to the upper-level design optimization. This limit may be more desirable for the lower-level optimization however; the upper-level optimization may not be able to achieve the desired performance. On the other hand, loose bounds may allow the upper-level design optimization to define a set of target values far from the current design. Consequently, the lower-level optimization may have difficulty in realizing the target values. Hence, a safeguard is necessary if the bounds defined by Eq. (6.16) become too large or too small. A minimum allowable size ϵ_l and a maximum allowable size ϵ_u have been set for the bounds. That is, $\Delta u_i = \epsilon_l$ in Eq. (6.16) if $\Delta u_i < \epsilon_l$, and $\Delta u_i = \epsilon_u$ if $\Delta u_i > \epsilon_u$. As the cycles between the upper and lower-levels progress, the allowable sizes will be continuously reduced to ensure the convergence.

Another important numerical consideration in this proposed two-stage optimization is the degree of accuracy required in targeting each intermediate variables. The accuracy of the targeting is not stringent for those intermediate variables to which the performance functions (e.g., global eigenvalues) in the upper-level are not sensitive. However, the accuracy of the targeting for the highly sensitive intermediate variables should remain high. To implement this consideration numerically, the sensitivity derivatives of the global eigenvalues with respect to the intermediate variables are used as the weighting coefficients in constructing the objective function in the lower-level design optimization

problem. Thus, the objective function in the lower-level design optimization problem (P6.2) is modified as

$$\min_{\mathbf{b}} \quad \phi_0(u_i, u_i^*) = \sum_{i=1}^{m} \left|\frac{\partial \lambda^g}{\partial u_i}\right| (u_i - u_i^*)^2 \tag{P6.3}$$

where the derivatives are computed at the optimal values u_i^*. The numerical issues discussed above will be demonstrated in the next section.

6.5 Numerical Results

The proposed method has been applied to a simple fixed-fixed beam and to a simplified model of an engine cradle (shown in Figs. 2.4 and 2.5) to demonstrate the numerical procedure and the applicability of the method.

The design modification problem has been set up to increase the first global eigenvalue by 10 percent by modifying only one of the components while the weight remains at a value less than the original value.

For these examples, the upper- and lower-level design optimization problems are set up as given below.

Upper level:

$$\min_{u_i} \quad \left[\sum_{i=1}^{m} \left(u_i - u_i^0\right)^2\right] W_1 + \left(\lambda_2^g - \lambda_2^{g^0}\right)^2 W_2 \tag{6.18}$$

subject to

$$\begin{aligned} \lambda_1^g &> 1.1\lambda_1^{g^0} \\ u_i^{bl} &< u_i < u_i^{bu} \end{aligned} \tag{6.19}$$

Lower Level:

$$\min_{\mathbf{b}_i} \quad \sum_{j=1}^{m} \left|\frac{\partial \lambda_1^g}{\partial u_j}\right| \left(u_j - u_j^*\right)^2 \tag{6.20}$$

subject to

$$\begin{aligned} V &< V_o \\ b_i^l &< b_i < b_i^u \end{aligned} \tag{6.21}$$

In Eq. (6.18), u_i^0 are the achieved intermediate variables in the previous cycle, and $\lambda_2^{g^0}$ is the initial value of the second eigenvalue of the global structure. The first term in Eq. (6.18) minimizes the change in the current design; the second term tries to preserve λ_2^g when λ_1^g is subjected to a 10- percent increase. The constants W_1 and W_2 in Eq. (6.20), are the weighting coefficients and are chosen to be 3.0 and 1.0, respectively. In Eq. (6.20), the sensitivities of the first global eigenvalue with respect to the intermediate variables $\frac{\partial \lambda_1^g}{\partial u_i}$ are used as the weighting coefficients (discussed in section 6.4), which determine the accuracy of the target required for those corresponding intermediate variables.

6.5.1 Fixed-Fixed Beam

A fixed-fixed beam considered in the previous chapters (i.e., Fig. 2.4) is shown here in Fig. 6.3. The beam is assembled from two identical cantilever beams α and two identical free-free beams β. However, in this case the beam is considered to be assembled in only one level. In previous chapters, it was considered to be a multilevel assembly.

Because component β is unconstrained, it has rigid-body modes. Components α and β are modeled with 2 nodes and 4-degree-of-freedom beam elements with transverse deflection and rotation as the nodal degrees of freedom. Component α is discretized into four elements, and component β is discretized into three elements. Hence, the components have 8 degrees of freedom each. When all components are assembled together, as shown in Fig. 6.3, the global structure has a total of 26 degrees of freedom. In this example, only one of the α components has been chosen for the modification to achieve the 10-percent increase in the first eigenvalue of the global structure.

Eigenmodes and static modes of each of the four components are obtained, as described in chapter 2. The component mode synthesis is performed by considering the two eigenmodes and the two static modes of each component as basis vectors. For component β, the two eigenmodes are the rigid-body modes. Eigenvalues obtained with

the component mode synthesis are listed in Table 6.1. These eigenvalues are compared with the exact values computed using the finite-element analysis of the entire structure. Notice that the first few eigenmodes are computed with a high degree of accuracy, which is fundamental to component mode synthesis.

At the upper-level, a total of 10 intermediate variables result from 2 eigenvalues, 2 interface degrees of freedom for each of the 2 eigenmodes, and 2 attachment modes. The boundary partition of the attachment modes, which corresponds to the degrees of freedom at which the unit forces are applied (i.e., Ψ_{ss}^{i}) is simply the boundary partition of the flexibility matrix of the component that corresponds to the same degrees of freedom; therefore, it is symmetric. Hence, among the four components of matrix Ψ_{ss}^{i}, only three are independent. As a result, out of 10 intermediate variables only 9 are considered as design variables for the upper-level design optimization.

For the lower-level, the element cross-sectional areas are treated as design variables. Because the cross section is rectangular, both its height and width are taken as design variables, and the component of concern is discretized into four elements. Hence, eight design variables exist for the lower-level design optimization.

The results obtained are shown in Table 6.2. The table shows that in just two iterations, a good target has been achieved between the upper and lower-levels. The primary reason for such an accurate target is the small ratio of the number of intermediate variables to be targeted to the number of primary design variables. The variation in the design variables after successive cycles is given in Table 6.3. In this example, the applicability of the proposed design modification technique for use with component mode synthesis has been demonstrated.

The second example, which is a simplified model of an engine cradle, is more complicated because it has a greater number of degrees of freedom and a larger ratio between the number of intermediate variables and the number of primary design variables. With this second example, we demonstrate the importance of the two-stage optimization

scheme and the dynamic adjustment of the bounds in the entire design process proposed here.

6.5.2 Simplified Model of Engine Cradle

The simplified model of an engine cradle is shown in Fig. 2.5. The structure can be divided into four components. Information on each component is given in Table 6.4. These components are discretized with 2 nodes and 12-degree-of-freedom circular-tube beam elements. When the components are assembled, the global structure has 198 degrees of freedom. In this example, component 3 has been chosen for modification.

The eigenmodes and the static modes of each component are obtained as explained in chapter 2. Because components 1 and 2 are unconstrained, the attachment modes are obtained by constraining the rigid-body degrees of freedom at one end and applying the unit forces at the other end. The number of eigenmodes and static modes considered for each component is given in Table 6.4. Component mode synthesis has been performed with these modes used as basis vectors.

At the upper-level, 137 intermediate variables result from 5 eigenvalues and 12 interface degrees of freedom for each of the 5 eigenmodes and 6 attachment modes. As explained in the previous section, the boundary partition of the attachment modes, which corresponds to the degrees of freedom at which the unit forces are applied, is symmetric. Hence, among the 36 components of matrix Ψ^i_{ss}, only 21 are independent. Therefore, out of 137 intermediate variables, only 122 are considered as design variables for the upper-level design optimization.

For the lower-level, the element cross-sectional areas are treated as design variables. Because the cross section of a single element is a circular tube, both its inner and outer radii are treated as design variables. Component 3 is discretized into 10 elements; therefore, 20 design variables result for the lower-level design optimization. The bounds on the design variables are set up to allow a variation of 15-percent in either direction.

(See Table 6.5) Note that for this problem the number of intermediate variables is greater than the number of primary design variables for the lower-level optimization.

The optimization results are listed in Table 6.6. The maximum percentage of change in λ_1^g that could be achieved was 6.2 percent after four cycles. More cycles did not improve the result significantly. However, the optimization process achieved a reduction of 24-percent in the volume of the component. The single-stage optimization was performed by treating only the radii of the elements related to component 3 as the design variables and subjecting the variables to the same volume reduction of 24-percent. As a result, a 6.3-percent improvement was achieved in the first global eigenvalue. Hence, the proposed methodology can achieve results very close to those results achieved by the single-stage optimization. The final design and bounds on the design variables in the lower-level are listed in Table 6.5. Notice that six of the design variables reached the bounds and two others were close. By relaxing the bounds on the lower-level design variables, a 7.3-percent improvement was achieved in the first eigenvalue; at the same time, the volume was further reduced to 34-percent of the initial value.

Table 6.6 shows that the achieved percentage of improvement in λ_1^g steadily increased from 3.6 at the end of the first cycle to 6.2 after four cycles. The key to this improvement lies in the systematic way that the bounds are adjusted on the intermediate variables to force the upper-level optimization to result in a design that can be realized in the lower-level design space. To illustrate the importance of adjusting the bounds, the variations of the values of the first 5 eigenvalues and the 6 interface degrees of freedom at point A in Fig. 2.5 of the first static mode, as well as their bounds for the successive cycles, are listed in Tables 6.7 and 6.8. Table 6.7 gives variations of the bounds, and Table 6.8 gives the required target and the achieved values of these intermediate variables. The values given in the tables are normalized with respect to their initial values. Initial bounds on all intermediate variables are taken as 20-percent of the initial value. As the cycles progress, the maximum allowable size ϵ_u of the bounds is reduced to 15, 12, and 10-percent for the

successive cycles; the minimum allowable size ϵ_l is kept at 5 percent for all cycles. These tables clearly show that the eigenvalues of the component are not targeted accurately, whereas the static-mode components are very close to the target values. This difference can be attributed to the fact that the sensitivities of the global eigenvalues with respect to the static-mode components are an order of magnitude higher than the sensitivities of the global eigenvalues with respect to the eigenvalues of the components.

The proposed two-stage approach was compared with the conventional single-stage approach in terms of the size of the problem to be solved and the number of optimization iterations required by each. The two-stage optimization required approximately 30 iterations and 30 function evaluations for the upper-level; for the lower-level, 145 iterations and 1100 function evaluations were required for the 4 cycles between the upper and lower-levels. The single-stage optimization took only 20 iterations and 376 function evaluations; however, the difference in the size of the problems analyzed in these two cases is noticeable. In the two-stage optimization, the size of the problem at the upper- and lower-level is 29×29 and 54×54, respectively. At the upper-level, only the eigenvalue analysis is required; at the lower-level, both the eigenvalue and the static analysis is required. The single-stage optimization solves a 198×198 eigenvalue problem. Although achievement of a perfect target is not possible, the entire design modification problem has been successfully divided into a number of smaller and tractable optimization problems without a significant increase in the computational effort. Above all, this research effort was directed toward characterization of the individual component as a design entity; this ultimately enables criteria to be set for the components so that this approach can be used for the efficient design modification of large structures by modifying only a few significant components.

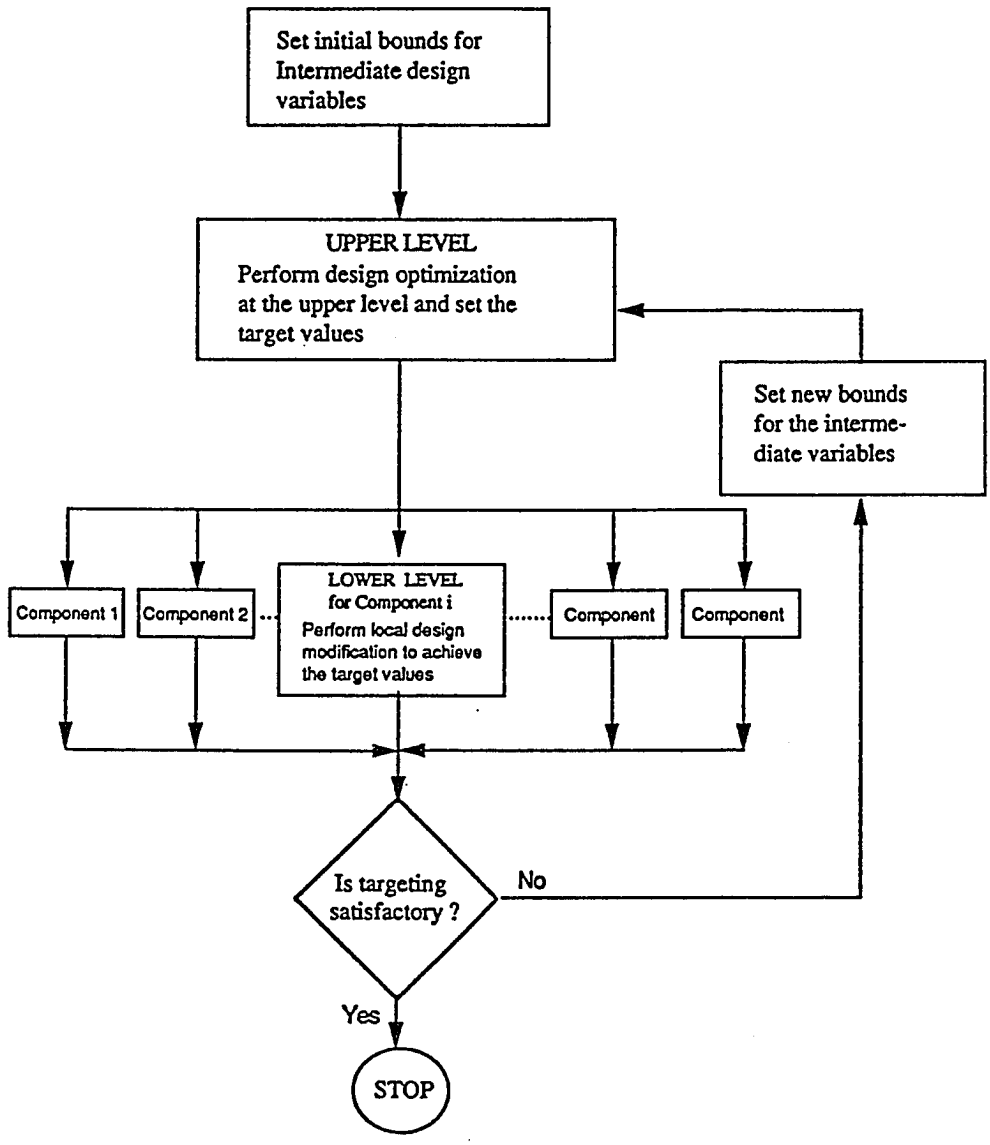

Figure 6.1 Multilevel design optimization.

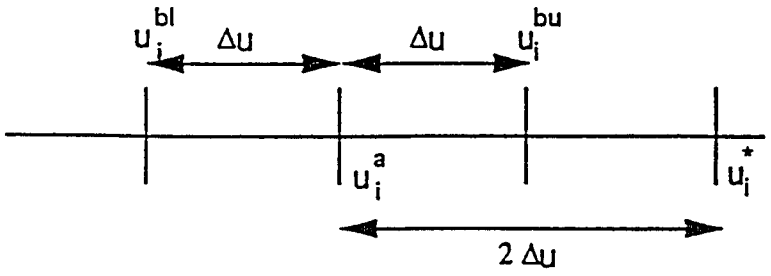

Figure 6.2 Adjustment of bounds for intermediate variables.

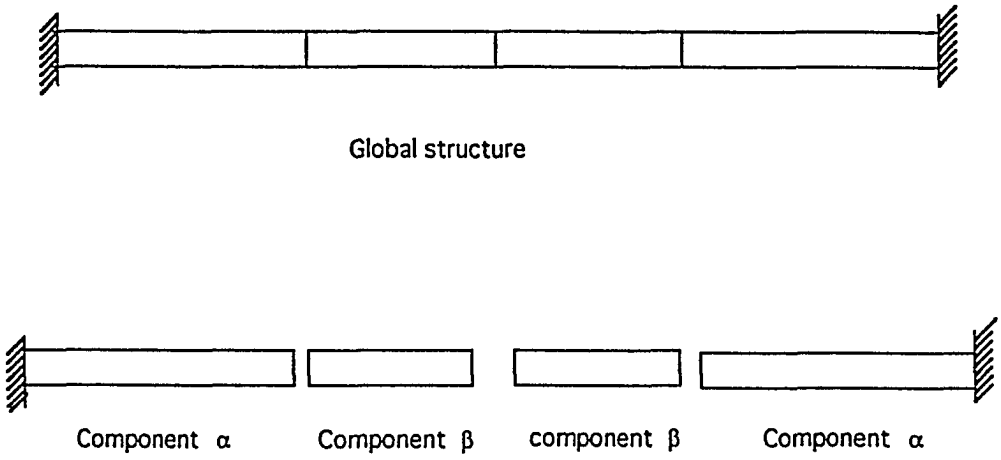

Figure 6.3 Fixed-fixed beam assembled in one level.

Table 6.1 Eigenvalues of Global Structure

(Fixed-Fixed Beam)

Computed	Exact
0.87506	0.87499
6.632265	6.63098
25.41630	25.36150
68.57203	68.43479
153.47555	151.14935
295.67301	292.31895
565.37267	507.57260
3097.08620	821.13760

Table 6.2 Change in First Eigenvalue of Global Structure

(Fixed-Fixed Beam)

Cycle no.	Target λ_1^g	Achieved λ_1^g
1	10.0%	8.3%
2	10.1%	10.7%

Table 6.3 Variation in Design Variables

(Fixed-Fixed Beam)

Element no.	Initial		After cycle I		After cycle II	
	Width (b)	Height (h)	Width (b)	Height (h)	Width (b)	Height (h)
1	2.0	4.0	1.4549	4.7987	1.4819	4.8158
2	2.0	4.0	1.4085	4.7028	1.5598	4.7962
3	2.0	4.0	1.3721	4.6498	1.3097	4.7244
4	2.0	4.0	1.3622	4.6125	1.2706	4.5191

Table 6.4 Component Data

(Simplified Model of Engine Cradle)

Component no.	Degrees of freedom	No. of Eigenmodes	No. of static modes	Total no. of modes
1	54	9	6	15
2	60	10	6	16
3	54	5	6	11
4	54	5	6	11

Table 6.5 Bounds on Lower Level Design Variables

(Simplified Model of Engine Cradle)

No.	Lower bound	Intial design	Final design	Upper bound
1	19.125	22.5	25.875	25.875
2	12.750	15.0	15.019	17.250
3	38.250	45.0	45.558	51.750
4	25.500	30.0	29.318	34.500
5	38.250	45.0	51.022	51.750
6	25.500	30.0	34.450	34.500
7	38.250	45.0	45.715	51.750
8	25.500	30.0	33.568	34.500
9	38.250	45.0	45.843	51.750
10	25.500	30.0	34.450	34.500
11	44.625	52.5	46.763	60.375
12	29.750	35.0	40.246	40.250
13	44.625	52.5	47.493	60.375
14	29.750	35.0	40.239	40.250
15	44.625	52.5	48.653	60.375
16	29.750	35.0	39.791	40.250
17	44.625	52.5	47.180	60.375
18	29.750	35.0	33.580	40.250
19	31.875	37.5	34.900	43.125
20	21.250	25.0	22.878	28.750

Table 6.6 Iteration History of Optimization Results

(Simplified Model of Engine Cradle)

Cycle no.	Target λ_1^g	Achieved λ_1^g
1	10.0%	3.6%
2	8.3%	4.8%
3	7.6%	5.7%
4	9.6%	6.2% (6.3%)*

* Result of single-stage design optimization for same reduction (24 percent) in volume of component.

Table 6.7 Dynamic Modification of Bounds of Upper Level Problem

(Simplified Model of Engine Cradle)

	Initial values		Cycle 2		Cycle 3		Cycle 4	
	Lower	Upper	Lower	Upper	Lower	Upper	Lower	Upper
Eigenvalues								
1	0.8	1.2	1.0934	1.2084	1.1366	1.2562	1.1815	1.3059
2	0.8	1.2	1.0744	1.1875	1.1055	1.2219	1.1324	1.2516
3	0.8	1.2	1.0351	1.1441	1.0679	1.1803	1.1319	1.2510
4	0.8	1.2	1.0751	1.1883	1.1137	1.2309	1.1652	1.2878
5	0.8	1.2	1.0637	1.2028	1.1119	1.2289	1.1454	1.2660
Static-mode components								
1	0.8	1.2	0.7622	0.9116	0.7125	0.8452	0.6869	0.7925
2	0.8	1.2	0.4979	0.6737	0.4083	0.4680	0.3052	0.3730
3	0.8	1.2	0.8632	0.9541	0.8116	0.9066	0.7684	0.8493
4	0.8	1.2	0.8738	0.9657	0.8442	0.9330	0.8321	0.9197
5	0.8	1.2	0.8022	0.9103	0.7578	0.8376	0.7110	0.7858
6	0.8	1.2	0.4363	0.5904	0.2761	0.3514	0.1607	0.1964

Table 6.8 Comparison of Required and Achieved Target Values

(Simplified Model of Engine Cradle)

	Cycle 1		Cycle 2		Cycle 3		Cycle 4	
	u^*	u^a	u^*	u^a	u^*	u^a	u^*	u^a
Eigenvalues								
1	1.1623	1.1509	1.2084	1.1964	1.2562	1.2437	1.3059	1.2683
2	1.1910	1.1310	1.1875	1.1637	1.2219	1.1920	1.2516	1.1971
3	1.1556	1.0896	1.1441	1.1241	1.1803	1.1914	1.2510	1.2258
4	1.0291	1.1317	1.1883	1.1723	1.2309	1.2265	1.1652	1.2481
5	0.9941	1.1332	1.2028	1.1704	1.2289	1.2057	1.2660	1.2057
Static-mode Components								
1	0.9863	0.8369	0.9116	0.7789	0.8452	0.7397	0.6869	0.7321
2	1.0430	0.5858	0.4979	0.4382	0.4083	0.3391	0.3045	0.3200
3	0.9421	0.9087	0.9541	0.8591	0.8116	0.8088	0.7684	0.7871
4	0.9786	0.9197	0.8738	0.8886	0.8442	0.8759	0.8321	0.8843
5	0.9643	0.8562	0.8022	0.7977	0.7578	0.7484	0.7110	0.7330
6	1.0014	0.5134	0.5904	0.3137	0.3514	0.1786	0.1964	0.1448

u^* = Required.

u^a = Achieved.

Chapter 7

CONCLUDING REMARKS AND FUTURE WORK

The objective of this research was to develop practical design techniques for structural synthesis and modification. Both the structural synthesis technique and the modification technique consider structural components as design entities. The structural synthesis technique selects the proper components to build an optimal structure and the structural modification technique selectively modifies the proper components to improve the performance of an existing structure.

The above objectives are accomplished by adopting the component mode synthesis technique as a vibration analysis tool for the global structure and establishing the functional relationship between the responses of the global structure and the responses of the individual components. This relationship facilitates the computation of the sensitivity derivatives of the global responses with respect to the responses of the individual components, which leads to determination of the contribution of the individual components to the responses of the global structure. With this relationship, the individual components are successfully characterized as design entities by using their dynamic and static responses as representative variables.

The structural synthesis technique proposed in this study is formulated as an integer programming problem that treats the various choices of the components as the design variables and is then solved with a genetic algorithm. After the required responses of the individual components have been obtained, the component mode synthesis method provides an efficient means for analyzing the global structure for the possible combinations of the assembled components. The component mode synthesis method is used as

an efficient reanalysis technique, in conjunction with a genetic algorithm, which requires the repetitive analysis of the global structures. This method is successfully demonstrated in finding the proper cross members for an engine cradle.

A local vibration targeting technique was presented for the efficient modification of the structure. This method selects the most significant components in the assembly and finds the optimum value for their vibration and static responses, so that the desired change in the performance of the global structure is achieved. Then, the local design modification is performed on the individual components to change the design variables such as elemental cross-sectional areas to achieve the set optimal values for these vibration and static responses. The sensitivity derivatives of the global responses with respect to the responses of the individual components were utilized to measure the significance of each component in terms of the vibration contribution to the global structure. A linear programming technique was used to determine the target values for the individual components of the structure. Local design modification of the individual components was performed with conventional gradient-based optimization techniques.

To deal with the problem of local vibration targeting more rigorously, a two-stage iterative design optimization scheme is presented. The local optimum of the two-stage problem is proven to be the local optimum of conventional single-stage problem. Although the proposed two-stage optimization may not be as computationally efficient, however, this method makes the structural modification problem tractable by allowing a set of smaller optimization problems to be solved. The proposed method for adjusting the bounds on the intermediate variables was useful in the given numerical examples.

Although the applicability of the developed methodologies were demonstrated on simple problems, these sample problems are general and can potentially be applied to the design modifications of realistic structures. However, a number of issues still must be addressed. For example, the accuracy of the component mode synthesis and its effect on the proposed design modification and synthesis techniques must be examined.

A more systematic method of measuring the significance of each component must be established. To this end, the possibility of establishing the physical meaning of the sensitivity derivatives of the global responses with respect to the various dynamic and static responses of the individual components must be explored.

The future efforts related to this work should be directed toward implementation of the proposed methodologies in commercially available, finite-element analysis and design optimization packages. These methodologies utilize the finite-element method to analyze the various components and conventional design optimization techniques to perform targeting, as well as the local design modification. Therefore, by effectively interfacing the finite-element analysis and the design optimization packages with the user-developed component mode synthesis program, a general-purpose modification tool can be developed. Other future work should be directed toward increasing the computational efficiency of the methodologies by implementing them on parallel machines. Because the analysis, as well as the local design modification, of the individual components can be performed independently from the rest of the components this particular feature can be effectively exploited to increase efficiency by implementing them in parallel.

REFERENCES

1. Hurty, W.C., "Dynamic Analysis of Structural Systems Using Component Modes," *AIAA Journal*, Vol. 3, No. 4, April 1965, pp. 678–685.

2. Craig, R. R., Jr., *Structural Dynamics — An Introduction to Computer Methods*, J. Wiley & Sons, Inc., New York, 1981.

3. Craig, R. R., Jr., "A Review of Time-Domain and Frequency-Domain Component Mode Synthesis Methods," *International Journal of Analytical and Experimental Modal Analysis*, Vol. 2, No. 2, 1987, pp. 59–72.

4. Bamford, R. M., "A Modal Combination Program for Dynamic Analysis of Structures," NASA TM 33–290, Jet Propulsion Laboratory, 1966.

5. Craig R. R., Jr., and Bampton, M.C., "Coupling of Substructures for Dynamic Analysis," *AIAA Journal*, Vol. 6, No.7, 1968, pp. 1313–1319.

6. Hintz, R.M., "Analytical Methods in Component Modal Synthesis," *AIAA Journal*, Vol. 13, No. 8, 1975, pp. 1007–1016.

7. Craig, R. R. Jr., and Chang, C-J., "On the Use of Attachment Modes in Substructure Coupling for Dynamic Analysis," *Proceedings AIAA/ASME 18th Structures, Structural Dynamics & Materials Conference*, Vol. B, 1977, pp. 89–99.

8. Kirsch, U., Reiss, M. and Shamir, U., "Optimum Design by Partitioning into Substructures," *Journal of the Structural Division, ASCE*, Vol. 98, No. ST1, 1972, pp. 249–267.

9. Kirsch, U., "Multilevel Approach to Optimum Structural Design," *Journal of Structural Design, ASCE*, Vol. 101, No. ST4, pp. 957–974.

10. Arora, J. S. and Govil, A. K., "An Efficient Method for Optimal Structural Design by Substructuring," *Computers and Structures*, Vol. 7, No. 4, 1977, pp. 507–515.

11. Okuma, M., Sok-Chu, P., Nagamastu, A. and Nanpe, M., "A Technique of Structural Dynamic Modification (Use of Mathematical Pseudo Inverse Method and Substructure Synthesis Method)," Pressure Vessels and Piping Conference, PVP, Vol. 179, 1989, pp. 155–160.

12. Heo, J. H. and Ehmann, K. F., "A Method for Substructural Sensitivity Synthesis," *Journal of Vibration and Acoustics, ASME*, Vol. 113, No. 4, 1991, pp. 201–208.

13. Schmit, L. A. and Ramanathan, R. K., "Multilevel Approach to Minimum Weight Design Including Buckling Constraints," *AIAA Journal*, Vol. 16, No. 2, 1978, pp. 97–104.

14. Sobieszczanski-Sobieski, J., James, B. B., and Dovi, A. R., "Structural Optimization by Multilevel Decomposition," *AIAA Journal*, Vol. 23, No. 11, 1985, pp. 1775–1782.

15. Haftka, R. T., "An Improved Computational Approach for Multilevel Optimum Design," *Journal of Structural Mechanics*, Vol. 12, No. 2, 1984, pp. 245–261.

16. Barthelemy, J. M., "Improved Mutlilevel Optimization Approach for the Design of Complex Engineering Systems," *AIAA Journal*, Vol. 26, No. 3,1988, pp. 353–360.

17. Schmit, L. A. and Mehrinfar, M., "Multilevel Optimum Design of Structures with Fiber-Composite Stiffened-Panel Composites," *AIAA Journal*, Vol. 20, No. 1, 1982, pp. 138–147.

18. Yates, K., Gurdal, Z. and Thangjitham, S., "Multilevel Optimization Using a Continuum Model for Structures," AIAA Paper No. 92–4786–CP, *Proceedings of the Fourth AIAA/USAF/NASA/OAI Symposium on Multidisciplinary Analysis and Optimization*, September 21–23, 1992, Cleveland, Ohio, pp. 773–783.

19. Kirsch, U., "Multitlevel Optimal Design of Reinforced Concrete Structures," *Engineering Optimization*, Vol. 6, 1983, pp. 207–212.

20. Kirsch, U., "An Improved Mutlilevel Structural Synthesis Method," *Journal of Structural Mechanics*, Vol. 13, No. 2, 1985, pp. 123–144.

21. Sobieszczanski-Sobieski, J., James, B. B., and Riley, M. F., "Structural Sizing by Generalized, Multilevel Optimization," *AIAA Journal*, Vol. 25, No. 1, 1987, pp. 139–145.

22. Patel, H. D., "Multidisciplinary Design Optimization with Superelements in MSC/NASTRAN," AIAA-92–4732–CP, *Proceedings of the Fourth AIAA/USAF/NASA/OAI Symposium on Multidisciplinary Analysis and Optimization*, September 21–23, 1992, Cleveland, Ohio, pp. 340–348.

23. MacNeal, R. H., "A Hybrid Method of Component Mode Synthesis," *Computers & Structures,* Vol. 1, No. 4, 1971, pp. 581–601.

24. Rubin, S., "Improved Component-Mode Representation for Structural Dynamic Analysis," *AIAA Journal*, Vol. 13, No. 8, 1975, pp. 995–1006.

25. Herting, D. N., "A General Purpose, Multi-Stage Component Modal Synthesis Method," *Finite Elements in Analysis and Design*, Vol. 1, 1985, pp. 153–164.

26. Klahs, J. W., and Townley, G. E., "Determining Component Loads and Stresses With Improved System Modeling Techniques," *Proceedings of the 3rd International Modal Analysis Conference,* Union College, Schenectady, N.Y., Vol. II, 1985, pp. 941–948.

27. Lamontia, M. A., "On the Determination and Use of Residual Flexibilities, Inertia Restraints, and Rigid-Body Modes," *Proceedings of the 1st International Modal Analysis Conference*, Union College, Schenectady, N. Y., 1982, pp. 153–159.

28. Yuan, M., Xiong, S. and Chen, X., "Multiple Level Dynamic Substructure Analysis," *Engineering Computations*, Vol. 8, 1991, pp. 231–244.

29. Haftka, R. T. and Gurdal, Z., *Elements of Structural Optimization*, 3rd ed., Kluwer Academic Publishers, Boston, Massachusetts, 1992.

30. Adelman, H. M. and Haftka, R. T., "Sensitivity Analysis of Discrete Structural Systems," *AIAA Journal*, Vol. 24, No. 5, pp. 823–832, 1986.

31. Fox, R. L. and Kapoor, M. D., "Rates of Changes of Eigenvalues and Eigenvectors," *AIAA Journal*, Vol. 6, No. 12, pp. 2426–2429, 1968.

32. Nelson, R. B., "Simplified Calculation of Eigenvector Derivatives," *AIAA Journal*, Vol. 14, No. 9, pp. 1201–1205, 1976.

33. Haug, E. J., Choi, K. K. and Komkov, V., *Design Sensitivity Analysis of Structural Systems*, Academic Press, New York, N. Y., 1986.

34. Goldberg, D. E., *Genetic Algorithms in Search, Optimization, and Machine Learning*, Addison-Wesley Publishing Co. Inc., Massachusetts, 1989.

35. IMSL User's Manual, Vol. 3, IMSL Problem Solving Software Systems, 1987.

36. Vanderplaats, G. N., "ADS — A Fortran Program for Automated Design Synthesis," NASA CR-177785, NASA Ames Research Center, September 1985.

37. *MATLAB User's Guide*, The Mathworks Inc., South Nalick, MA, 1991.